University of Stavanger

FACULTY OF SCIENCE AND TECHNOLOGY

MASTER'S THESIS

Study programme/specialisation: Engineering Structures and Materials/ Civil Engineering	Spring/ semester, 2020 Confidential
Author: Mohammad Afaghi	
Programme coordinator: Kjell Tore Fosså Supervisor(s): Kjell Tore Fosså	
Title of master's thesis: The Effect of CO2 Curing on Cement-Based Materials	
Credits: 30	
Keywords: Early Carbonation Curing; Cement Paste and Mortar; Different Water-Cement Ratio; Mechanical Properties; Micro-Structural Changes; CO2 Uptake; SEM; XRD; TGA; Chemical Reactions; Porosity; Density; pH.	Number of pages: ……112…… + supplemental material/other: …61…… Stavanger, …14/07/2020…. date/year

Abstract

Early carbonation curing of concrete elements has been shown to be a promising sustainable technology for CO_2 capture and utilization, which would be beneficial for the environment. It has been found that carbonation curing would also improve the mechanical properties as well as permeability. In this study, the effect of early age carbonation curing on the mechanical, chemical and micro-structural properties of cement paste and mortar with two different water-cement ratio of 0.3 and 0.6 was examined. Five hours of initial controlled air curing in the climate chamber with RH of 60% and temperature of 25°C, prior to four and eight hours of carbonation curing with CO_2 pressure and concentration of 6 bars and 99%$\geq$, respectively, was carried out. This study confirms that, carbonation curing would mainly happen in the first two hours. Water-cement ratio is an important parameter for the process, w/c of 0.3 shows higher capacity of CO_2 uptake. Besides, mortar elements, due to their porous nature, show higher potential for CO_2 uptake, around 15% of cement weight, compare to 9% for cement paste, thermogravimetric's results serve as supporting evidence. In terms of mechanical properties, the results show that, with proper mix design and pre-conditioning, carbonation curing would result in a high rapid 1-day compressive strength development rate up to 125% and 45% for mortar and cement paste specimens, respectively, in comparison with normal air curing specimens. Besides, carbonation curing results in higher strength, after 14 days, compare to the reference. Carbonation curing also results in reduction of both suction and macro porosity, it decreases the total porosity up to 10% and 7% for mortar and cement paste elements, respectively, which resulted in higher density for carbonation cured samples. In spite of the traditional belief regarding a reduction in pH level as a result of the carbonation procedure, the results show the pH level above 12 for all the carbonation cured samples. Micro-structural changes are evaluated by using multiple techniques. X-Ray Diffraction, Thermogravimetric Analysis and Scanning Electron Microscopy examinations indicate that the early carbonation curing results in rapid formation of $CaCO_3$ crystals due to the reaction of CO_2 with cement phases and hydration products itself to create a micro-structure with higher strength contributor than conventional hydration. The results also show less amount of CH and high amount of calcite in carbonation cured samples.

Preface

I would like to thank my supervisor, professor Kjell Tore Fosså for his guidance and support during this research, besides, a great appreciation goes to Kværner company that offered me the interesting general topic regarding the global concern for utilization of carbon dioxide which made me motivated in this research.

Further, I would like to thank John Grønli, Samdar Kakay and Jarle Berge that have provided me with materials and equipment in the concrete laboratory.

A great gratitude also goes to Johannes Steinnes Jensen and Caroline Einvik that helped me to assemble the airtight chamber for carbonation curing.

I would like to thank two key persons during my experiment; Anna Cecilie Åsland that patiently accompanied me during the long process of thermogravimetric test and Mona Wetrhus Minde that gave me the opportunity to work with SEM and X-Ray Diffraction instrument.

In the end, special thank to my mother and my friend Andreas Teslo Kjos that have encouraged me during the research.

In spite of COVID-19 restrictions, this study has been completed satisfactorily.

Table of Contents

List of Tables

List of Figures

Notations

Symbol	=	definition
C_M	=	Cement mortar
C_P	=	Cement paste
CH	=	Calcium hydroxide
C-S-H	=	Calcium silicate hydrate
cm^3	=	Centimeter
dm^3	=	Cubic decimeter
DTG	=	Differential thermogravimetric
EDS	=	Energy-Dispersive X-Ray Spectroscopy
g	=	Gram
H	=	Hours
K	=	Kelvin
kg	=	Kilogram
kJ	=	Kilojoule
kN	=	Kilonewton
kV	=	Kilovolt
L	=	Liter
m^2	=	Cubic meter
mA	=	Milliampere
$mBar$	=	Millibar
mg	=	Milligram
min	=	Minute
ml	=	Milliliter
mm	=	Millimeter
MPa	=	Megapascal
N	=	Newton
nm	=	Nanometer
ppm	=	Parts-per-million
RH	=	Relative humidity
RPM	=	Revolutions per minute
s	=	Second
SEM	=	Scanning Electron Microscopy
TGA	=	Thermogravimetric Analysis
Vol%	=	Volume percentage
w/c	=	water to cement
wt%	=	Weight percentage
XRD	=	X-Ray Diffraction
μm	=	Micrometer
°C	=	Celsius
3D	=	Three dimensional

Chapter 1

Introduction

Water vapor (H_2O), carbon dioxide (CO_2), methane (CH_4), nitrous oxide (N_2O) and ozone (O_3) are considered the primary greenhouse gases in Earth's atmosphere. Predominant gas of these greenhouse gases is carbon dioxide (CO_2). Around 1750, since the industrial revolution, human activities have resulted in an increase of 45 percent in the atmospheric concentration of carbon dioxide, from 280 ppm to 415 ppm in 2019 [11]. Cement production has so far contributed about 5 percent of total CO_2 emissions. It has been reported that carbon dioxide capture and utilization remain an issue with those who are concerned about global warming. Many scientists agree that the rate of warming on Earth is faster than any time in the last 10,000 years which is caused by increasing carbon dioxide into the atmosphere, this will lead to increase the possibility of catastrophic consequences; the ocean water level would rise due to melting glaciers and Antarctic ice caps and then can threaten many coastal cities. Severe impact of global warming on humans and nature is undeniable.

In 2009, More than 120 heads of government participated the Copenhagen Climate Change Summit, they agreed to reduce their emissions. Some developed countries committed to fund and support clean energy technologies. Besides, 197 countries have adopted the Paris Agreement to reduce global greenhouse gas emissions to limit the global temperature increase to 2 degrees of Celsius in this century, thus, it is necessary to develop new technologies and new products to reduce the carbon dioxide emission into the atmosphere.

While carbon capture and storage (CCS) is promising in geologic formation, carbon capture and utilization (CCU) seems more satisfying. A part of emitted carbon dioxide can be recycled and utilized into early age of concrete curing to form thermodynamically stable calcium carbonates.

As the population of the Earth is growing, the concrete productions are getting more demanded. According to The Global Cement Report, 13^{th} Edition, world cement consumption has 2.8% growth reaching to 4.08 billion tons in 2019 which leads to increasing of worldwide man-made CO_2 emission. This emission is the result of the chemical process

and burning fuel in cement industry (fabrication of 1 ton of cement would emit 900 kg of CO_2). Carbonation curing of concrete productions can be a promising way to utilize a part of this CO_2 emission.

The influence of CO_2 curing of concrete on development of compacted cement pastes and mortars has been investigated from 1970s [12–14].
CO_2 curing of concrete has several benefits. It was found that calcium carbonates and silica gel can be formed by the reaction of calcium silicates with CO_2 [15], which results in higher density that means lower porosity [16]. Moreover, the rapid strength gain induced by carbonation prompted research into its mechanism [17], in order to get the best performance of concrete, both in compressive strength and durability, curing should be implemented right after casting fresh concrete. The most usual way of curing is water.
Recently, many studies have shown that carbon dioxide can be an effective alternative for water curing, since it reduces the water permeability of carbonated concrete due to the precipitation of calcium carbonate crystals [18]. As for environmental benefits, saving millions liter of water annually and helping to reduce the carbon dioxide from the atmosphere, can be mentioned. In addition, the energy required for steam curing of 1 m^3 of concrete is around 0.59 gigajoule, by deploying carbonation curing it can be reduced to less than 0.013 gigajoule and huge amount of energy can be preserved [19]. Accelerating early strength and improving durability of the products are mechanical benefits of carbonation curing.

Carbonation curing can be applied to building products such as masonry block, paving stone, cement board and fiberboard. In the United States and Canada, annual cement consumption by these building products is near 14 million tones [20]. It has been found that if all of these products are cured by carbon dioxide, the net annual sequestration of CO_2 in concrete can reach 1.8 million tones [20]. Precast pipes can also be used for carbonation curing. Annual production of concrete pipes in the USA is about 22 million tons, if the amount of cement usage is considered 15.5% of total mass and carbon dioxide uptake of 10% by cement mass, “the US concrete pipe industry could consume 275,000 tons of CO_2 per year” [6].

1.1 Capacity of Norway to Reduce Carbon Dioxide for Utilization into Concrete Products

The concrete products in each country is divided into three types of production. Ready-Mix concrete, precast elements and precast concrete production.

- Ready-Mix concrete (RMC) classified into productions like; walls, slabs, foundations, structures.
- Precast element (PEC) classified into productions like; roof, walls, facades, columns, beams and slabs.
- Precast concrete products (PCP) classified into productions like; paving, blocks, pipes, etc.

The Norway's annual production of concrete in 2003 was gathered by Wallevik [21]. Table 1.1 illustrates a summary of report based on the volume and cement consumption for three different concrete products.

Table 1.1: Concrete products and cement consumption of three concrete products in Norway (2003)

Concrete Productions	Volume Production in 2003 (m^3)	Cement Consumption 2003 (Kg)
RMC	2.4 million	800 million
PEC	307500	108.7 million
PCP	492308	192 million
Total	3.5 million	1100.7 million

According to a study [20], it can be estimated an average of 7% carbon dioxide (flue gas at a net efficiency of 84%) or 12.8% recovered carbon dioxide (at net efficiency of 87.1%) uptake for all kinds of concrete products in the USA.
If these percentages are used for Norway's concrete production, it can be expected to utilize annually, 77,000 tons of carbon dioxide flue gas, or 140,900 tons of recovered carbon dioxide into concrete by carbonation curing.

1.2 Objectives and Scope

In this research, the effect of early age CO_2 curing of cement paste and mortar on mechanical, chemical and micro-structural changes has been investigated. The study is limited to concentrate on the following properties:

- **The effect of fresh properties on CO_2 uptake**
  - Fresh density
  - Air content
  - slump
- **The effect of carbonation curing on mechanical properties**
  - Early compressive strength
  - 14-days compressive strength
- **The effect of carbonation curing on chemical changes**
  - X-Ray diffraction analysis
  - Thermogravimetric analysis
  - CO_2 uptake
  - Degree of hydration
  - pH level

- **The effect of carbonation curing on micro-structural changes**
  - Scanning electron microscopy
  - Porosity
- **The effect of mixing design on CO_2 uptake**
  - Cement paste and mortar
  - Different water to cement ratio

1.3 Thesis Structure

An overview of the thesis structure is presented below;

- **Chapter 1: Introduction**
- **Chapter 2: Literature Review**
- **Chapter 3: Experimental Program**
- **Chapter 4: Results and Discussions**
- **Chapter 5: Conclusions**
- **Chapter 6: Future Work**

Chapter 2

Literature Review

The purpose of this chapter is to provide the reader with relevant theory within the field of cement phase, carbonation process and a brief explanation of tests methods. This also will be followed by a review of previous research has done on carbonation curing of concrete.

2.1 Chemical Composition of Cement

Chemical composition of cement clinker is expressed in terms of chemical oxides; table 2.1 shows the typical composition of clinker [22].

Table 2.1: Typical composition of Portland clinker (wt%)

CaO	Calcium oxide/ lime	60-67
SiO_2	Silicon dioxide/ silica	17-24
Al_2O_3	Aluminum oxide/ aluminia	4-7
Fe_2O_3	Iron oxide	1.5-5
MgO	Magnesium oxide/ magnesia	1-5
SO_3	Sulfite	0.5-3.5
$K_2O + Na_2O$	Alkali	0.2-1.5

There are four major phases in Portland clinker that make chemical formula in cement chemistry (table2.2), which are expressed as sums of oxides, mentioned in table 2.1. These phases are highly reactive in the presence of water that the products of the reactions are mainly calcium silicate hydrate (C-S-H) and calcium hydroxide ($Ca(OH)_2$).

Table 2.2: Four major phases in Portland clinker

Major Phase	Mineralogical term	Cement chemical notation	Shortened chemical notation
Tricalcium silicate	Alite	$3\,CaO \cdot SiO_2$	C_3S
Dicalcium silicate	Belite	$2\,CaO \cdot SiO_2$	C_2S
Tricalcium aluminate	Aluminate	$3\,CaO \cdot Al_2O_3$	C_3A
Tetracalcium aluminoferrite	Ferrite	$4\,CaO \cdot Al_2O_3 \cdot Fe_2O_3$	C_4AF

2.2 Carbonation of Concrete

Concrete can be subjected to two different types of carbonation. The first and natural one, weathering carbonation, which concerns mature concrete to react over an extended period when it is exposed to carbon dioxide in the atmosphere and it will continue reacting until the lifetime of the specimen. The second is early age carbonation, which includes injection and utilization of carbon dioxide into the concrete when it comes to curing at early age.

2.2.1 Weathering Carbonation

Weathering or atmospheric carbonation occurs in concrete when calcium compounds react with carbon dioxide from the atmosphere and water in the concrete pores.
The first reaction would be CO_2 with water in the pores to form carbonic acid (H_2CO_3). Then the carbonic acid reacts with the calcium hydroxide ($Ca(OH)_2$) contained in the hydration products of a mature concrete. According to the following chemical reactions, the result is the formation of calcium carbonate ($CaCO_3$):

$$CO_2 + H_2O \longrightarrow H_2CO_3$$

$$Ca(OH)_2 + H_2CO_3 \longrightarrow CaCO_3 + 2\,H_2O$$

Once the $Ca(OH)_2$ has carbonated and is depleted from the cement paste, the calcium-silicate-hydrate gel (C-S-H) can be decalcified, thereby allowing the liberated CaO to carbonate;

$$H_2CO_3 + CaO \longrightarrow CaCO_3 + H_2O$$

Or more general reaction would be;

$$C-S-H + 2\,CO_2 \longrightarrow SiO_2 + 2\,CaCO_3 + H_2O$$

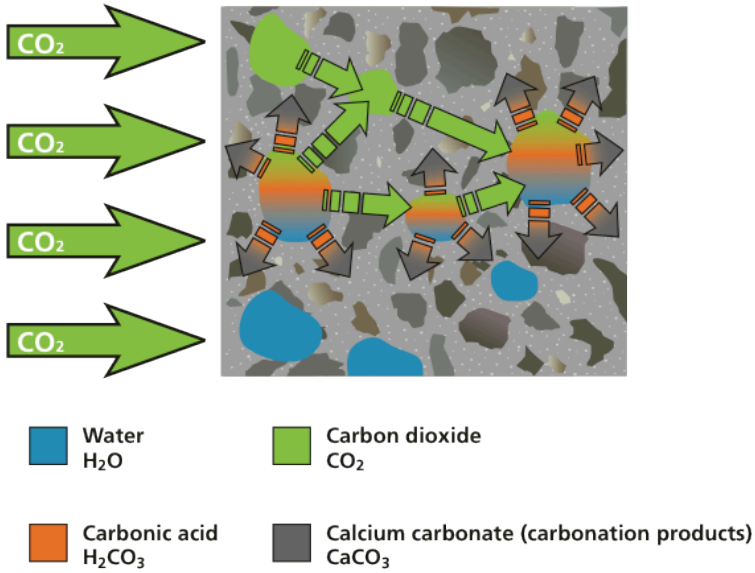

Figure 2.1: schematic of weathering carbonation [1]

The depletion of calcium hydroxide ($Ca(OH)_2$) will reduce the pH level below 13 and this level can reach 8 for fully carbonated concrete. Low pH level can deteriorate the protective passive layer of reinforcement on its surface and when reinforcement is exposed to aggressive agents such as chloride ions, would lead to corrosion.
When steel is placed into the concrete with a high pH level, it creates a passive film that protects the rebars from corrosion and can be deteriorated by low pH level as a result of calcium hydroxide reaction with carbon dioxide in cement paste. Once the iron ions are released from the anode and react with oxygen, the ion-oxide is formed that occupies a larger volume than the uncorroded steel. As a result of this expansion, cracking and spalling of the concrete may occur. It has been found that a 25 micro millimeter of corrosion may cause cracking, however, this value depends on the amount of concrete's cover over the reinforcement [23].
On the contrary, prolonged weathering carbonation of hydrated cement has been proven to have some advantages; increasing compressive strength in the long term [24, 25], decreasing sorptivity due to the reduction in capillary porosity in the surface through replacement of carbonates products [26]; hence, water permeability also would be decreased [27].

One of the primary factors that can have a significant effect on the depth of carbonation and the CO_2 uptake over time, is relative humidity (RH). In general, carbonation only occurs when the RH is in range of 40 to 90 percent and that is because of the amount of water in the pores for CO_2 to dissolve to form the carbonic acid which is needed to react with the calcium compounds. Besides, if the RH is too high, then the CO_2 pores are full of water, which makes it inhibited for CO_2 to ingress.

Carbonation Rate Exposed to Environment

When carbon dioxide in the atmosphere reacts with calcium hydroxide, carbonation of concrete will occur in the hydrated cement paste. According to previous studies [28], the carbonation rate is assumed to be governed by using the following equation:

$$\text{Depth of carbonation(mm)} = C.T^{0.5} \tag{2.1}$$

Where;
T is time in years.
C is the coefficient, dependent on concrete quality.

According to table 2.3, the value of C is highly dependent on the water-cement ratio [28]. By using the data, the carbonation depth of concrete with a specific w/c ratio, can be estimated in a long time.

Table 2.3: Value of C for different w/c ratio

W/C	C (for normal portland cement)
0.70	8
0.60	4.9
0.50	4
0.40	1

2.2.2 Early Age Carbonation

Although carbonation of mature concrete exposed to weathering CO_2 is not a desirable chemical reaction, however; carbonation of early age is beneficial to both mechanical properties and durability performance due to the elimination of CH [6]. In addition, it is found that the early carbonation of precast concrete can decrease the carbonation shrinkage of assembled concrete structures in service [29].
Carbonation curing of concrete is a complicated process involving chemical reactions and physical changes. Once water is mixed with Portland cement, hydration of cement would start. The carbonation of hydration products and hydration of cement itself make little contribution compare to the reaction between CO_2 and cement mineral that contribute to the structure and performance of carbonation cured concrete.
Carbonation curing is an accelerated curing process that injects carbon dioxide gas into the curing chamber. CO_2 is diffused into the concrete specimens right after casting and transforms the gaseous CO_2 into calcium carbonates, it is expected that the carbonation of fresh $2\,CaO \cdot SiO_2$ (C2S) and $3\,CaO \cdot SiO_2$ (C3S) pastes in an accelerated curing process, equations 2.2 and 2.3 indicate the reactions. The products in these reactions are hybrid of calcium-silicate-hydrate (C-S-H) and calcium carbonate. The early strength can be achieved within a few minutes to a few hours [17, 30, 31].

$$3\,CaO \cdot SiO_2 + (3\text{-}x)CO_2 + yH_2O \longrightarrow C_xSH_y + (3\text{-}x)CaCO_3 \tag{2.2}$$

$$2\,CaO \cdot SiO_2 + (2\text{-}x)CO_2 + yH_2O \longrightarrow C_xSH_y + (2\text{-}x)CaCO_3 \tag{2.3}$$

Where; C_xSH_y is $xCaO \cdot SiO_2 \cdot yH_2O$

Equations 2.2 and 2.3 are spontaneous and exothermic.
The nine steps below and figure 2.2 are the summations of various reactions for the early age carbonation [2]:

- The CO_2 gas diffuses through the pores of the concrete specimen.
- Solvation of CO_2 gas to CO_2 aqueous.
- Reaction of water with CO_2(aq) to produce H_2CO_3.
- Ionization of H_2CO_3 to H^+, $HCO_3{}^-$, $CO_3{}^{2-}$ instantaneously which depends on the presence of $Ca(OH)_2$ that keeps the pH level higher than 10. When $Ca(OH)_2$ reacts with CO_2, the lower source of calcium hydroxide make the pH level lower. However, the pH can recover as the concrete matures.
- Then the cement phases (C_3S and C_2S) dissolve exothermically and rapidly. Cement particles are covered by a layer of C-S-H gel which release Ca^{2+} and $SiO_4{}^{4-}$ ions as a consequence of dissolution of C-S-H gel.
- Then Nucleation of C-S-H gel and $CaCO_3$ happens with slight high temperature.
- Vaterite and aragonite are two $CaCO_3$ crystals that can be formed at the beginning, but finally, they revert to calcite which is more stable than vaterite and aragonite.
- The formed C-S-H gel would be progressively decalcified and silicate hydration (S-H) and $CaCO_3$ would be formed.

$$3\,CaO \cdot SiO_2(s) + 3\,CO_2\,(aq) + nH_2O \longrightarrow SiO_2 \cdot nH_2O + 3\,CaCO_3$$

$$2\,CaO \cdot SiO_2(s) + 2\,CO_2\,(aq) + nH_2O \longrightarrow SiO_2 \cdot nH_2O + 2\,CaCO_3$$

There are two approaches regarding carbonation curing; if carbonation is performed right after casting, reaction would occur between C_3S and C_2S, or reaction would occur between cement phases and hydration products if carbonation is performed after a while, however, the contribution of hydration products in early carbonation is lower than carbonation of cement mineral. The following reactions show the carbonation of hydration products [32];

Carbonation of calcium hydroxide;
$Ca(OH)_2\,(aq) + CO_2\,(aq) \longrightarrow H_2O + CaCO_3$

Carbonation of C-S-H gel;
$xCaO \cdot SiO_2 \cdot yH_2O\,(s) + CO_2\,(aq) \longrightarrow CaCO_3 + (x\text{-}1)\,CaO \cdot SiO_2 \cdot yH_2O$

Carbonation of ettringite[1];
$3\,CaO \cdot Al_2O_3 \cdot 3\,CaSO_4 \cdot 32\,H_2O\,(s) + 3\,CO_2\,(aq) \longrightarrow 3\,CaCO_3 + 3\,CaSO_4 \cdot 2\,H_2O + 2\,Al(OH)_3\,(s) + 9\,H_2O$

[1] In the presence of gypsum (calcium sulfate), C_3A hydrates and forms ettringite (AFt).

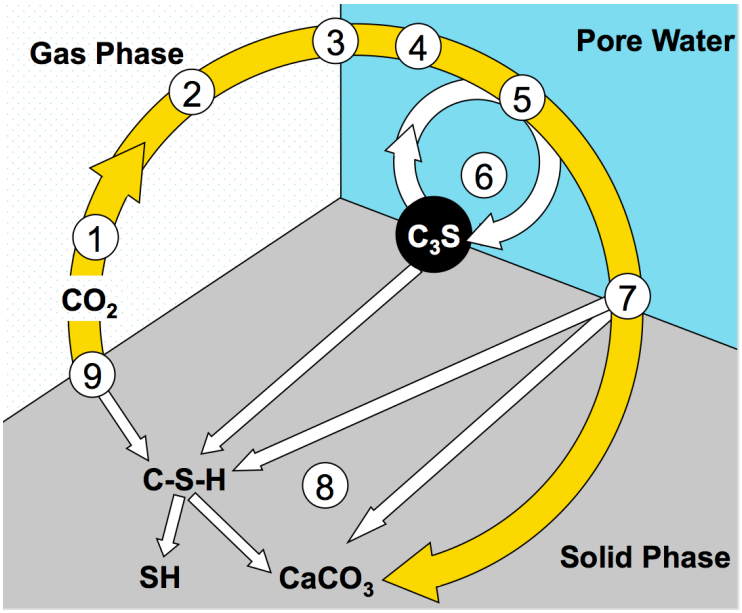

Figure 2.2: Schematic of nine steps for early carbonation reactions [2]

The difference of the weathering carbonation and early age carbonation can be written in the simple words;
In the weathering carbonation, CO_2 would react with $Ca(OH)_2$, which is a part of hydration products; this reaction would deplete $Ca(OH)_2$ from concrete and as a result, the pH would reduce since $Ca(OH)_2$ is alkaline. However, in early age carbonation, the CO_2 would contribute to the reaction of hydration and produce $CaCO_3$ instead of $Ca(OH)_2$.

Maximum Theoretical CO_2 Uptake by Cement

The maximum theoretical CO_2 consumption by cement (equation 2.4) and the degree of CO_2 curing (equation 2.5) can be calculated by the following equations [33]:

$$M_{max} = 0.785(\mathrm{CaO} - 0.7\mathrm{SO_3} + 1.09\mathrm{MgO} + 1.42\mathrm{Na_2O} + 0.93\mathrm{K_2O} \tag{2.4}$$

Where;
All the oxides represent their mass percentages in cement clinker.

$$\alpha\% = \frac{M_{\mathrm{CO_2}}}{M_{max}} \times 100 \tag{2.5}$$

Where;
α is the degree of carbonation.

2.2.3 Solidia Tech

Solidia Tech company is commercializing a reduced carbon footprint in concrete industry in both producing calcium-silicate-based cement and curing technology by injecting CO_2 gas. The cement has a lower amount of CaO and belite ($(CaO)_2 \cdot SiO_2$) in its main mineral phase and due to the lower amount of CaO, much less calcium carbonate ($CaCO_3$) should be calcined, as a consequence, less CO_2 would be emitted during the production (565 kg of CO_2 per one tone of cement production).
Besides, the company uses non-hydraulic curing by injecting CO_2 gas in the presence of water in early age, which causes an improvement in performance. The solidia Tech cement can utilize around 230 kg of CO_2 per tone of cement usage [34].

$$(CaO)_2 \cdot SiO_2 + 2\,CO_2 \xrightarrow{H_2O} 2\,CaCO_3 + SiO_2$$

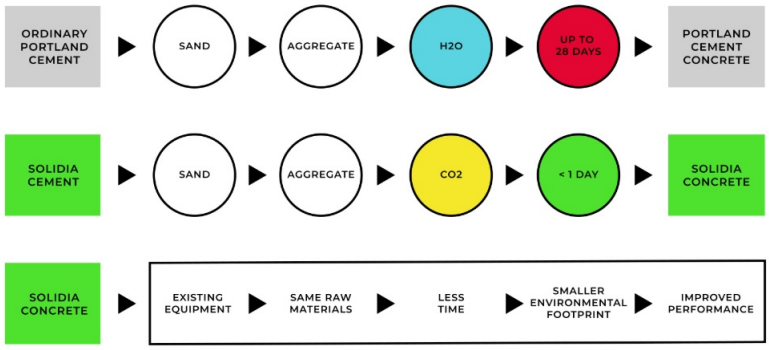

Figure 2.3: A schematic of Solidia Tech technology [3]

2.2.4 Measuring CO_2 Uptake

Three common methods can be used to measure the percentage of CO_2 uptake after carbonation curing;

- Mass Gain Method
- Mass Curve Method
- TGA Method

Mass Gain Method

Comparison of sample mass before and after carbonation. Since it is an exothermic reaction, water loss should be considered in the mass difference. This mass of lost water, that is condensed on the wall of the chamber, can be obtained by absorbent paper. Then CO_2

uptake can be calculated by using equation 2.6:

$$\text{CO}_2 \text{ uptake}\% = \frac{Mass_{\text{(after carbonation)}} - Mass_{\text{(before carbonation)}} + Water_{\text{(lost)}}}{Mass_{\text{(cement)}}} \quad (2.6)$$

Mass Curve Method

In this method, the chamber is placed on a digital scale to record the mass of the entire system. Before the injection of CO_2 gas, the scales should be zeroed and then the subsequent mass curve is used to determine the carbon uptake percentage by cement paste after correction for residual gas in the chamber [6].

TGA Method

This method is completely described in the section 3.5.10

2.3 Chloride-Induced Corrosion

Chloride-induced corrosion has a vital role in determining the durability and serviceability of the reinforced concrete structures, especially the ones exposed to marine environments. Chloride ion presents in the marine environment or seawater affects the passivity of steel film and its protective layer and provokes the initiation of corrosion; the chloride can oxidize and corrode the surface of rebars. In addition, the corrosion of the surface of the rebars compromises the bond between the concrete and steel reinforcement, leading to separation of concrete and steel reinforcement. The chloride ion ingression into concrete can also make excessive cracking in the concrete itself.

One of the common chloride ion penetration mechanism is absorption through capillary suction. As a concrete surface exposed to environment, it will undergo wetting and drying cycles. When water containing chloride drawn into the pore structure, the water dries out during the drying process and the chloride remains in the concrete. This process may cause a high enrichment of chloride content after some drying and wetting cycles. Therefore, the water penetration depth and the porosity of the surface layer of concrete are two important factors affecting the initiation of corrosion.

The most common chloride ion penetration mechanism is through diffusion, which is driven by the presence of a concentration gradient. It occurs when chloride ions move from a high concentration area to a low concentration area to reach a uniform concentration equilibrium. Figure 2.4 shows the chloride ion ingression into the concrete.

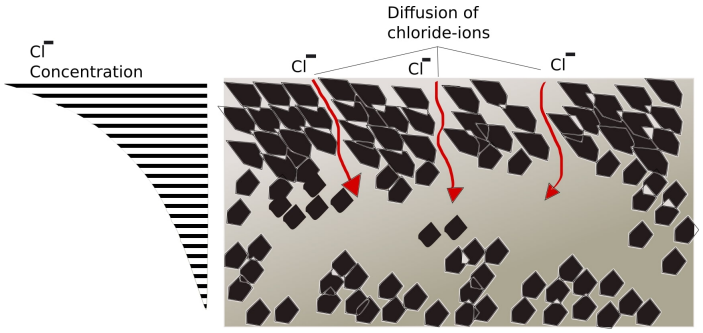

Figure 2.4: Chloride ion ingression through pores into concrete

2.4 Previous research

The following sections will present previous research has done on CO_2 curing of concrete or lightweight concrete blocks. The previous selected research is designated in terms of the experimental mechanisms.

2.4.1 Compressive Strength

It has been found by many studies that carbonation curing has a significant influence on early compressive strength.

A study showed an effect of carbonation curing on compressive strength of precast reinforced concretes with different water to cement ratio [4] illustrated in figure 2.5. The test was conducted after 1 and 28 days from casting.

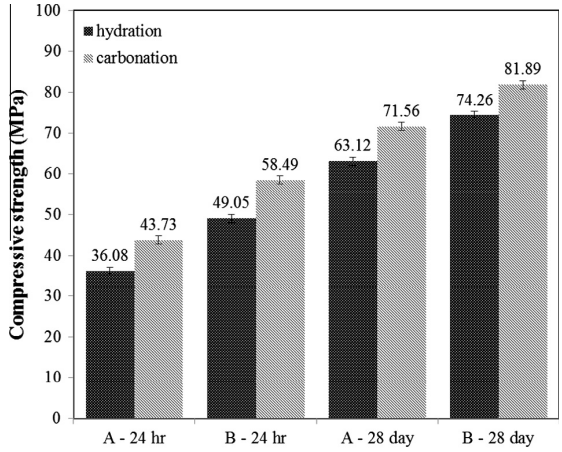

A: w/c ratio of 0.4 B: w/c ratio of 0.3

Figure 2.5: Comparison of compressive strength in two different periods [4]

As it can be observed, on the first day, there is an almost 20% increase in carbonated specimens in both batches, this value reduced to almost 11% after 28 days.

Another study [5] showed a good comparison of compressive strength for a different types of batches with w/c ratio of 0.15, after 2 hours, 3 and 28 days of curing. This comparison is illustrated in figure 2.6. The abbreviation used in the graph is explained in figure 2.7.

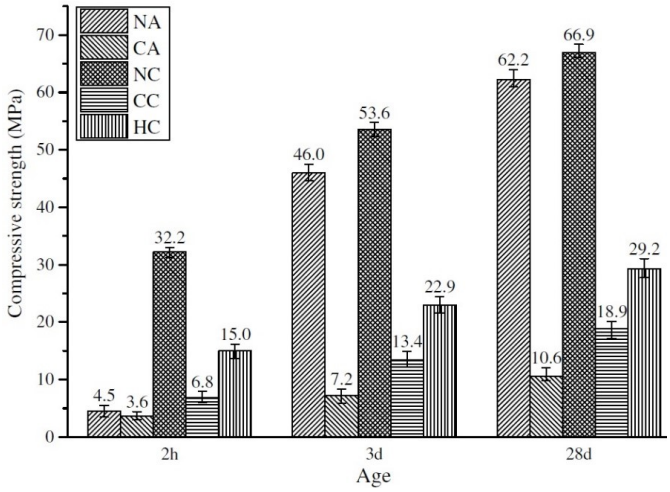

See figure 2.7 for the abbreviations

Figure 2.6: Comparison of compressive strength for different mixing and curing mechanisms with respect to curing time [5]

	Mixing stage	Curing stage	
Identifier	Method	Method	Curing age
NA	Normal air mixing (N)	Air curing (A)	2hA, 3dA, 28dA
CA	Carbonation mixing (C)	Air curing (A)	2hA, 3dA, 28dA
NC	Normal air mixing (N)	Carbonation curing (C)	2hC 2hC + 3dA 2hC + 28dA
CC	Carbonation mixing (C)	Carbonation curing (C)	2hC 2hC + 3dA, 2hC + 28dA
HC	Hybrid mixing (H)	Carbonation curing (C)	2hC 2hC + 3dA, 2hC + 28dA

Note: 2hA = 2 h air curing; 2hC = 2 h carbonation curing; 3dA = 3 days air curing; 28dA = 28 days air curing.

Figure 2.7: Abbreviation used in figure 2.6 [5]

It can be seen that, after just 2 hours of carbonation curing, NC (carbonation curing)

achieved 52% of 28 days compressive strength related to air curing, however, it did not show a significant effect in the long term.

2.4.2 Heat of Hydration

According to a study, the temperature of the specimens elevated very quickly in the presence of CO_2 in carbonation curing; this can be the result of chemical reactions during carbonation curing that mainly happens within the first 2 hours [35], however, the temperature growth depends on many factors such as CO_2 pressure, CO_2 concentration, preconditioning, humidity and concrete matrix content.

2.4.3 Chloride Induced Test

The effect of early carbonation curing on resistance to chloride-ion penetration was investigated by using the Rapid Chloride permeability Test (RCPT), RCP test measures the electrical conductivity of the concrete which depends on both chemistry of the pore solution and pore structure, however, the main criticisms of using this method are:

- The passed current is related to all ions in the pore solution, not just chloride ions.
- The high voltage applied to specimens can lead to an increase in temperature and then further increase in the charge passed [36].

According to Rostami and et al. [6], the carbonation cured specimens showed lower coulomb passing compare to steam cured specimens, which means that carbonation cured specimens are more resistant to chloride penetration than steam cured specimens. It may be the effect of lower initial (up to 6 hours) capillary suction of carbonated samples compare to steam cured samples [6], which this reduction of initial capillary suction can be a result of shrinkage of capillary tubes and connectivity lost in the pore space.

2.4.4 Change of pH Level

Using early carbonation treatment is not likely detrimental, since the value of pH in both, reference specimen (without carbonation curing) and carbonation curing, remains over 12 in the depth of more than 10 mm [6]. Figure 2.8 illustrates the difference of pH level in different depth respect to the curing method.

(2S) means 2 hours of steam curing,
(2C) means 2 hours of carbonation curing.

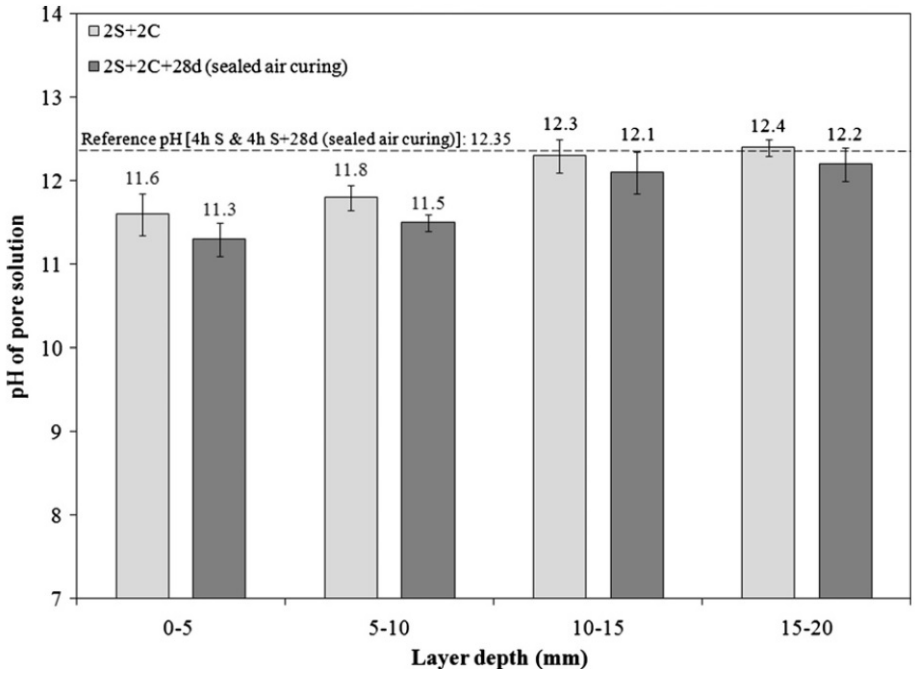

Figure 2.8: pH value in different layer depth respect to curing mechanism [6]

It can be concluded that the pH level of CO_2 cured specimens after 4 hours, satisfies the needed pH value, even in the outer layer.

2.4.5 Durability

Using carbonation curing of concrete elements can offer an improvement for durability performance. Some advantages of this curing method, found by previous studies, are listed below:

- The reduction of calcium hydroxide content in concrete samples, due to early carbonation, leads to better sulfate resistance [6].

- The early carbonation curing of concrete samples leads to a reduction in chloride-ion migration since hydroxyl ions are eliminated and calcium carbonate is precipitated within the surface layer [6]. The RCPT results regarding ion conductivity are described in section 2.4.3

- In addition to the aforementioned durability improvements, early carbonation curing shows better performance and resistance for concrete exposed to freeze-thaw cycles [6].

2.4.6 Preconditioning Effect (initial curing)

Preconditioning of concrete, right after casting, can have a significant effect on the reaction of CO_2 with cement minerals during carbonation curing, which leads to mechanical and chemical changes.

A study found that [7], concrete specimens which were preconditioned in fog room (wet environment) showed a slight increase in the temperature profile (from 20 °C to 30 °C after 15 minutes of CO_2 curing) during the curing process, thus; a slow reaction between CO_2 and cement clinker mineral in the 4 hours of CO_2 curing would happen, on the contrary; in dry preconditioning, the temperature increased significantly (from 20 °C to 58 °C after 15 minutes of CO_2 curing), thus, the reaction between CO_2 and cement clinker minerals at the beginning of the curing process happened very fast. Figure 2.9 illustrates the temperature profiles of specimens during carbonation curing with different preconditioning.

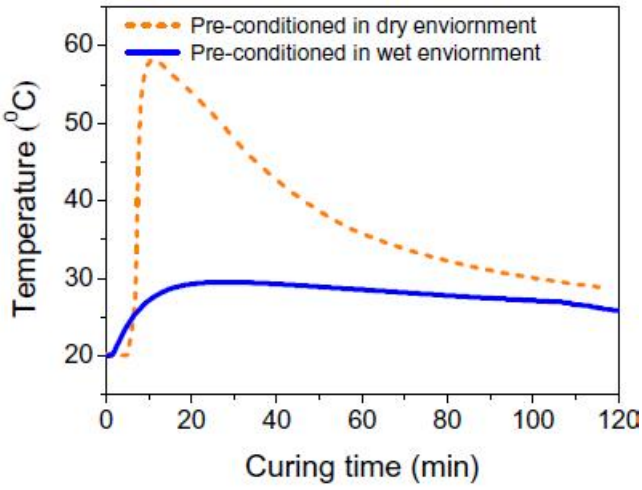

Figure 2.9: The temperature profiles during CO_2 curing for different preconditioning [7]

Another study indicated the effect of relative humidity, during the pre-curing time, on both compressive strength and CO_2 curing degree. It was shown that, the higher the relative humidity, the more CO_2 curing degree and the less the moisture loss during pre-curing [8]. The optimum moisture loss is around 4.5% for carbonation curing, as the moisture loss increased both strength and CO_2 uptake increased, however, as the moisture loss was greater than the optimum value, the strength decreased sharply [35]; this optimum value would be different for different matrix content. Besides, more moisture loss increases the possibility of having crack. More CO_2 curing degree would imply more compressive strength [8].
In conclusion, in order to get appropriate CO_2 curing degree and high compressive strength, 3 hours of pre-curing with RH of 60-70% and temperature of 25°C is needed [8].

2.4.7 Effect of CO_2 concentration

According to a study [7], the effect of different CO_2 concentration during carbonation curing on compressive strength was investigated. It indicated that, the higher CO_2 concentration would result in a higher CO_2 curing degree and higher compressive strength. Figure 2.10 illustrates the compressive strength with different CO_2 concentrations during the carbonation curing process.

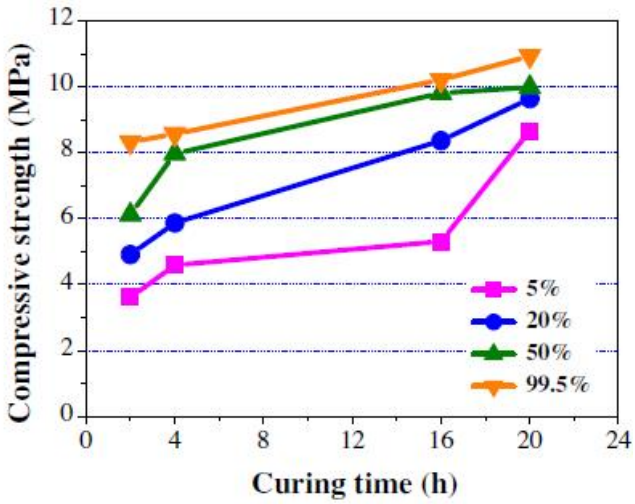

Figure 2.10: Compressive strength profile during CO_2 curing for different CO_2 concentrations [7]

2.4.8 Effect of CO_2 Pressure

One of the factors that can influence the carbonation curing is CO_2 pressure in the airtight chamber. The more CO_2 pressure results in the higher diffusion of carbon dioxide into the depth of the specimen, which means more carbonation curing degree, however, the relation between CO_2 pressure and CO_2-curing degree is not linear. A study showed that an increase in CO_2 pressure up to 0.2 MPa would significantly increase the CO_2-curing degree, however, this increase is slight for further pressure [8]. Figure 2.11 illustrates the effect of different CO_2 pressure on both CO_2-curing degree and compressive strength.
It is important to mention that the effect of CO_2 pressure would vary for specimens with different compositions and curing conditions.

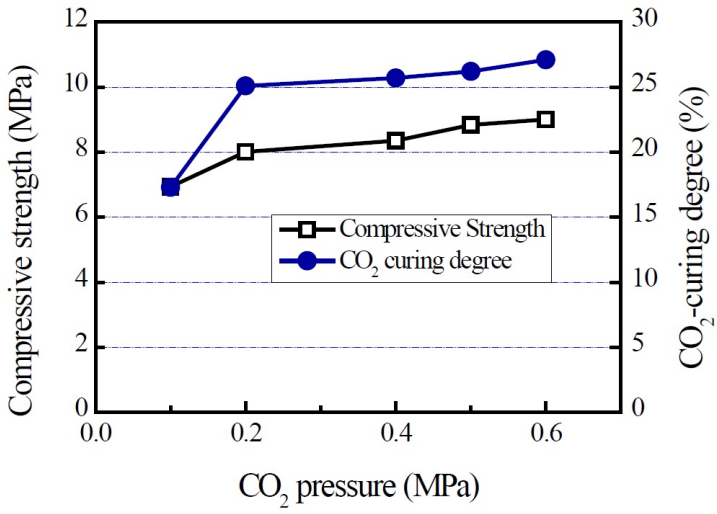

Figure 2.11: Effect of CO_2 pressure on CO_2-curing degree and compressive strength [8]

Chapter 3

Experimental Program

In this research, the effect of carbonation curing on cement paste and mortar with the different water-cement ratio in terms of mechanical strength (compressive strength), permeability (porosity, pH level), chemical changes (CO_2 uptake, degree of hydration) and the micro-structural changes is investigated with the purpose of increasing the knowledge of carbonation curing. The chapter is classified into sections that follow the logical order of performing the experimental program: The experimental procedure is illustrated in section 3.1. Section 3.2 is dedicated to materials. Section 3.3 is dedicated to specimens' preparation. The curing set-ups is described in section 3.4. Section 3.5 presents the different variety of experiments followed by the test set-up. An overview of chapter three is listed below:

- Chapter 3.1: Experimental Work Plan
- Chapter 3.2: Materials
- Chapter 3.3: Specimen's Preparation
- Chapter 3.4: Curing Procedure
- Chapter 3.5: Test Procedure

3.1 Experimental Work Plan

The experimental work plan for carbonation curing is illustrated in figure 3.1. The test is performed for two different cement-based materials (cement paste and mortar) with different water to cement ratio and CO_2 curing time, but the same curing procedure (see section 3.4). Each set of specimens cured with carbon dioxide are compared with a reference specimen, which is cured in the same pre-curing condition (5 hours in the climate chamber) and the same water to cement ratio. After 13 hours from casting, all specimens are places into the water for additional curing until 14 days. The compressive strength of specimens are tested and compared after one day (initial compressive strength) and 14 days from casting. Besides, the porosity test is started after seven days from casting. TGA, XRD tests are done after six days from casting. pH and SEM tests are done after 14 days from casting. Figure 3.2 illustrates the schematic of the whole experiment. Table 3.1 illustrates the number of specimens used for each test.

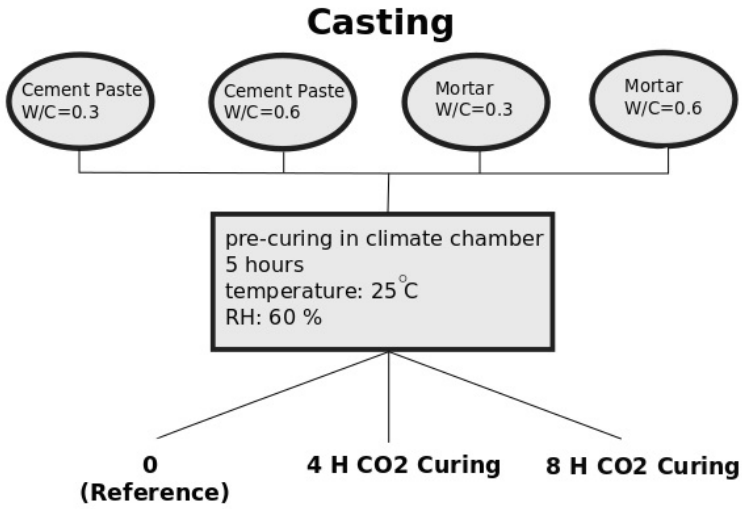

Figure 3.1: Experimental work plan for different curing condition

Table 3.1: Number of Specimens used for tests

Type of Test	Number of Specimens
Early compressive strength	3(40×50 mm) cubes
Compressive strength (14 Days)	3(40×50 mm) cubes
Porosity	1(50×50 mm) cube
pH level	Crushed samples
TGA	Crushed samples
SEM and XRD	Crushed samples

Note: Crushed and powder samples are used for SEM, TGA, XRD and pH level tests which are taken from used specimens of compressive strength test.

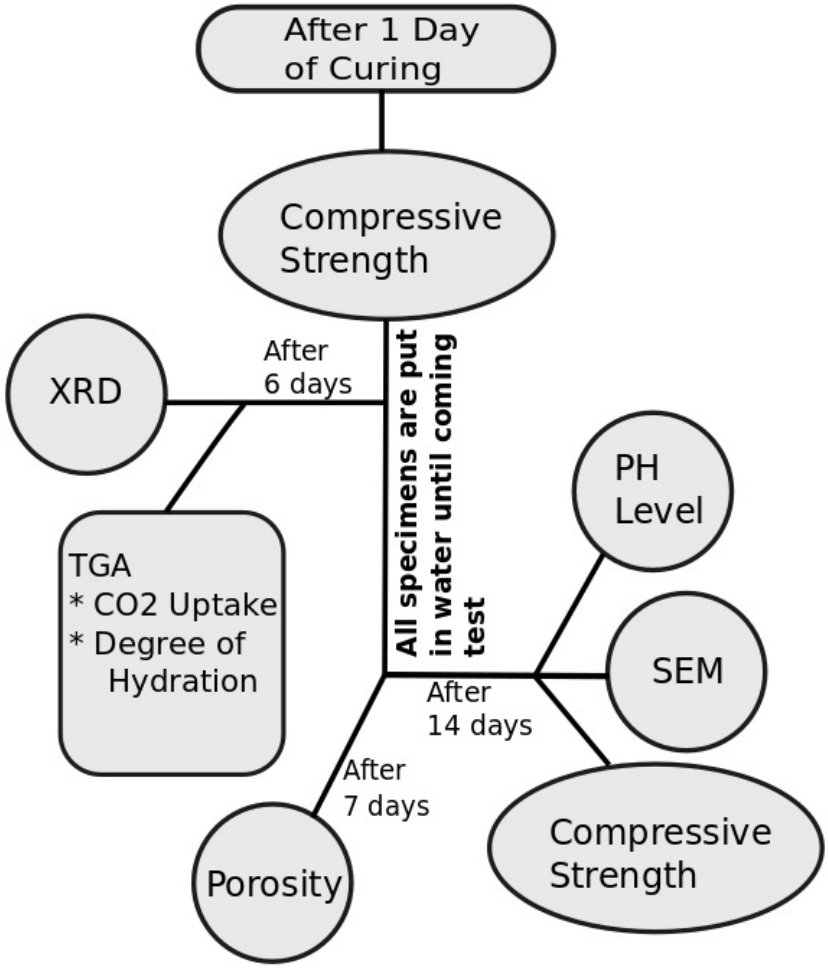

Figure 3.2: Schematic of whole experiment

3.2 Materials

In the following section, all the materials which are used in this experiment are described.

3.2.1 Portland Cement

Cement used for the experiment is provided by Norcem company in Norway. The cement is industrial (CEM I 52.5R). Norcem Industri is a cement, suitable for wintertime since it gains high early strength. The cement makes it possible to do concrete works in cold weather. All the requirements regarding the Portland cement, mentioned in the standard EN 197-1-CEM I 52.5R, are satisfied. Tables 3.2 and 3.3 show the chemical composition and physical properties of cement NORCEM INDUSTRI 52,5R.

Table 3.2: Chemical composition of NORCEM INDUSTRI 52,5R

CaO	SiO_2	MgO	SO_3	Na_2O	K_2O
62%	19.4%	2.5%	3.9%	0.5%	1.1%

Table 3.3: Some chemical and physical data of NORCEM INDUSTRI 52,5R

Fineness (Blaine)	547 m^2/kg
Tricalciumaluminate C_3A	7.6 %
Alkali	1.2 %
Mineral additives	3.7 %
Sulfate content (AS SO_3)	3.8 %
Chloride content	0.05 %
Specific weight	3.1 kg/dm^3

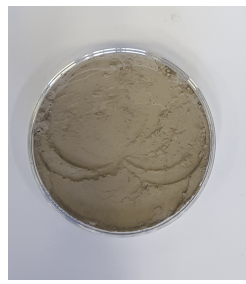

Figure 3.3: CEM I 52.5R

According to NS-EN 196-1:2016, the cement is kept in an airtight container to avoid exposure of air before mixing.

3.2.2 Sand

According to NS-EN 196-1:2016, CEN reference sand with specif particle size should be used to make mortar. Reference sand consists of rounded particles and has at least 98% silica content. The moisture content should be less than 0.2%. The Particle size distribution of the CEN reference sand is shown in table 3.4.

Table 3.4: Particle size distribution of the CEN Reference Sand

Square mesh size (mm)	2.00	1.60	1.00	0.50	0.16	0.08
Cumulative sieve residue (%)	0	7 ± 5	33 ± 5	67 ± 5	87 ± 5	99 ± 1

Since the CEN reference sand is not available in the laboratory, the aim is to use similar sand with a close value of particle distribution. The aggregates with the size range of 0-2 mm used in this research, are supplied by TØRRSAND in Norway. The cumulative mass retained curve is obtained by sieve analysis, in accordance with NS-EN 196-1:2016, shown in figure 3.4.

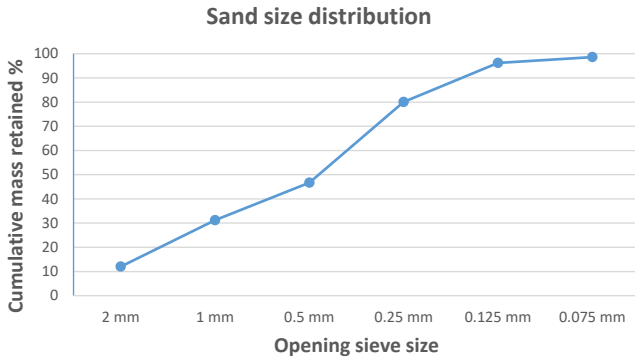

Figure 3.4: Cumulative mass retained (%) of used aggregate

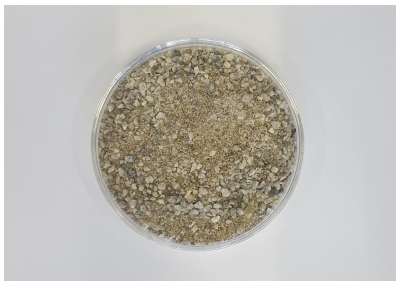

(a) Sand

(b) Sieving procedure

Figure 3.5: Sand and sieving procedure

Moisture in Sand

According to NS-EN 196-1:2016, the moisture content of CEN reference sand should be less than 0.2%. In this research, to have a similar moisture content of sand, they are dried at 105°C for 5 hours. By using the speedy moisture tester, the moisture in the aggregates is then calculated. This method is based on measuring the gas pressure generated by a reaction between the available moisture in aggregates and a pulverized calcium carbide reagent.

Method:

20g of the aggregates are needed to place in a vacuum container (figure 3.6) and then two scoops of reagent are added into the container's inverted cap to separate it from the aggregates sample. The cap is placed on the container on the horizontal position, then should be closed to be airtight. The container is shaken and turned 180 degrees for 20 seconds, then again shaken for another 20 seconds. The gauge underneath shows the percent of moisture by wet weight. It can be converted to percent of dry weight by using equation 3.1:

$$Moisture_{(Dry)}\% = \frac{Moisture_{(wet)}\% \times 100}{100 - Moisture_{(wet)}\%} \tag{3.1}$$

Figure 3.6: Speedy moisture test

By using the equation 3.1, The $moisture_{(dry)}$ is measured 0.11% which satisfies the requirement in NS-EN 196-1:2016 standard.

3.2.3 Water

Water is a key ingredient in the production of cement-based materials, however, since it has a small effect on the quality of specimens, little needs to be written about water quality. The most important factor regarding mixing water is an impurity, which can have a detrimental effect on concrete quality, setting time, drying shrinkage and durability.
The water used for the experiment is potable water. The quality of tap water used for

mixing is accepted. Twenty-four hours before mixing, the mixing water is tapped. The water container's temperature has kept constant at 20 °C.

3.2.4 Superplasticizer

Dynamon SX-N is a very efficient liquid superplasticising admixture, based on modified acrylic polymers. Superplasticiser is used to improve the workability and/or reduce the amount of water needed, yet retain the same workability. Lower water to cement ratio means higher mechanical strength, reduced permeability and increased durability. Dynamon SX-N is added in dosages between 0.4 and 2.0% of the amount of cement + fly ash + micro-silica. At least 80% of the mixing water should be added before Dynamon SX-N. Table 3.5 provides the technical data of the superplasticizer.

Table 3.5: Technical data of Dynamon SX-N

Appearance	Liquid
Color	yellowish brown
Viscosity	easy flowing; 30 $mPa.s$
Density (g/cm^3)	1.06 ± 0.02
pH	6.5 $\pm$ 1
Chloride content (%)	0.05
Alkali content (Na_2O-equivalents) (%)	2.0

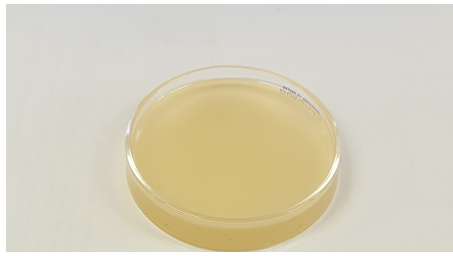

Figure 3.7: Dynamon SX-N superplasticizer

3.2.5 Carbon Dioxide Gas

The high-pressure carbon dioxide cylinder is provided from NIPPON GASES Company. The CO_2 regulator is used to control the pressure in order to have only the gas phase. The regulator then is linked by a hose to the airtight chamber for the carbonation curing process.

Physical and Chemical Properties of CO_2

Table 3.6 shows the information on the basic physical and chemical properties of CO_2.

Table 3.6: Information on basic physical and chemical properties of CO_2

Physical state at 20 °C/101.3 kPa	Gas
Color	Colorless
Odor	Odorless
PH	Not applicable for gases
Melting point/Freezing point	-78.5 °C at atmospheric pressure
Boiling point	-56.6 °C
Flammability	Nonflammable
Vapor pressure (20 °C)	57.3 bar
Relative density, gas (air=1)	1.52
Water solubility	2000 $mg/Liter$
Molar mass	44 g/mol

CO_2 Regulator

Like other kinds of pressurized gas cylinders, CO_2 cylinders, without dip tubes, must be used with a regulator to dispense gas so that the pressure can be reduced to a level appropriate for the intended purpose. The regulator should be specifically made for carbon cylinder to satisfy some requirements such as; inlet corrosion resistance, hand-adjustable pressure and inlet/outlet pressure gauge.

Figure 3.8: CO_2 cylinder regulator

Safety Measures While Using CO_2 Cylinder

Unlike simple asphyxiants, carbon dioxide gas has the ability to cause death even when normal oxygen levels (20%-20%) are maintained. 5% CO_2 has been found to act synergistically to increase the toxicity of certain other gases (CO, NO_2). Some remarkable safety measures are mentioned below:

- Adequate air ventilation.
- Opening the valve slowly to avoid pressure shock.
- Keep the cylinder below 50 °C.
- Wearing cold insulating gloves when using it.
- Use gas filters with a full face mask.
- Make sure to use proper regulator.
- Always secure the gas cylinder in an upright position.

3.3 Preparation of cement-based Specimens

In the following section, the preparation of two types of cement-based materials is described. The purpose of this research is the investigation of carbonation curing effect on cement paste and mortar. The effect of carbonation curing depends on some proportioning parameters such as; water to cement ratio and additives. In order to have a better understanding of the effect of carbonation curing on CO_2 uptake, based on the proportioning parameters, two different cement-based materials with different water-cement ratio are used.

3.3.1 Mix Design

According to the standard NS-EN 196-1:2016, the procedure of mix design is described and then adopted to the experiment. Tables 3.7 and 3.8 show the mix design of cement paste and cement mortar, respectively. According to NS-EN 196-1, the mass-ratio of sand to cement used is 3.

Previous studies have shown that specimens had to be designed with very low water to binder ratio in a range of 0.05 to 0.175 to achieve a high degree of CO_2 curing [37]. This will make the use of CO_2 curing method difficult for the use of full-scale industrial production. However; it was recently found that specimens with normal water to binder ratio could achieve acceptable CO_2 curing degree in the case of proper preconditioning in a dry environment, after they are molded, for a specific period [15, 35, 38, 39].
In this research, to understand the effect of water to cement ratio on carbonation curing, two different w/c ratio of 0.3 and 0.6 are used.

Table 3.7: Two different mixing design of cement paste

Batch number	Water-cement ratio	Cement quantity	Water quantity
1	0.3	1502 kg/m^3	450.6 kg/m^3
2	0.6	992 kg/m^3	595 kg/m^3

Table 3.8: Two different mixing design of cement mortar

Proportions of materials	Batch 1 (w/c 0.3)	Batch 2 (w/c 0.6)
Cement	442 kg/m^3	468 kg/m^3
Sand	1326 kg/m^3	1404 kg/m^3
Water	132.6 kg/m^3	280.8 kg/m^3
Superplasticizer	1.5 % Cement weight	-

- The cement, sand and water have a temperature of 20 ± 2 °C .
- All the materials are stored in a controlled laboratory environment with a temperature of 20 ± 2 °C. The cement is kept in a sealed and airtight container. The sand is kept in closed chambers to avoid reaching humidity and water.

3.3.2 Molds

Plastic cubic molds with dimensions of $50\ mm \times 50\ mm \times 50\ mm$ are used for specimens with porosity test and steel beam molds with dimensions of $40\ mm \times 160\ mm \times 40\ mm$ are used for specimens with compression test. According to NS-EN 12930-2:2019, the inner surface of the molds are covered with thin non-reactive oil to prevent the material from adhering to the mold.

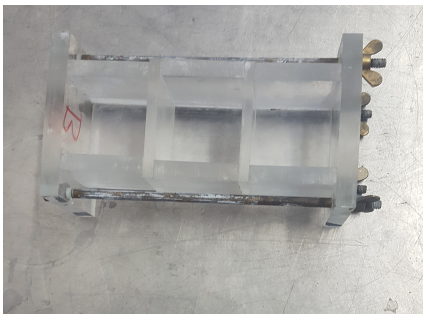

(a) Plastic cubic molds

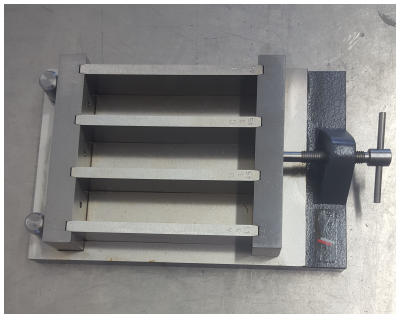

(b) Steel beam molds

Figure 3.9: Plastic cubic and steel beam molds

3.3.3 Mixing of Fresh Cement Paste and Mortar

All the material components are weighed up according to the mix design and keep in separate containers.
According to NS-EN 196-1:2016, the timing of the various mixing stages refers to the times at which mixer power is switched on/off and shall be maintained within ± 2 Sec. The mixing procedure of cement paste and mortar is illustrated in table 3.9 and table 3.10, respectively. Hobart Mixer with different mixing speeds described in table 3.11 is used.

Table 3.9: Procedure of mixing cement paste

Step	Time	Procedure
1	0	Adding cement and water to mixture
2	30 Sec	Mixing water and cement with low speed
3	30 Sec	Mixing with high speed
4	30 Sec	Stop mixer and remove material adhering to wall
5	60 Sec	Continue mixing

Table 3.10: Procedure of mixing cement mortar

Step	Time	Procedure
1	0	Adding cement and water to mixture
2	30 Sec	Mixing water and cement with low speed
3	30 Sec	Adding sand steadily during 30 sec
4	30 Sec	Mixing with high speed and adding superplasticizer
5	30 Sec	Stop mixer and remove mortar adhering to wall
6	60 Sec	Continue mixing

Table 3.11: Speed of mixer blade

	Rotation $[min^{-1}]$	Planetary movement $[min^{-1}]$
Low Speed =Hobart N-50 Low (136 RPM)	140 ± 5	62 ± 5
High Speed =Hobart N-50 Low (136 RPM)	285 ± 10	125 ± 10

(a) Hobart N-50 Mixer **(b)** Flat Beater

Figure 3.10: Hobart mixer

3.3.4 Molding and Compaction Procedure

According to NS-EN 196-1:2016, molding the specimens starts right after casting. As an alternative for jolting compaction, a vibration table is used. The condition and procedure of using the vibration table are listed below;

- The maximum load on the table (including molds) should be lower than 43 kg.

- Make sure that the lower surface of the molds base plate is clean.
- The total compaction duration is 120 seconds.
- Molds are filled within the first 45 seconds;
  - First 15 seconds, half of the mold depth is filled without switching off the vibration.
  - Let the table keep vibrating for another 15 seconds.
  - Add the next layer for another 15 seconds.

Figure 3.11: Vibration table

3.4 Curing

In this section, three curing processes are explained;

- Pre-carbonation curing including demolding
- Carbonation curing
- After carbonation curing

3.4.1 Pre-carbonation Curing

Pre-curing conditions, before starting carbonation curing, can have an effect on the amount of CO_2 diffusion through the concrete samples.
It has been found that a dry preconditioning before CO_2 curing is critical to achieve a high CO_2 curing degree [7]. Moreover; As it is described in section 2.4.6, there should be an optimum moisture loss to have the highest carbon dioxide uptake. It is suggested that the appropriate pre-carbonation curing is keeping the samples in an environment with RH of 60-70% for a couple of hours [8].

The best time to demold the specimens to start carbonation curing is based on two facts; when the specimens achieve initial setting time and when part of the water in pores are absorbed and reacted with cement. It has been shown that a decent CO_2 uptake happens when the specimen is demolded after 5 hours and started carbonation curing immediately [4].

In this research, after casting and filling the molds, all the specimens (cement paste and mortar) with different water to cement ratio are placed into the climate chamber (CTS climate chamber C-40/600) with a relative humidity of 60% and temperature of 25 °C for 5 hours and then are demolded right after. The reason behind 5 hours of initial curing is using industrial cement with earlier setting time and obtaining acceptable moisture loss, besides, after 5 hours, the specimens are hardened enough to be transported without any physical damage.

Figure 3.12: Climate chamber CTS C-40/600

Demolding

After 5 hours of initial curing in the climate chamber, the specimens are demolded carefully to avoid any physical damage. All the surfaces of specimens exposed to the oil are wiped with a clean towel to make sure any residual oil remained on the surfaces is removed. All the specimens are then marked based on the work plan, without damaging the surfaces.

3.4.2 CO_2 Curing Methodology

All the specimens are divided into two groups (reference group and carbonation group) in accordance with the type of sample (cement paste or mortar) and water to cement ratio. Reference specimens are placed in laboratory environment with RH of 45% and temperature of 20 ± 2 °C and impermeable plastic wrap is applied around them until the end of carbonation curing (figure 3.13a). The carbonation group is divided into two groups (cement paste and mortar) in order to be cured separately into the airtight chamber (figure 3.13b). The chamber is placed in laboratory environment with a temperature of 20 ± 2 °C.

(a) Plastic wrap around reference specimens

(b) Two separated carbonation groups

Figure 3.13: Specimens after demolding

In order to have the equal condition for all the specimens inside the chamber, specimens are placed on top of a metal net sheets with a thickness of 1 cm to allow the bottom side of the specimens to be exposed to CO_2 gas, in addition, one more metal net sheet is placed on the top of the specimens to put the rest of the specimens on them (figure 3.15). To control the CO_2 concentration and pressure, inlet and outlet valves are fixed to the chamber. The value of relative humidity and temperature, inside the chamber, are measured every 5 minutes during the whole process by using Temperature and Humidity Data Logger-USB recorder (figure 3.14). The inlet valve is connected to the regulator to stabilize and control the gas pressure inside the chamber.

Figure 3.14: Temperature and Humidity Data Logger

Figure 3.15: Inside the airtight chamber

An increase in CO_2 concentration and pressure would increase CO_2 curing degree and compressive strength [7]. Since CO_2 concentration and the gas pressure in the chamber would drop as a result of CO_2 absorption of specimens, the general trend is keeping both the high CO_2 concentration and pressure of 0.6 MPa constant over time of carbonation curing. To make sure to have a high concentration of CO_2 gas ($\geq 99.0\%$), a vacuum machine is used to remove the air inside the chamber completely before injecting CO_2 gas. Then, CO_2 gas is injected until the pressure gauge shows 6 bars (0.6 MPa), the chamber is kept pressurized with CO_2 gas at the pressure of 0.6 MPa for the whole carbonation curing time.
In order to measure the CO_2 uptake in the carbonation process, a digital scale is placed under the airtight chamber to record the weight. At the beginning of the process, the chamber is vacuumed from the air and then the scale is set to zero, by injecting the CO_2 gas, it records the increased mass, then at the end of the carbonation process (for each four and eight hours of curing) the airtight chamber is again vacuumed and the value that scale shows is the amount of CO_2 reacted with cement phase.
The whole carbonation curing framework is illustrated in figure 3.16.

Figure 3.16: Carbonation curing framework

Another purpose of this study is to compare the effect of carbonation curing time on CO_2 uptake, mechanical and chemical changes. So, 4 and 8 hours of carbonation curing are selected based on industrial capabilities and acceptance. After 4 hours of carbonation curing, the set of specimens which are supposed to be cured for 4 hours, are taken out from the chamber and sprayed with water to compensate the moisture loss during carbonation curing and then placed in the laboratory environment and plastic wrap is applied around them to make an equal condition with their references. Afterward, the chamber is again closed, vacuumed and pressurized (0.6 MPa) with CO_2 gas and carbonation curing will continue for other designated curing time (8 hours) and the process of spraying water and plastic wrap is applied in the same way as described above. A schematic of the carbonation framework is shown in figure 3.17.

3.4.3 After Carbonation Curing (Water Curing)

After carbonation curing, all the specimens (Cement paste and mortar, including their references) are placed in water at a temperature of 20 ± 2 °C for the rest of the curing in accordance with NS-EN 196-1:2016.

Figure 3.17: 3D schematic of carbonation framework

3.4.4 An Overview of Curing Procedure

To have a better understanding of the curing procedure, table 3.12 is made to illustrate the number of specimens used for each curing time and curing method.

Table 3.12: An overview of marked specimens based on the curing procedure and time

Specimen groups	Pre-curing	Carbonation curing	After CO_2 curing
Cement paste ↓ Reference (R_P)	5 hours in climate chamber 25 °C and RH 60%	0	Immersed in water
4 Hours of CO_2 curing (4_P)		4 Hours	
8 Hours of CO_2 curing (8_P)		8 Hours	
Cement mortar ↓ Reference (R_M)	5 hours in climate chamber 25 °C and RH 60%	0	
4 Hours of CO_2 curing (4_M)		4 Hours	
8 Hours of CO_2 curing (8_M)		8 Hours	

3.5 Tests Procedure

The following section is dedicated to explaining the procedure of variety of experiments which are listed below:

- Density of fresh mortar and cement paste
- Air content of fresh mortar
- Slump measurement
- Porosity and hardened density
- Compressive strength
- Microstructure-Scanning Electron Microscopy (SEM)
- X-Ray diffraction test (XRD)
- Thermogravimetric analysis
- CO_2 uptake
- Degree of hydration
- pH level

3.5.1 Density of Fresh Cement Paste and Mortar

According to NS-EN 1015-7, the density of fresh mortar is determined and the procedure is adopted for the cement paste.

Procedure:

Clean the density container and dampen with a moist cloth prior to starting the test. Weigh the density container to determine its mass (M_1) to the nearest 0.01 kg. The density container is filled in two layers and the thickness of each layer is around half of the height of the container. Each layer is compacted by hand with a compacting rod to achieve full compaction. Ensuring that each layer is subjected to number of 15 strokes and compacting rod does not forcibly strike the bottom of the container when compacting the first layer, nor penetrate significantly in any previous layer. The top layer is smoothed and leveled with the top of the density container. Weigh the density container with its contents to determine its mass (M_2). The density of fresh material is then calculated by the following equation 3.2:

$$D = \frac{M_2 - M_1}{V} \tag{3.2}$$

Where:
D is the density of fresh material in kg/m^3
V is the volume of the density container (1 L)

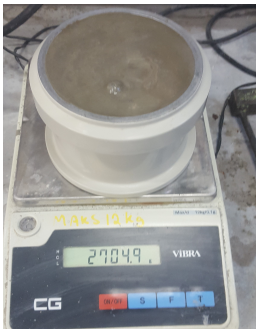

Figure 3.18: Density container filled with fresh cement paste

3.5.2 Determination of Air Content of Mortar

According to NS-EN 1015-7: *Determination of air content of fresh mortar*, the air content of fresh mortar can be determined by using air entrainment meter.

Procedure:
Clean the container and dampen with a moist cloth prior to starting the test. The container is filled in two layers and the thickness of each layer is around half of the height of the container. Each layer is compacted by hand with a compacting rod to achieve full compaction. Ensuring that each layer is subjected to number of 15 strokes and compacting rod does not forcibly strike the bottom of the container when compacting the first layer, nor penetrate significantly in any previous layer. The top layer is smoothed and leveled with the top of the container. Clean the bucket edge with sponge or similar. Place the cap on the bucket and lock it with the quick-release clips. Open both valves and fill it with water through one of the valves until water comes out from another valve. Unscrew the air pump handle and Pump up the pressure until the pressure gauge (clockwise) passes the red alignment mark. Close both valves again and depressurize the container and read the value from the pressure gauge.

Figure 3.19: Mortar air entrainment meter

3.5.3 Slump Measurement

The workability of fresh mortar can be measured by slump measurement in accordance with NS-EN 1015-3:1999+A1:2004.

Procedure:

The cone-shaped mold with dimensions of 100 mm at bottom, 70 mm at top and 60 mm height with a volume of 0.344 liters is used. The cone mold is moistened before using it. Fresh material is filled in three layers. Each layer is compacted by hand with a compacting rod to achieve full compaction. Ensuring that each layer is subjected to number of 15 strokes and compacting rod does not forcibly strike the bottom of the container when compacting the first layer, nor penetrate significantly in any previous layer. The top layer is smoothed and leveled with the top of the cone. The mold is raised vertically in a smooth manner over a five seconds period to allow fresh material flow freely. The vertical displacement of the surface of the free fresh material is measured with respect to the crone's height. As an example, figure 3.20 shows the slump test for cement paste.

Figure 3.20: Slump test for cement mortar (W/C=0.3)

3.5.4 Porosity and Hardened Density

According to publication 14-637 The Norwegian Public Roads Administration, the porosity of hardened concrete is measured by limited PF method. The limited procedure involves only the determination of porosity of specimens based on its density without considering the suction speed value. This method is adopted for hardened mortar and cement paste specimens. The specimens used in this test have dimensions of $50\ mm \times 50\ mm \times 50\ mm$.

The procedure is described step by step:

- According to the test, the specimens should have a volume of 100-150 cm^3 and a thickness of not more than 50 mm. The cubic samples satisfy the requirements.

- The specimens are dried in an oven at a temperature of 105 °C for seven days (the weight loss is less than 0.01% per hour), which is followed by a minimum of 2 hours of cooling at room temperature of 25 °C.
- Specimens are then weighed by a digital scale (g_1).
- Specimens are placed in a water container, totally immersed in water, for 7 days. Specimens are then taken out from the water and any surface water is removed by a damp cloth, then they are weighted in the air (g_2) and water (g_3) (Figure 3.21a).
- The specimens are immersed in water and placed in a pressure tank at 50 atm for at least one day. In order to prevent the water from being squeezed out of the specimens, the specimens are weighted immediately after taking out from the pressure tank (g_4) (Figure 3.21b).

Porosity and hardened density are determined by using the following equations 3.13:

Table 3.13: Porosity and density equations

Sample volume: $V\ (m^3)$	$= g_3/\rho_w$
Normal density: $\rho\ (kg/m^3)$	$= g_2/V$
Dry density: $\rho_1\ (kg/m^3)$	$= g_1/V$
Solid density: $\rho_{fs}\ (kg/m^3)$	$= \frac{g_1}{V - \frac{g_4 - g_1}{\rho_w}}$
Suction porosity Vol%: P_s	$= \frac{g_2 - g_1}{V \times \rho_w}$
Macro porosity Vol%: P_m	$= \frac{g_4 - g_2}{V \times \rho_w}$
Total Porosity Vol%: P_1	$= P_s + P_m$
Water density: $\rho_w\ (kg/m^3)$	$= 1000$

The pore system can have a great effect on CO_2 uptake during carbonation curing. In general, porosity can be defined as the internal volume that can be filled with water. The reaction of water and cement causes a reduction in the volume and the entire volume change can be assigned to water, which means that "the chemically bound water has lost 25.4% of its volume before hydration (chemical shrinkage)" [22]. This volume change may cause self-desiccation since some pores would be partially emptied and water can be sucked during exposure to it (capillary force). Self-desiccation causes RH reduction when it is not exposed to water during curing time. Besides, a finer pore system can be a result of less w/c ratio that can produce lower relative humidity since the finer the pores, the more the tension in the water.
Gel and capillary pores, which can suck water directly, make suction porosity; gel pores (size around $0.002\ \mu m$) are the space between the solid parts of C-S-H gel phase which grows from the cement particles and capillary pores (size around 4 to $1000\ nm$) are some parts of the volume (water-filled volume) between the cement particles that did not fill up with hydration products [22]. The capillary porosity increases by increasing w/c ratio, and

gel porosity is related to the amount of cement that is reacted.
Macro pores (also called air pores) are generally larger than a few micro-meter. They are created as a result of mixing fresh concrete and can be there even after setting. These pores can only be filled with water at over-pressure [22]. The sum of macro porosity and suction porosity is considered as total porosity.

Normal density is considered as the density of specimen, including the water inside the pores. The dry density is the density of specimen without any residual water in pores. Solid density is considered as the density of specimen without including the pores volume.

(a) Weigh in water

(b) Pressure tank (50 bar)

Figure 3.21: Porosity, weigh in water and pressure tank

3.5.5 Compressive Strength

Compressive strength of specimens is measured in accordance with NS-EN 196-1:2016 with some modifications, which are described below.

Procedure:

Based on the curing time of each set of specimens, one-third of the prism, which is already cut by cutting machine (Brillant 285, figure 3.22a) with the dimensions of $40\ mm \times 40\ mm \times 53\ mm$, is arranged in the comrpressive testing jig. The two plates on top and down of the jig (ELE International) have the dimensions of $50\ mm \times 50\ mm$. As figure 3.22b shows, this means that the back face of the jig' plate overhangs the sample by $10\ mm$. The modifications are made in the load rate of the compression machine, which are listed below;

- Type of compressive testing machine: Toni Technik 1142

- Type of compressive testing jig: ELE International
- Load capacity of machine: 3000 kN
- Load capacity of compressive testing jig: 250 kN
- Constant loading rate for mortar: 320 N/s
- Constant loading rate for cement paste: 500 N/s

(a) Cutting machine Brillant 285 **(b)** Compressive machine including jig

Figure 3.22: Cutting and compression machine

The compressive strength is calculated according to NS-EN 196-1:2016:

$$F_c = \frac{F}{A_c} \tag{3.3}$$

Where:
F_c is the compressive strength (MPa).
F is the maximum load at failure (N).
A_c is the cross-sectional area of the specimen on which the force acts (2000 mm^2).

The compressive strength test is conducted after two periods, one and fourteen days from casting. In each of those periods, three specimens are selected and tested from each batch and group of curing procedures. The average of three compressive strength for each group is calculated. According to NS-EN 196-1:2016, the arithmetic average of three individual results should be expressed to the nearest 0.1 MPa.

3.5.6 Preparation of Powder Sample

This section is dedicated to the preparation of powder sample for the following tests (X-Ray diffraction test, thermogravimetric test and pH level test). Crushed samples, after compression test, are taken and used to make powder. First, they are dried for five hours at a temperature of 90 °C in the oven, then the jaw crusher machine (Retsch BB200) is used to make the sample in small pieces (figure 3.23a). The small pieces are then filled in a disc mill machine (Retsch DM 200) to make them powder (figure 3.23b). Sieve size 63 μm is used to get very fine particles out of it (figure 3.23c). Each powder sample from each set of batch and curing procedure is kept separately in an airtight container to avoid air moisture from them until the test is carried on. It is important to mention that, the way of making powder is in such that the whole part of the cubic sample, layer by layer, is distributed roughly in the powder and the heat does not generate during the process. Besides, all the equipment is cleaned after each process of making a powder sample.

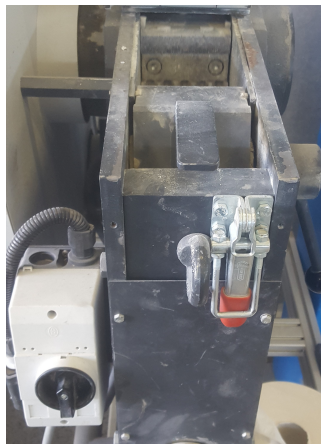

(a) Jaw crusher machine

(b) Disc mill machine

(c) 63 μm sieve size

Figure 3.23: Procedure of making powder out of cubic specimens

3.5.7 Micro-structure-Scanning Electron Microscopy (SEM)

Scanning Electron Microscopy (SEM) creates a digital image of the micro-structure by scanning the surface with a focused beam of electrons. The electron gun shoots a focused beam of electrons, the beam hits the surface of the sample and penetrates to the depth of a few microns, depending on the accelerating voltage and the density of the sample. The atoms in the sample are interacted by electrons, creating different signals like; secondary electrons (SE), backscattered electrons (BSE), X-ray and light (cathodoluminescence)(CL), figure 3.24a illustrates the different types of signals used by an SEM. The emitted signals from this are then caught with some different detectors in the machine. For imaging with a resolution of below 10 nm, the SE and CL are used. X-ray is used to detect chemical element composition by Energy Dispersive X-ray Detector (EDS), the characteristic X-ray is emitted as a result of electrons which are knocked out from their original position in the atom by using a high-energy beam of particles [40]. In this process, an electron from a higher-energy orbital drops down to substitute the vacancy that is left by the knocked-out electron, as a consequence of this substitution, the electron releases energy as a characteristic X-ray. Schematics of Energy Dispersive X-ray are shown in figures 3.25. Figure 3.24b shows a schematic representation of the basic SEM components. Lenses are used to control the path of the electrons.

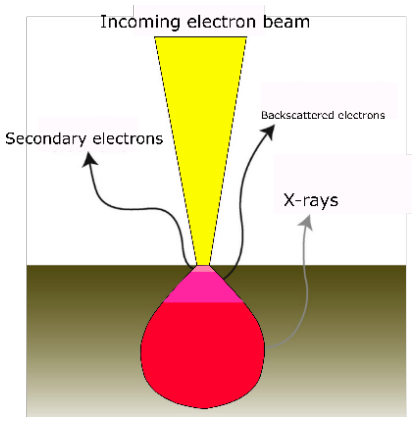

(a) Different types of signals used by SEM.

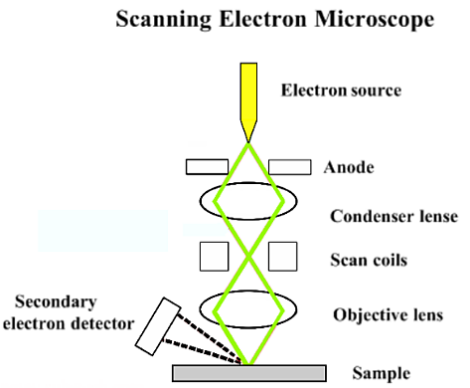

(b) Schematic of the basic SEM components.

Figure 3.24: Basic components of SEM and different types of signals [9]

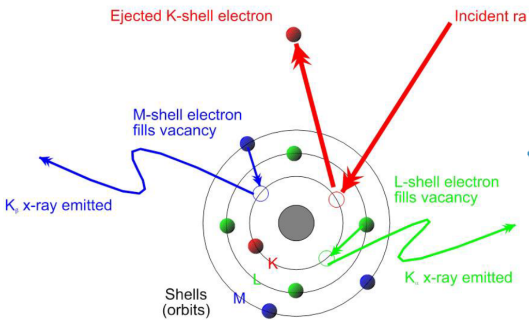

(a) Characteristic X-ray [41]

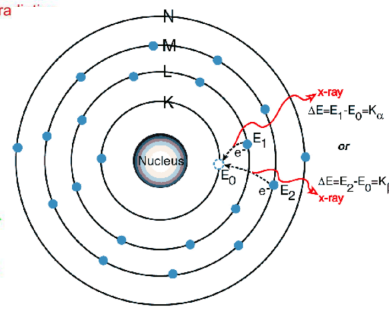

(b) X-ray emission and law of conservation of energy law [42]

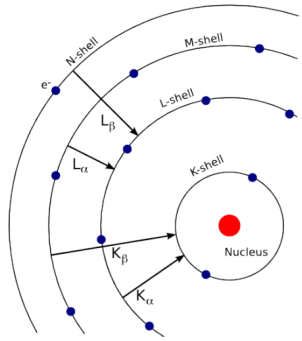

(c) Higher energy electrons drops down to fill the vacant position [43]

Figure 3.25: Schematics of Characteristic X-ray conservation of energy and electron dislodging

SEM Sample Preparation

The purpose of the sample preparation is to achieve a high-quality microscopic image without the presence of electric charge accumulation that can make noise, which can be seen white spots in the case of having electric charge accumulation. Preparation also protects the sample against contamination and vibration.

Small samples, in the range of $10\ mm \times 10\ mm$, are taken from the inner part of the specimens (these specimens are which that already used for compressive strength test). The crushed samples are then placed in the oven with a temperature of 85°C for five hours to lose its moisture. Then, they are placed in a small disc with a diameter of $10\ mm$ with conductive carbon tape. The purpose of using conductive carbon tape is to conduct the electric current away from the sample since the surface of the sample can also be accumulated by electric current. Each of the samples is coated with palladium in order to conduct the electric current away. In order to cover the samples with palladium, they are placed in a vacuum chamber with 0.07 $mbar$ pressure and start covering for 2.5 minutes. Figures 3.26a and 3.26b and 3.26c illustrate the process of palladium covering.

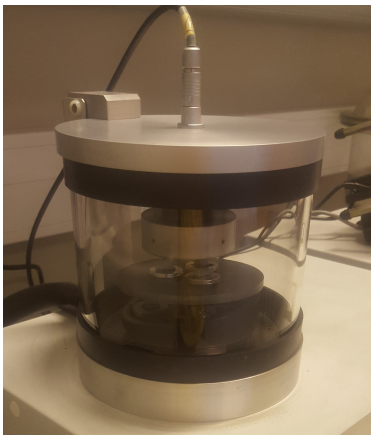

(a) Vacuum chamber

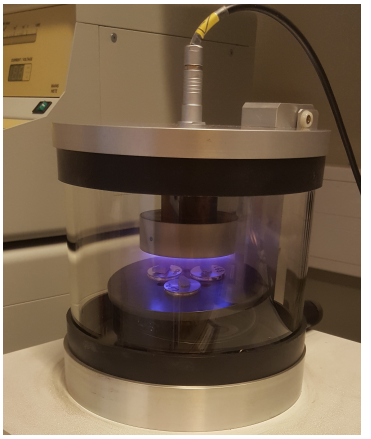

(b) Coating procedure

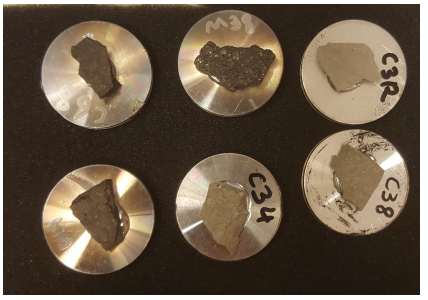

(c) Dark samples are coated

Figure 3.26: Process of palladium covering in vacuum chamber

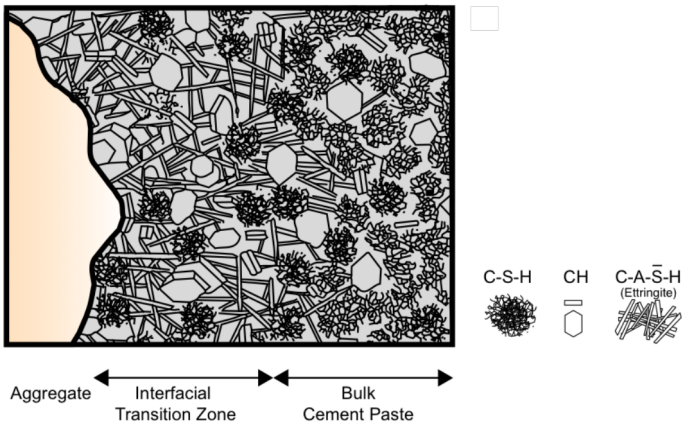

Figure 3.27: Microstructure – Interfacial Transition Zone and Bulk Cement Paste [10]

SEM Analysis Framework

In order to compare the SEM images for different samples, all the samples from different batches are taken after 14 days of curing. As figure 3.27 illustrates, both the bulk cement paste and the interfacial transition zone are analyzed for each sample. To have a better understanding of micro-structure of the samples, several images with different magnifications and the same scan speed of six are taken for each sample. Samples are tested and analyzed with Zeiss Supra 35VP Scanning Electron Microscope, shown in figure 3.28.

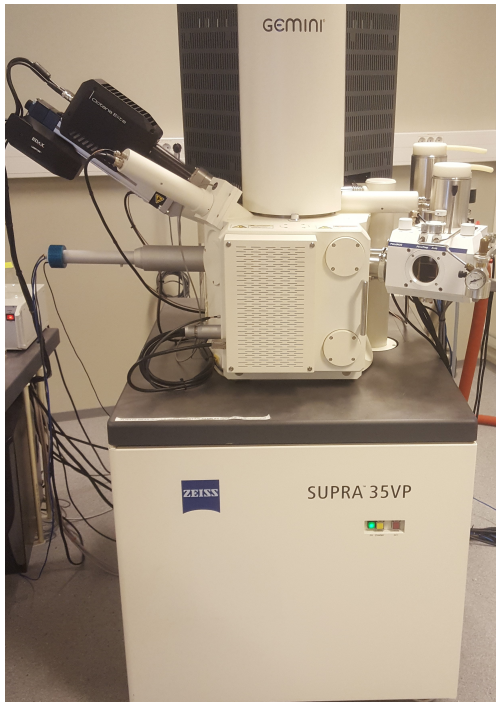

Figure 3.28: Zeiss Supra 35VP Scanning Electron Microscope

3.5.8 X-Ray Diffraction Test

X-ray diffraction is a technique to detect the crystal structures of an element. Cathode ray tube generates X-rays that are filtered to make monochromatic radiation, collimated to focus and directed toward the sample. When the X-ray beams interact with the sample, it produces constructive interference and diffracted X-ray, this happens if the conditions satisfy Bragg's Law ($n\lambda = 2d.\sin\theta$) which relates to the wavelength of electromagnetic radiation to the diffraction angle and the lattice spacing in a crystalline sample, then the diffracted X-rays can be detected and analyzed by using a database with a software. When the sample is scanned through a range of 2θ angles, then all the possible diffracted directions of the lattice can be obtained (because of the random orientation of the powdered

material). When the diffraction peaks convert to d-spacing[1], it allows to identify the mineral since each mineral has its own unique d-spacing. This identification achieves by comparing of d-spacing with standard reference patterns. Figure 3.29 illustrates a schematic of basic elements in X-ray diffraction test.

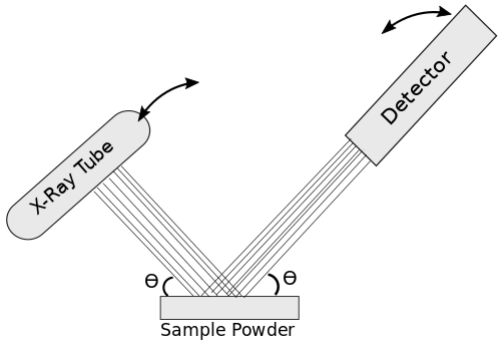

Figure 3.29: Basic elements in X-ray diffraction test

X-ray diffractometer consists of three basic elements: X-ray tube, sample holder and X-ray detector. X-rays are generated in a cathode ray tube by heating a filament to produce electrons, then the electrons are accelerated and bombarded toward the target in the sample by applying specific voltage. When the electrons have enough energy to dislodge inner shell electrons of the target material, characteristic X-ray spectra are produced. These X-ray spectra consist of several components with different wavelength, which the most common components are κ_α and κ_β. X-rays are collimated and directed towards the sample. As the detector and sample rotate, the intensity of the reflected X-ray is recorded. The detector processes this reflected X-ray signal and converts it to a count rate, which can be shown on the monitor. The X-ray diffractometer's geometry is such that the sample rotates in the path of the collimated X-ray beam at an angle of θ while the X-ray detector is mounted on an arm to collect the diffracted X-ray and rotates at an angle of 2θ.

In this test, the aim is to detect higher peaks of calcium carbonate crystals ($CaCO_3$, which consists of three different polymorphs: calcite[2], aragonite[3] and vaterite[4]) in CO_2 cured specimens compared to their reference. In addition to calcium carbonate crystals, tricalcium silicate (C_3S or Alite), dicalcium silicate (C_2S or Larnite/Belite), calcium hydroxide ($Ca(OH)_2$ or portlandite), ettringite ($Ca_6Al_2(SO_4)_3(OH)_{12} \cdot 26\,H_2O$), Albite ($NaAlSi_3O_8$) and quartz ($SiO_2$) are compared. The X-Ray instrument used in this

[1]Distance between planes of atoms that give rise to diffraction peaks, planes of atoms can be referred to a 3D coordinate system that can be described as a direction within the crystal.

[2]Calcite is a carbonate mineral and the most stable polymorph of calcium carbonate and crystal system of calcite is trigonal.

[3]aragonite are polymorphs of calcium carbonate but less stable than calcite and crystal system of aragonite is orthorhombic.

[4]vaterite is a carbonate mineral and less stable than calcite and aragonite polymorph of calcium carbonate. It has a higher solubility than either of these phases. Therefore, once vaterite is exposed to water, it converts to calcite.

research is Bruker D8 Advance Eco (figure 3.30) with Cu tube, $40kV$ and $25mA$. The 2θ angle is selected between a range of 5-100 degrees with a step size of 0.02 degrees and a step time of 0.5 seconds. This means that the X-ray beams direct toward the sample for 0.5 seconds from 5 degrees to 100 degrees in each step size of 0.02 degrees.

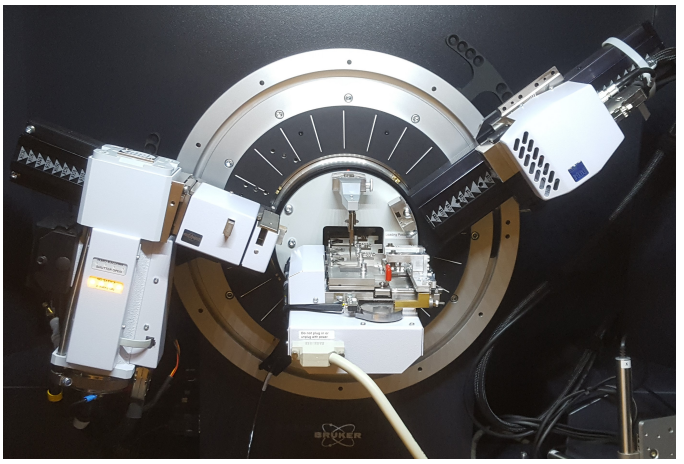

Figure 3.30: Bruker D8 Advance Eco, X-ray diffraction

Sample Preparation

After six days from casting, almost 2 grams of ground particles from each set of specimens are milled with mortar and pestle to get very fine powder and filled in the sample holder. Each test set-up takes 1 hour; hence, the whole test needs two days to be completed. Figure 3.31 shows sample preparation and installation.

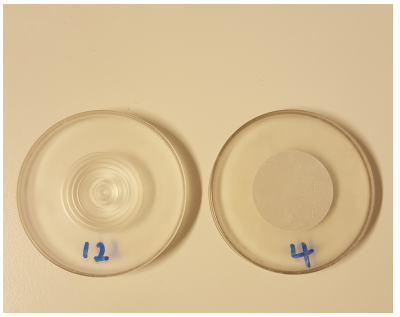

Figure 3.31: Sample holder and installation

3.5.9 Thermogravimetric Analysis (TGA)

Thermogravimetric analysis is a method of thermal analysis, performed to indicate the mineralogical changes and thermal decomposition in a sample. TGA is a technique of monitoring the mass of a substance as a function of temperature; the mass of the sample is measured over time as the temperature increases.

Procedure:

The proposed method of TGA measures an accurate quantitative profile expressed as the amounts of chemical phases in the specimen. After six days of curing, the specimens from different curing procedure, that are used for the compressive strength test, are selected for making the sample powder (see section 3.5.6) and passed from sieve size of 63 micro-meter, make sure that the powder samples should not contain coarse aggregates.
Before the TGA test, the sample powder for each specimen needs to be dried for 30 minutes in an oven at a temperature of 105 °C. Then the samples are preserved in airtight plastic bags while waiting to carry out the tests (figure 3.32).

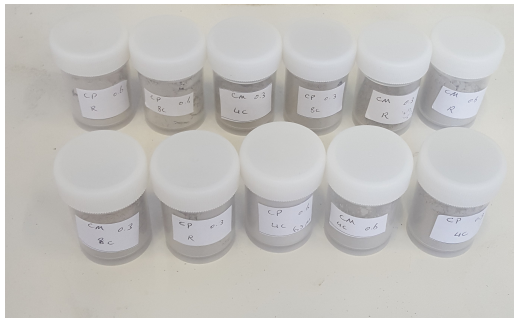

Figure 3.32: Powder samples in airtight containers

As figure 3.33 shows, the TGA measuring cup (crucible) is filled up to around 40 mg of the sample powder. The crucible is closed with a lid and placed into the TG machine (The machine model is TGA/DSC 3+ Mettler-Toledo with the accuracy of 0.1 micro-gram). Before conducting any analysis, a zero measurement with an empty crucible is made and the weight profile of an empty crucible will be subtracted automatically so that the measurement will be made only for the material in the crucible, this data (zero measurement) is used for every analysis. The sample starts to be heated from room temperature (25°C) up to 1000 °C with a rate of 20 K/min. The test is conducted under the protection of nitrogen gas. Each phase (including the hydrates) is characterized by its own temperature range of decomposition and specific mass loss; for instance, loss of water is related to portlandite and loss of CO_2 is related to calcium carbonate. The test takes approximately 1 hour to reach the desired temperature, then the system starts cooling down and the crucible can be taken out in order to be cleaned and used for the next sample.

(a) TGA/DSC 3+ Mettler-Toledo **(b)** crucible of TG filled with powder

Figure 3.33: TGA instrument

3.5.10 CO_2 Uptake (Using TG-DTG Analysis)

Measuring the degree of carbonation and the ability of cement-based material to capture carbon is called carbon dioxide uptake. A higher carbon dioxide uptake means lower carbon footprint of concrete [44]. The CO_2 uptake of specimens for each set of curing time is measured right after 6 days of curing. The calculation was based on TG-DTG (derivative thermo-gravimetry) analysis. Considering that the mass loss between 500 and 1000°C, represents the decomposition of $CaCO_3$ as a result of CO_2 loss. The difference between CO_2 loss% in carbonated curing sample (M) and normal air curing sample (N) is considered CO_2 uptake [45–47]. The equation 3.4 expresses below:

$$CO_2 \text{ uptake}\% = M_{\text{mass loss at 500-1000 °C}} - N_{\text{mass loss at 500-1000 °C}} \tag{3.4}$$

Mass Loss Principles According to TG-DTG Curves

According to the TG mass loss curve:

- The mass loss between 105 °C and 350 °C represents the mass loss of H_2O due to the dehydration of C-S-H gel, aluminate hydrate and ferro-aluminate hydrate.
- The mass loss between 350 °C and 500 °C corresponds to the dehydration of $Ca(OH)_2$.
- The mass loss between 500 °C and 1000 °C is due to the decarbonation of $CaCO_3$ [5].

For example, The degree of subsequent hydration after carbonation curing can be estimated by the mass loss, which is related to the decomposition of $Ca(OH)_2$, between the

temperature range of 350 °C and 500 °C [48].

All the decomposition temperature ranges, which mentioned above, are based on the hypothesis and there is no specific temperature to explain an accurate decomposition temperature. According to Ramachandran et al. [46], the decomposition temperature ranges are described with more details;

- Evaporation of water and decomposition of poorly formed C-S-H gel, happen below 105 °C.
- Loss of bound water in low temperature for C-S-H gel and ettringite[1] happens between 105 °C and 200 °C.
- Mass loss between 200 °C and 420 °C represents the decomposition of bound water in well-formed hydration products, including C-S-H gel and C-A-H (Calcium Aluminate Hydrate).
- Mass loss between 420 °C and 470 °C represents the decomposition of bound water in calcium hydroxide ($Ca(OH)_2$).
- Mass loss between 420 °C and 680 °C represents the decomposition of poorly crystalline calcium carbonates ($CaCO_3$) designated by aragonite and vaterite.
- Mass loss between 680 °C and 950 °C represents the decomposition of the well crystalline calcite.

3.5.11 Determination of Hydration Degree

Thermogravimetric analysis is an effective way for the evaluation of hydration degree. In this research, the methodology proposed by Bhatty[49] is investigated. Different regions of dehydration (Ldh), dehydroxylation[2] (Ldx) and decarbonation (Ldc) are defined based on the decomposition of hydrated compounds (mass loss%) in their temperature range, presented in the table 3.14 [49], although different decomposition temperature ranges are defined in section 3.5.10, it is decided to follow the Bhatty's methodology to determine hydration degree.

Table 3.14: Bhatty's temperature ranges for different decomposition regions

Region	Temperature range (°C)
Ldx	440-580
Ldc	580-1000
Ldh	105-440

By using equations 3.5 and 3.6, hydration degree can be determined [49].

$$W_{(B)} = Ldh + Ldx + 0.41.Ldc \tag{3.5}$$

[1] Ettringite is formed as the result of the reaction between calcium aluminate and calcium sulfate in hydrated portland cement.

[2] Decomposition of $Ca(OH)_2$

$$\alpha = \frac{W_{(B)}}{0.24} \tag{3.6}$$

Where;
α is the hydration degree in percentage.
The value of 0.41 is equivalent to dividing the molecular weight of H_2O to CO_2 [50]. The value of 0.24 in equation 3.6, corresponds to the maximum chemically bound water, which is required to hydrate the cement.

3.5.12 pH Level Measurement

The pH of the cement-based materials is measured by using digital pH probe meter (figure 3.34) in accordance with ASTM C 25 (Standard Test Methods for Chemical Analysis of Limestone, Quicklime, and Hydrated Lime [51]). The procedure is described below step by step;

Procedure:

- Using 14 days crushed samples from compressive strength test and make them powder with the procedure described in section 3.5.6.
- Calibrating the pH probe using appropriate buffer solutions.
- Mixing the sample powder with 10 mL of fresh distilled water in plastic stirrer at a temperature of 22 $\pm$ 1 °C and filtering the mixture using No. 40 filter paper.
- Inserting the pH probe into the mixture for a couple of minutes and reading the pH to one decimal place.

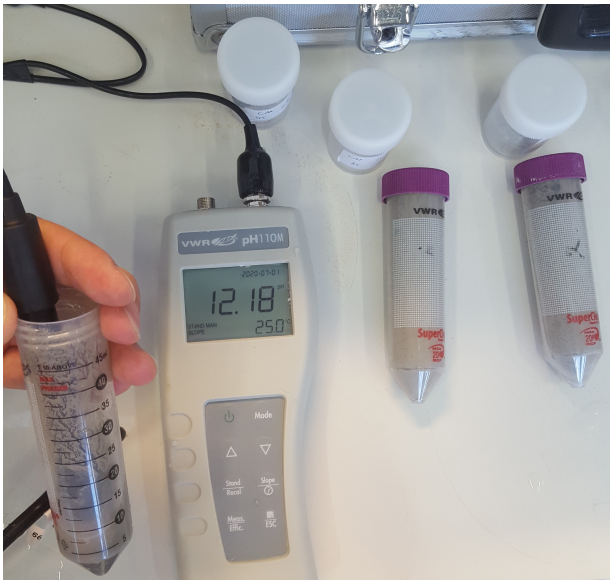

Figure 3.34: Determination of pH level with digital probe meter

Chapter 4

Results and Discussions

In the following chapter, the results and findings are presented and discussed based on the experimental program.

4.1 Fresh Properties of Cement Paste and Mortar

In this section, the results for fresh properties of cement paste and mortar with two different water to cement ratio are provided and discussed. Although carbonation curing was applied after initial setting time, the fresh properties of materials have influenced the efficiency of CO_2 curing.

4.1.1 Slump Measurement

Cement Paste

The slump of cement paste with w/c ratio of 0.6 and w/c ratio of 0.3 was completely opposite of each other. There was a total collapse for w/c ratio of 0.6, which was likely due to the high amount of water inside the sample without the presence of particle phase, which led to very low friction between cement Particles, on the contrary, the slump for w/c ratio of 0.3 was measured as zero. It was likely due to a very low amount of water-cement ratio that resulted in very low mobility and compactibility (like a high-stiff paste) with high friction between matrix phases.

Cement Mortar

The slump of the mortar with w/c ratio of 0.6 was measured as 12 mm. It means that the mortar was much stiffer compared to cement paste with the same w/c ratio; this is due to the high quantity of solid particles in the mortar (sand). The slump for w/c ratio of 0.3 was measured zero as a result of high friction between matrix and particle phases due to the low w/c ratio.

An overview of slump measurement is shown in table 4.1.

Table 4.1: Overview of slump measurement

	w/c: 0.3	w/c: 0.6
Cement paste	0	collapsed
mortar	0	12 mm

4.1.2 Air Content of Fresh Mortar

A very low w/c ratio would lead to low mobility and compactibility, which makes it hard to be compacted by rod strike in accordance with NS-EN 1015-7, so, high amount of air content was expected as for w/c ratio of 0.3. The amount of air content in the fresh mortar with w/c ratio of 0.6 and 0.3 is measured as 1.6% and 20%, respectively. This high portion of air content might be due to the different sources of air voids presented in fresh materials such as;

- Air originally present in the intergranular space in the cement and sand.
- The high volume of sand with a low amount of water makes a smaller portion of cement paste matrix around aggregates and a region with higher porosity near the surface of the sand would appear.
- The dissolved air in the mixing water.
- The in-folded and mechanically enveloped air which is trapped during mixing and casting.

Although finding the source of the air content is not the aim of this study, but the quantity of air content is desirable with respect to CO_2 gas diffusion. This means that the mortar with w/c ratio of 0.3 can be more efficient for CO_2 gas diffusion due to the higher air content.

The test did not conduct for the cement paste since one batch was like slurry and the other like stiff paste.

4.1.3 Density of Fresh Cement Paste and Mortar

The density of fresh cement paste and mortar is presented in table 4.2. In general, using more cement and high-dense sand particles with lower water-binder ratio, in a specific volume, would result in higher density, however; the density of mortar with w/c ratio of 0.3 is lower than the other batch with w/c ratio of 0.6 and it is related to the much higher air content for w/c ratio of 0.3 as discussed in section 4.1.2.

Table 4.2: Density of fresh materials

	w/c: 0.3	w/c: 0.6
Cement paste	1960 kg/m^3	1590 kg/m^3
mortar	1900 kg/m^3	2150 kg/m^3

4.2 Heat and RH Development During CO_2 Curing

During four and eight hours of carbonation curing, the data logger, inside the chamber, recorded the temperature and relative humidity for cement paste and mortar, which are illustrated in figure 4.1 and figure 4.2.

As it can be observed in figure 4.1, the temperature, inside the chamber, increased significantly to 52°C during first two hours of carbonation curing for cement paste specimens which was the result of exothermic reaction of CO_2 gas with water and dissolution of tricalcium silicate (C_3S) and dicalcium silicate (C_2S) as explained in section 2.2.2. The heat inside the chamber caused a part of the water vaporized and RH value increased from 60% to 65%. The sudden change in temperature and RH after about 4 hours, is due to the opening the chamber; temperature reduced significantly and water droplets went to the RH sensor caused a high value of RH (this also happened to figure 4.2 after opening the chamber for mortar specimens). Besides, a considerable amount of water observed in the chamber which might be the result of CO_2 reaction with $Ca(OH)_2$ that produces water, also the intensive heat inside the chamber can make the water vaporized out of the specimen and water droplets can be the result of condensation, this also applies to carbonation curing of mortar with less observable amount of water inside the chamber.
In the next four hours of curing, it seems that there was much less reaction compare to the first four hours of carbonation curing. It can be concluded that the carbonation happened mainly in the first two hours of carbonation curing for cement paste. According to Caijun et al.,2012 [35], the chemical reaction of early carbonation curing would mainly happen in the first two hours.

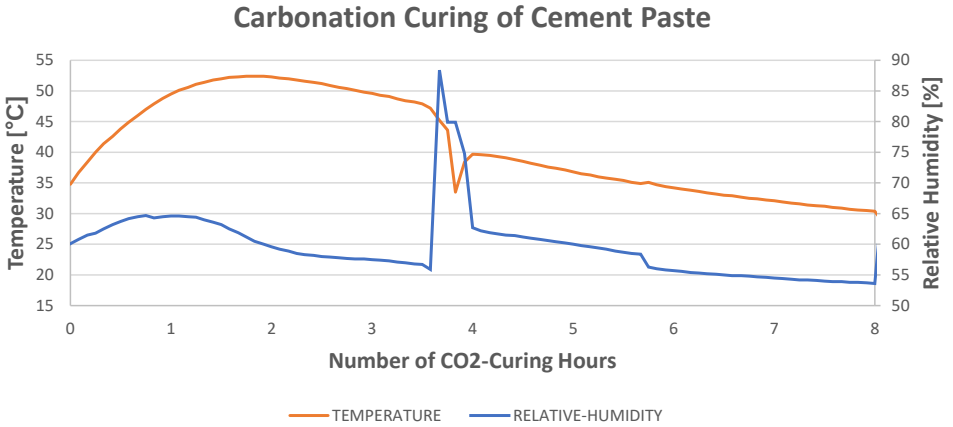

Figure 4.1: Temperature and RH development during carbonation for cement paste

In cement mortar, however, the temperate and RH increased significantly just in a short period of 30 minutes, which could be due to the lower amount of cement to react with CO_2. After this period, the temperature and RH value reduced slightly until about the room condition. A small sudden change in temperature (in both graphs) around 6 hours of curing can be due to the room temperature as a result of opening the entrance door.

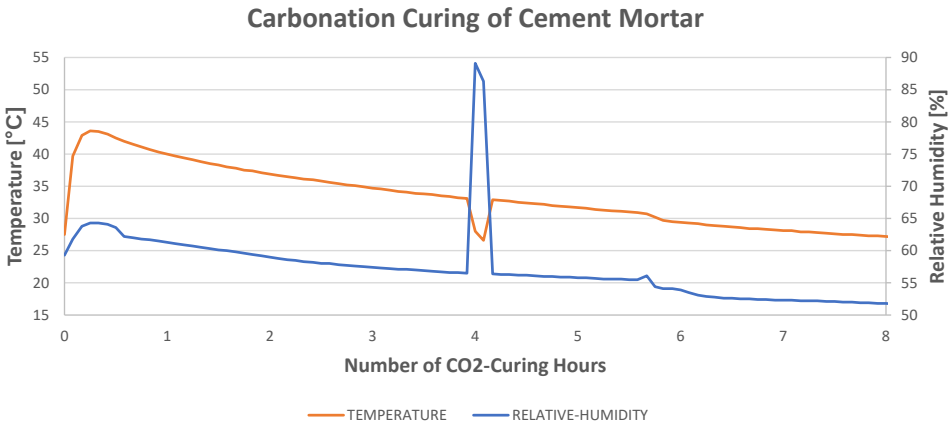

Figure 4.2: Temperature and RH development during carbonation for mortar

4.3 CO_2 Uptake by Mass Curve Method

CO_2 uptake was measured based on the digital scale value through the whole carbonation procedure as described in section 3.4.2. Figure 4.3 and table 4.3 illustrate the percentage of CO_2 uptake by cement weight% in two different carbonation curing hours.

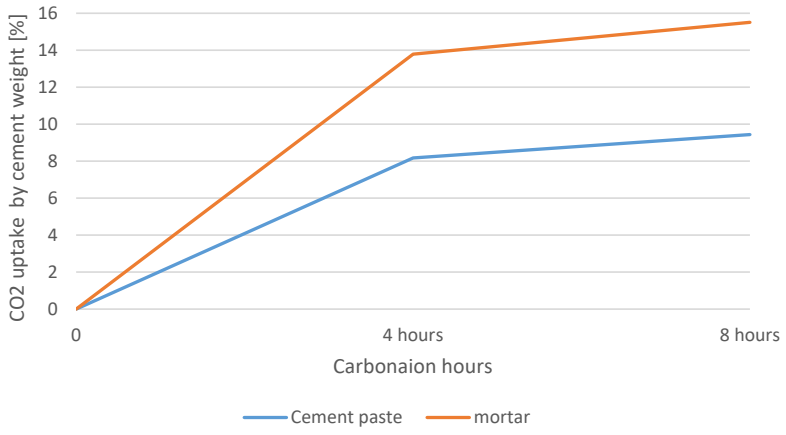

Figure 4.3: CO_2 uptake by cement wt% for cement paste and mortar

Table 4.3: CO_2 uptake% for cement paste and mortar with respect to cement wt%

	CO_2 uptake after 4 H by cement weight	CO_2 uptake after 8 H by cement weight
Cement paste	8.18%	9.44%
Mortar	13.79%	15.51%

Interesting to mention that CO_2 uptake (kg) of cement paste and mortar with respect to 1 m^2 of the cement-based wall with a thickness of 20 cm of products[1] is provided in table 4.4, although cement paste (without sand) does not use commonly in wall production. In this method, since the amount of CO_2 uptake, for each batch with different w/c ratio, could not be measured separately, the average is taken to calculate the values.

Table 4.4: CO_2 uptake (kg) for cement paste and mortar with respect to 1 m^2 of the cement-based wall with a thickness of 20 cm

	CO_2 uptake after 4 H of carbonation	CO_2 uptake after 8 H of carbonation
Cement paste	20.4 kg	23.5 kg
Mortar	12.5 kg	15.1 kg

Based on the mixing design of each batch and total volume of specimens in the airtight chamber, the amount of cement is calculated for two separate carbonation process; one for cement paste and the other for mortar, then based on the mass residual of scale, after vacuuming the chamber, the amount of CO_2 which was reacted with cement phase is calculated. Being incapable of measuring CO_2 uptake for each set with different w/c ratio is an obstacle in this method. All the data is provided in Appendix B.
As it can be observed in figure 4.3, after 4 hours of carbonation curing, cement mortar shows 13.79% of CO_2 uptake compare to cement paste with 8.18%. This higher value may be the result of being more porous in mortar compare to cement paste, so that CO_2 gas can diffuse more into the depth of specimens to react with cement phases. Of course, the real graph should be non-linear (higher slop within first two hours following by decreasing slope while carbonation continues), however, since two carbonation hours were selected, the scarce of data for a lower interval of carbonation period has made an obstacle to make a non-linear graph.
In the second 4 hours of CO_2 curing, the CO_2 uptake increased slightly in both cement paste and mortar, which means that carbonation curing mainly is efficient in the first four hours. This also corresponds to the high increase of heat development inside the chamber within the first 2 hours of carbonation curing discussed in section 4.2.

The maximum theoretical CO_2 consumption by cement can be calculated by the following equation [33]:

$$M_{max} = 0.785(\mathrm{CaO} - 0.7\mathrm{SO_3} + 1.09\mathrm{MgO} + 1.42\mathrm{Na_2O} + 0.93\mathrm{K_2O} \qquad (4.1)$$

[1] 20 cm thickness seems to be a perfect value for both the concrete wall production as well as high CO_2 ingress through the deep layers.

By using the chemical composition of the cement, from table 3.2, the maximum theoretical CO_2 uptake by cement weight is calculated as 50.984%. By using equation 2.5, the degree of carbonation, for cement paste and mortar, can be calculated. The results are presented in table 4.5;

Table 4.5: Carbonation degree of cement paste and mortar after 4 and 8 hours of CO_2 curing

	Carbonation degree after 4 H of carbonation curing	Carbonation degree after 8 H of carbonation curing
Cement paste	16%	18.5%
Mortar	27%	30.4%

The carbonation degree of mortar, as expected, was higher than cement paste, due to the higher amount of CO_2 uptake (since carbonation degree is measured as dividing the value of CO_2 uptake by cement wt% by maximum theoretical CO_2 uptake as measured as 50.984%)

4.4 Compressive Strength

4.4.1 1-Day Compressive Strength

1-day compressive strength was tested to understand the effect of carbonation curing on early strength, which previously was proven that early carbonation would result in higher early strength [17].

Figure 4.4 illustrates the comparison of 1-day compressive strength for cement paste with w/c ratio of 0.3 and 0.6 in different carbonation curing time.
As it is explained in section 3.3.1, it can be observed from figure 4.4 that w/c ratio is an important parameter for an efficient carbonation curing. In specimens with w/c ratio of 0.3, carbonation curing of four and eight hours has shown 38.5% and 45.7% of increase in compressive strength compared to their reference. It seems that diffusing CO_2 gas into specimens reacted with cement mineral (C_2S and C_3S) and formed calcium carbonate ($CaCO_3$). The compressive strength did not increase significantly from four to eight hours of CO_2 curing, which corresponds to the CO_2 uptake that mainly happened within the first 2-3 hours of carbonation curing that discussed in section 4.3.
Specimens with w/c ratio of 0.6, however, have not been influenced dramatically by carbonation curing, both carbonation curing time showed almost 5% increase. The reason might be that, the water filled the pores of specimens and did not let the CO_2 to diffuse into the deep layers and specimens did not have optimum moisture loss during pre-carbonation curing.

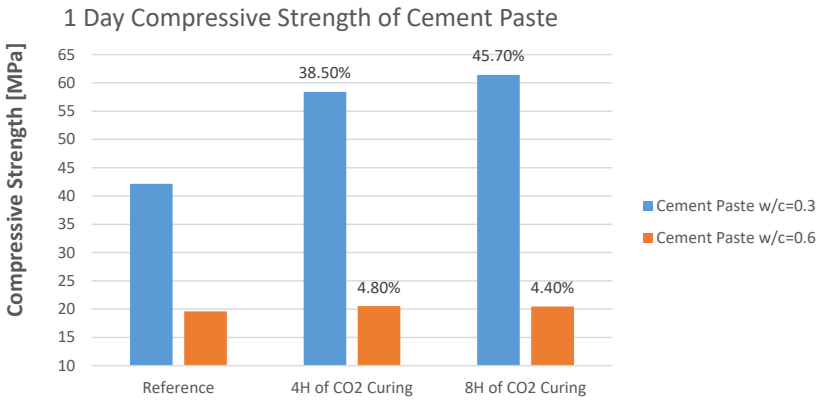

Figure 4.4: Comparison of 1-day compressive strength for cement paste specimens

Figure 4.5 shows the comparison of 1-day compressive strength for mortar specimens in different carbonation curing time. As it can be observed, there is a significant increase in the compressive strength of carbonation cured specimens compare to their references. For specimens with w/c ratio of 0.3, a high increase of 89.9% and 125.9%, respectively, for 4 and 8 hours of carbonation curing have achieved. The higher rate of increase in the mortar, compare to cement paste, could be due to presence of sand that made it more porous and lower effective w/c ratio; the effective w/c ratio had to be lower than 0.3 since a part of the water was absorbed by sand. Hence, CO_2 might react with more amount of cement phases (C_3S and C_2S) to form calcium carbonate. This also corresponds to both, the higher CO_2 uptake in mortar compare to cement paste and the high amount of air content discussed in section 4.1.2.
It also shows a moderate increase for w/c ratio of 0.6 in carbonation cured specimens; the reason behind this might be due to the lower effective w/c ratio, which made it easier for CO_2 to diffuse into deep layers.

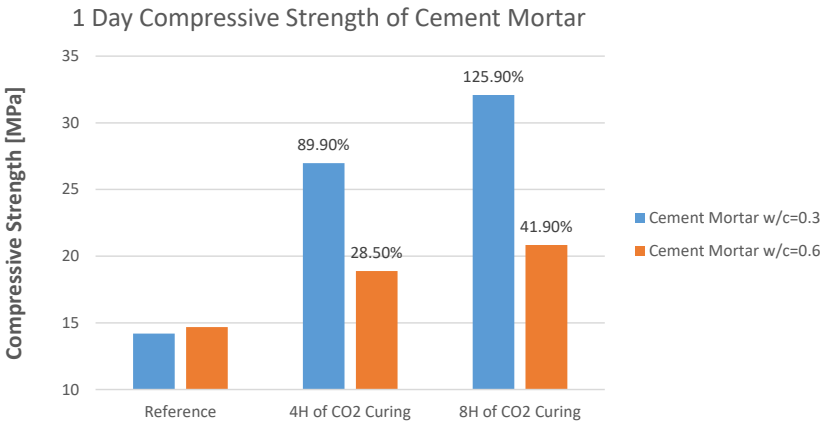

Figure 4.5: Comparison of 1-day compressive strength for mortar specimens

4.4.2 14-Days Compressive Strength

14-days compressive strength was tested to evaluate the effect of carbonation curing in a long time.
Figure 4.6 illustrates the compressive strength for cement paste after 14 days. As it can be observed, the carbonation cured specimens, still showed higher strength compare to their reference. Although all the specimens gained more strength after 14 days due to the maturity, however, after 14 days, the difference in strength between reference and carbonation cured samples, for w/c ratio of 0.3, decreased; the reference's strength increased 49% after 14-days, but four and eight hours of carbonation cured samples gained 16% and 15% more, respectively, it might be due to the much higher amount of cement phases (C_2S and C_3S) left in the reference sample to hydrate. On the contrary, since the specimens with w/c ratio of 0.6 did not show high difference between carbonation cured and reference in 1-day compressive strength, the difference did not change significantly after 14 days; reference, four and eight hours carbonation cured samples gained 39%, 39% and 42%, respectively after 14-days, suggesting that the amount of cement phases to hydrate, in reference and carbonation cured samples, did not differ significantly.

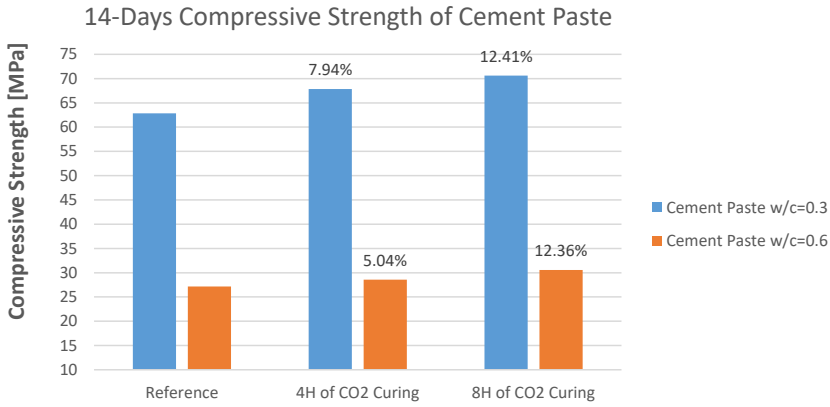

Figure 4.6: Comparison of 14-days compressive strength for cement paste specimens

Figure 4.7 illustrates the compressive strength for the mortar after 14 days. In specimens with w/c ratio of 0.3, reference, 4 and 8 hours of carbonation cured samples, gained 43%, 13% and 12% increase compared to the 1-day strength; reference gained more increase due to the more cement phases left to hydrate, however, carbonation cured samples still showed higher strength by 49% and 76% for 4 and 8 hours of carbonation, respectively.
Interestingly, specimens with w/c ratio of 0.6 gained the highest rate of increase in strength after 14 days, making the difference between their strength really small.
Generally, it is conclusive that specimens with more cement phases to hydrate gain more rate of increase in strength in a long time; however, it does not mean that carbonation cured samples would result in lower strength in a long time.

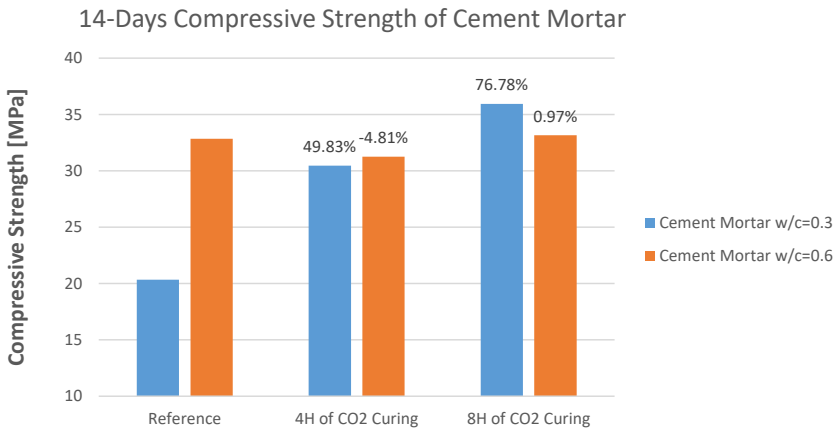

Figure 4.7: Comparison of 14-days compressive strength for mortar specimens

4.5 X-Ray Diffraction Results

The X-ray diffraction test was done at the age of 6 days from casting. Major diffracted peaks in cement paste and mortar with different w/c ratio, from angle 2θ of 5° to 100° have been investigated. The X-ray patterns are presented until 65° since there was no major peak after that degree. The peaks imply how strong a particular mineral exists in the sample, making it a good way of comparing the different carbonated specimens and their reference in terms of their minerals.
In figure 4.8, X-ray patterns of cement paste with w/c ratio of 0.3 are plotted for reference, 4 and 8 hours of carbonation curing. As it can be observed, two major peaks at angle 2θ of 18° and 29° are mainly different between carbonated and reference patterns. At 18°, calcium hydroxide ($Ca(OH)_2$) has a higher peak in reference compare to 4 and 8 hours of carbonation curing, on the contrary, at 29°, calcite ($CaCO_3$) has a higher peak in carbonated specimens compare to reference. It is conclusive that the intensity of peaks for calcite correspond to the reaction of CO_2 with cement phases to form more calcium carbonate rather than calcium hydroxide.

Figure 4.9 provides the relative percentage of major minerals in each set of samples. The higher percentage of portlandite ($Ca(OH)_2$) and lower calcite in reference specimens corresponds to the X-ray diffracted patterns. It also shows a lower percentage of Larnite (C_2S or Belite) in carbonated samples compare to the reference, which can be conclusive that C_2S was consumed more to form calcium carbonate. Moreover, C_2S has lower reactivity with water compare to alite (C_3S), due to this, belite contributes little in the early strength, on the contrary, since belite forms the most C-S-H per unit reacted material, it contributes significantly in the long term of compressive strength. This can serve as supporting evidence in higher rate of increase in compressive strength of reference, after 14 days, compare to carbonation cured specimens.

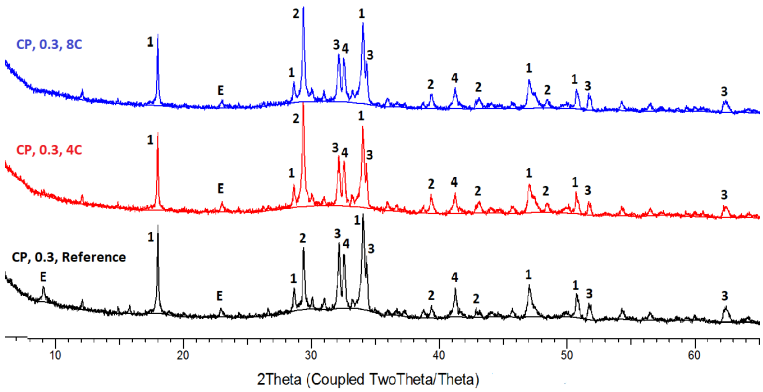

1: Portlandite($Ca(OH)_2$) 2: Calcite 3: Alite(C_3S) 4: Larnite(C_2S) E: Ettringite

Figure 4.8: Diffracted X-Ray patterns for cement paste specimens with w/c ratio of 0.3

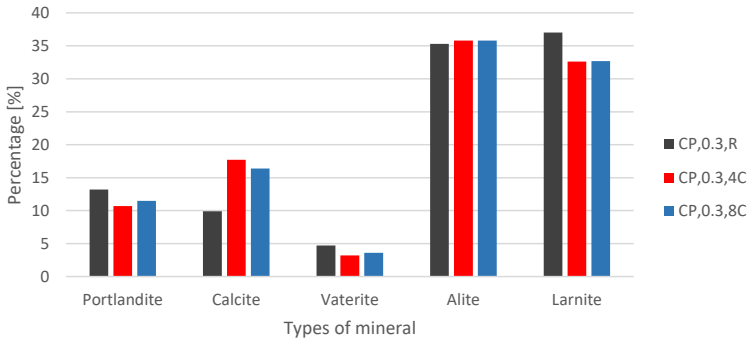

Figure 4.9: Relative percentage of major minerals in cement paste with w/c ratio of 0.3

In figure 4.10, X-ray patterns of cement paste with w/c ratio of 0.6 are plotted for reference, 4 and 8 hours of carbonation curing. As it can be observed, two major peaks at angle 2θ of 29° and 34° are mainly different between carbonated and reference patterns. At 29°, calcite has higher peaks in carbonated samples compare to reference, also two more calcite peaks appeared in carbonated samples at 36° and 43°. At 34°, calcium hydroxide has a higher peak in reference compare to carbonated samples, which means that CO_2 reacted with cement phases to form more calcium carbonate rather than calcium hydroxide, besides, carbonation of calcium hydroxide itself can be another reason. However, this does not correspond to increased 1-day compressive strength for w/c ratio of 0.6 (around 5% increase), it might be due to the distribution of mineral in X-ray's powder sample that was taken from the whole specimen which was mixed from outer and inner layers; in outer layers, there has to be more calcium carbonate than inner layers. It can be also observed in carbonated samples that, at 48° and 51°, Aragonite and Vaterite (two polymorphs of calcium carbonate) have been formed instead of $Ca(OH)_2$, respectively.

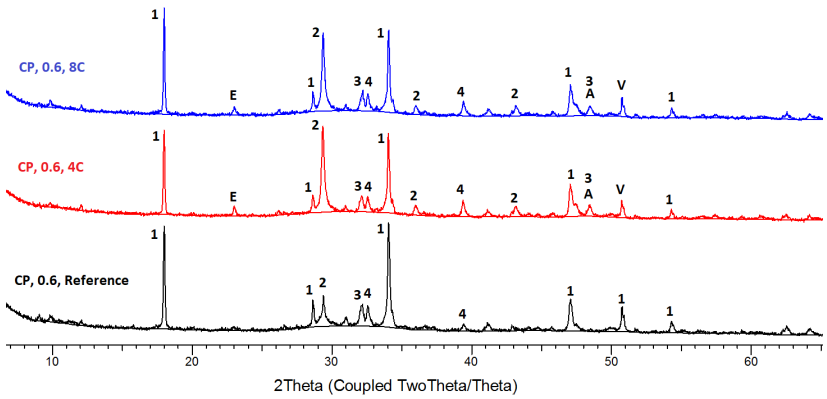

1: Portlandite($Ca(OH)_2$) 2: Calcite 3: Alite(C_3S) 4: Larnite(C_2S) E: Ettringite A: Aragonite V: Vaterite

Figure 4.10: Diffracted X-Ray patterns for cement paste specimens with w/c ratio of 0.6

Figure 4.11 provides the relative percentage of major minerals in each set of samples. It has to be mentioned that, each mineral's relative percentage in the chart has been counted from all the peaks in each pattern, whether can be detected by eyes or not. For instance, the detectable Vaterite peaks appeared in the carbonated samples' pattern, however, in figure 4.11, it shows more percentage of Vaterite for the reference sample. Besides, a lower relative percentage of alite in reference sample may be due to the higher reactivity of alite with water, the C_3S is more consumed in the reference sample since reference had lower moisture loss in comparison with carbonation cured specimens. The reason for lower Larnite (belite) in carbonated cured specimens is the same as discussed for w/c ratio of 0.3 (figure 4.9).

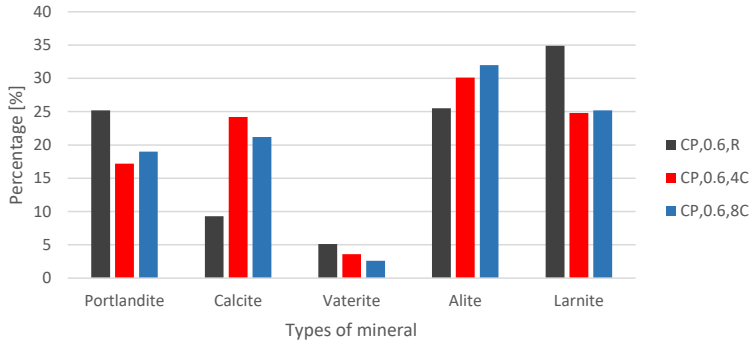

Figure 4.11: Relative percentage of major minerals in cement paste with w/c ratio of 0.6

In figure 4.12, X-ray patterns of mortar with w/c ratio of 0.3 are plotted for reference, 4 and 8 hours of carbonation curing. As it can be observed, there are some peaks related to quartz due to the sand particles inside the powder that are not relevant. The most relevant

peaks in this study, relate to calcite and calcium hydroxide. There are more intense peaks of calcium hydroxide at 18° and 34° in reference sample due to the normal hydration products of cement phases, however, in carbonation cured samples, the patterns show less calcium hydroxide and more intense calcite ($CaCO_3$) peaks at 29°, which means that more CO_2 reacted with cement phases to form calcite instead of calcium hydroxide. Besides, calcite was detected at 39°, 43° and 54° for the carbonated samples. The difference of calcite peaks in the mortar, compare to their reference, is more intense than cement paste compares to its reference, with the same w/c ratio, which also corresponds to higher increase rate of compressive strength in the carbonated mortar than carbonated cement paste samples.

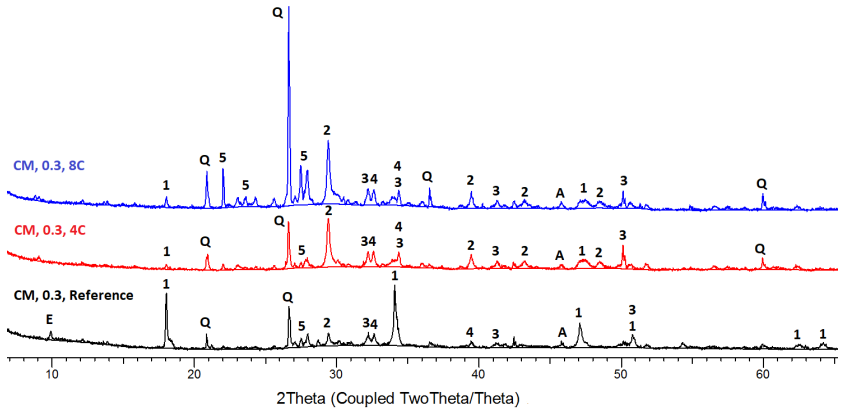

1: Portlandite($Ca(OH)_2$) 2: Calcite 3: Alite(C_3S) 4: Larnite(C_2S) 5: Albite
E: Ettringite A: Aragonite Q: Quartz

Figure 4.12: Diffracted X-Ray patterns for mortar specimens with w/c ratio of 0.3

The reasons behind the higher relative percentage of alite and calcite, lower relative percentage of larnite and portlandite, in the carbonation cured samples (figure 4.13), are similar as discussed in the cement paste part.

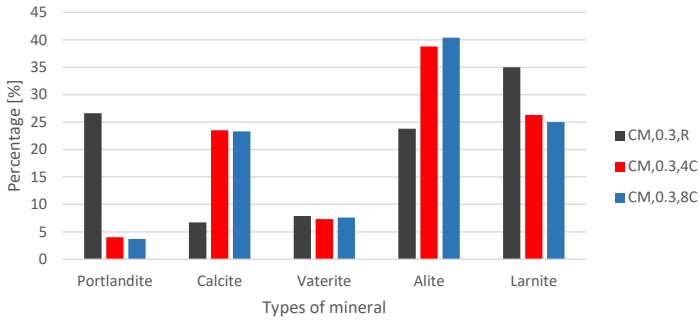

Figure 4.13: Relative percentage of major minerals in the mortar with w/c ratio of 0.3

In figure 4.14, X-ray patterns of mortar with w/c ratio of 0.6 are plotted for reference, 4 and 8 hours of carbonation curing. Like mortar with w/c ratio of 0.3, lower calcium hydroxide and higher calcite peaks in carbonated specimens, are the result of CO_2 reaction with cement phases to form more calcite rather than calcium hydroxide. Since the X-ray patterns and relative percentage of minerals in figure 4.15 are similar to mortar (w/c ratio of 0.3) discussed above, it is unnecessary to discuss the reasons again.

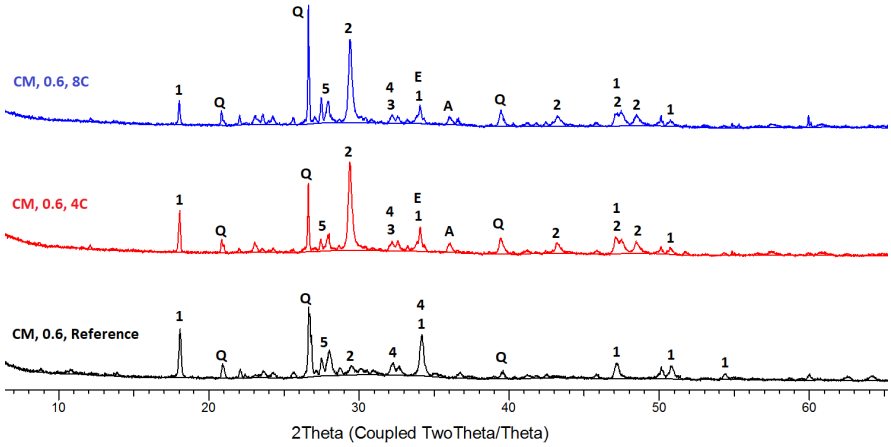

1: Portlandite($Ca(OH)_2$) 2: Calcite 3: Alite(C_3S) 4: Larnite(C_2S) 5: Albite
E: Ettringite A: Aragonite Q: Quartz

Figure 4.14: Diffracted X-Ray patterns for mortar specimens with w/c ratio of 0.6

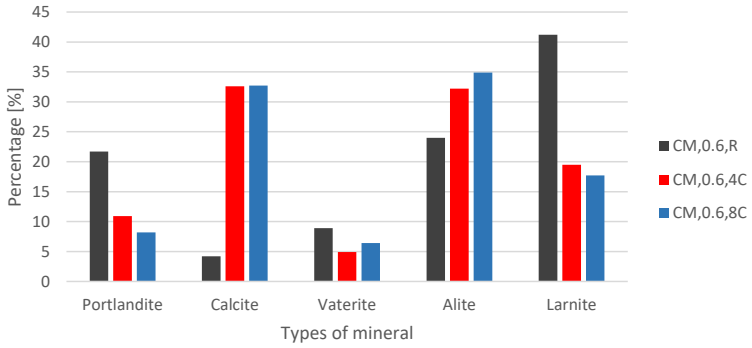

Figure 4.15: Relative percentage of major minerals in the mortar with w/c ratio of 0.6

4.6 Thermogravimetric Analysis

TGA was done at the age of 6 days from casting. Thermal decomposition of hydration and carbonation products in their specific range are analyzed and discussed. To fresh the mind, decomposition of products in their specific range of temperature are summarized below [46, 52]: (for more details see section 3.5.10)

- 105°C-420°C ⇒ Loss of H_2O due to the dehydration of C-S-H, aluminate hydrate and ferro-aluminate hydrate.

- 420°C-500°C ⇒ Dehydration of $Ca(OH)_2$

- 500°C-1000°C ⇒ Decarbonation of $CaCO_3$

Mass loss percentage of cement paste with w/c ratio of 0.3 for reference, four and eight hours of carbonation curing at the temperature range of 30°C to 1000°C is illustrated in figure 4.16, First derivative of mass loss is presented in figure 4.17. Table 4.6 also shows the mass loss% in different temperature ranges.
In figure 4.16, lower slop of mass reduction at the beginning of the process for carbonated sample (from 30°C to 105°C) is likely due to the less free water left inside the samples as a result of the exothermic reaction during carbonation curing, this also is similar for cement paste with w/c ratio of 0.6. According to table 4.6, both carbonation cured samples, compared to their reference, showed lower mass loss due to the decomposition of C-S-H and $Ca(OH)_2$, however, they showed a noticeable increase in the mass loss due to the decarbonation of $CaCO_3$, which is likely due to the CO_2 reaction with cement phases (C_3S and C_2S) to form more calcium carbonate than hydration products, resulting in higher early compressive strength [6]. Eight hours of carbonation sample did not show noticeable differences in mass loss compared to four hours, which seems that no significant reactions happened in the next 4 hours of carbonation curing. This also corresponds to the heat development discussed in section 4.2.

Table 4.6: Mass loss% of cement paste with w/c ratio of 0.3 in different temperature ranges

	Mass loss% 105-420°C	Mass loss% 420-500°C	Mass loss% 500-1000°C
Reference	11.41 %	4.46 %	3.14 %
4 hours of carbonation	7.42 %	3.43 %	9.93 %
8 hours of carbonation	7.03 %	3.18 %	11.14 %

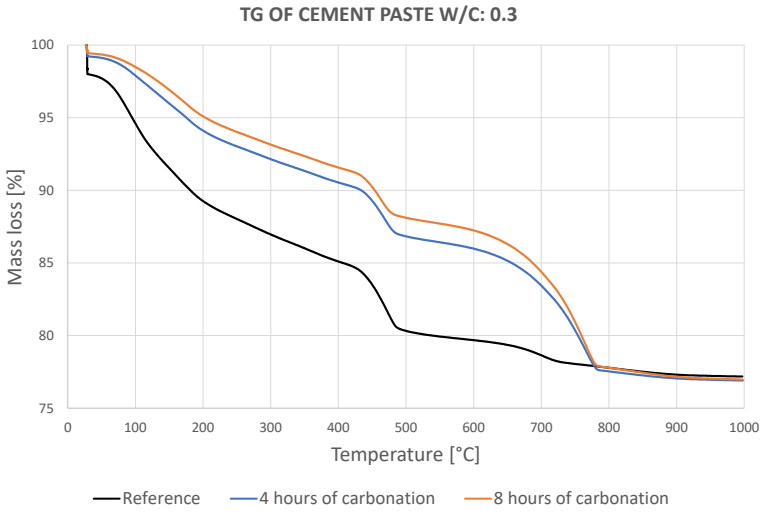

Figure 4.16: Thermal mass loss% for cement paste with w/c ratio of 0.3

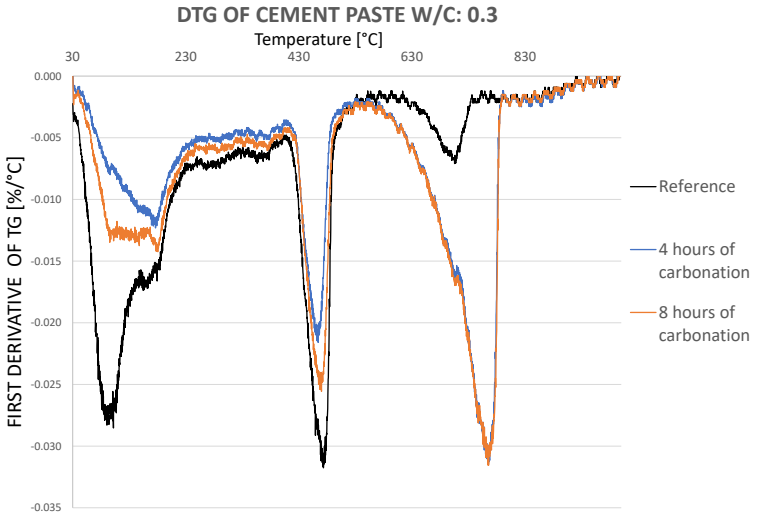

Figure 4.17: DTG for cement paste with w/c ratio of 0.3

According to table 4.7, the main observable differences in cement paste with w/c ratio of 0.6, compare to w/c ratio of 0.3, are lower quantity of products in both, hydrated and carbonated compounds, it seems that the higher amount of unreacted water, inside the specimens, delayed the hydration products as well as the formation of calcium carbonate. This also corresponds to lower compressive strength compared to the other batch.

Table 4.7: Mass loss% of cement paste with w/c ratio of 0.6 in different temperature ranges

	Mass loss% 105-420°C	Mass loss% 420-500°C	Mass loss% 500-1000°C
Reference	8.27 %	3.30 %	2.55 %
4 hours of carbonation	7.00 %	2.88 %	6.94 %
8 hours of carbonation	6.81 %	2.86 %	6.64 %

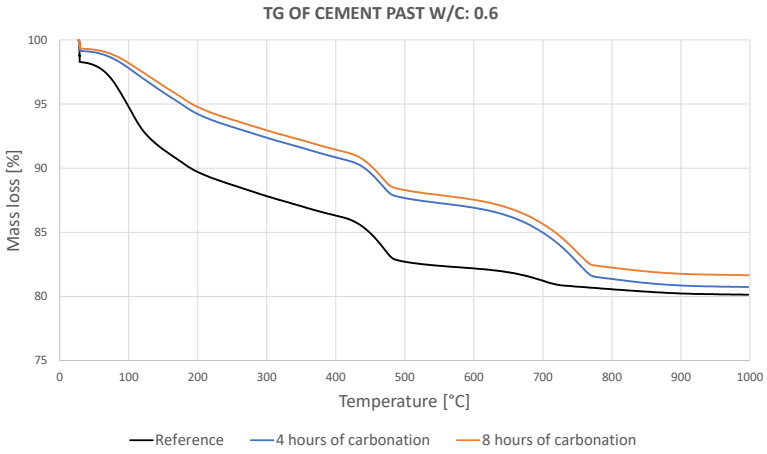

Figure 4.18: Thermal mass loss% for cement paste with w/c ratio of 0.6

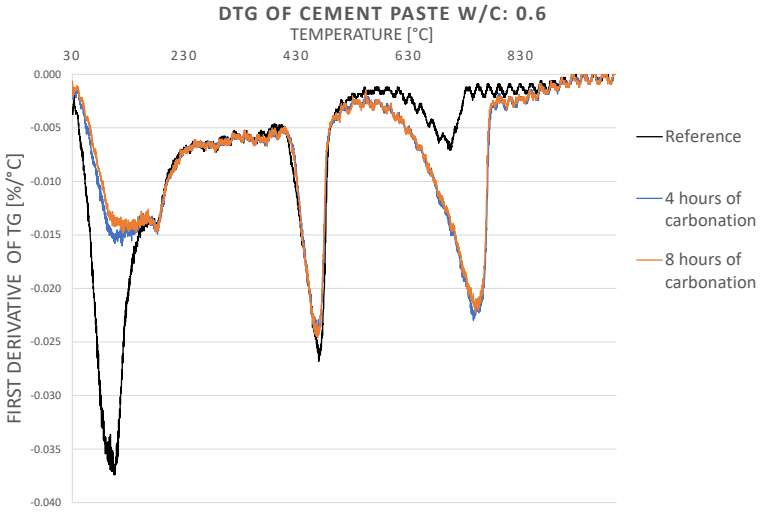

Figure 4.19: DTG for cement paste with w/c ratio of 0.6

As it can be observed in both figures 4.20 and 4.22, the slope of mass losses in the temperature range of 30°C and 105°C, are almost similar in all mortar samples, which is likely due to the water absorption of sand to reduce the free-water inside the specimens. In general, reference mortar specimens showed a lower quantity of C-S-H products compared to reference samples in cement paste, which intensively suggesting that the lower amount of cement used in the mortars has caused this reduction.
Carbonation cured mortars with w/c ratio of 0.3 showed the maximum mass loss in temperature range of 500°C and 1000°C among all other batches (around 15%), due to the proper combination of two important factors; lower effective water-cement ratio [37] and having enough pores for the diffusion of CO_2. In addition to increased formation of $CaCO_3$ in carbonation cured samples, lower quantity of hydration products (CH and C-S-H), has been achieved due to the both, less cement phases left for hydration and carbonation of $Ca(OH)_2$ and C-S-H itself. It is conclusive that, the mortar-like elements, such as masonry block, are perfect and ideal for early age carbonation to uptake a high amount of carbon dioxide.

Table 4.8: Mass loss% of mortar with w/c ratio of 0.3 in different temperature ranges

	Mass loss% 105-420°C	Mass loss% 420-500°C	Mass loss% 500-1000°C
Reference	5.13 %	3.20 %	3.45 %
4 hours of carbonation	4.33 %	1.48 %	15.37 %
8 hours of carbonation	4.20 %	1.29 %	14.76 %

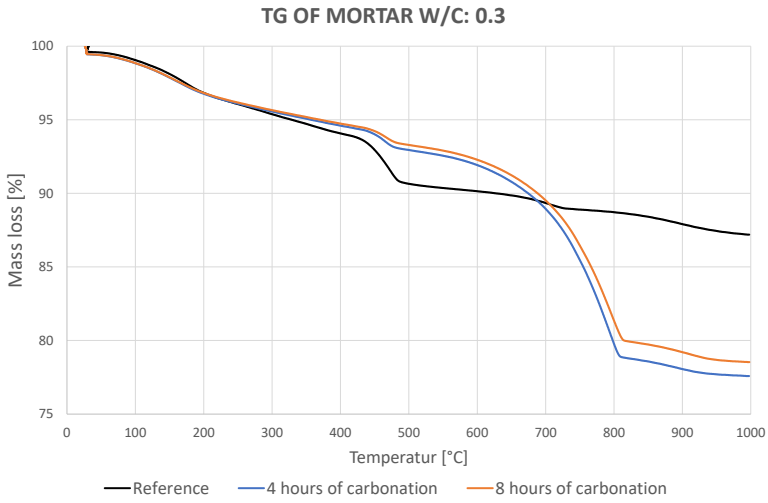

Figure 4.20: Thermal mass loss% for mortar with w/c ratio of 0.3

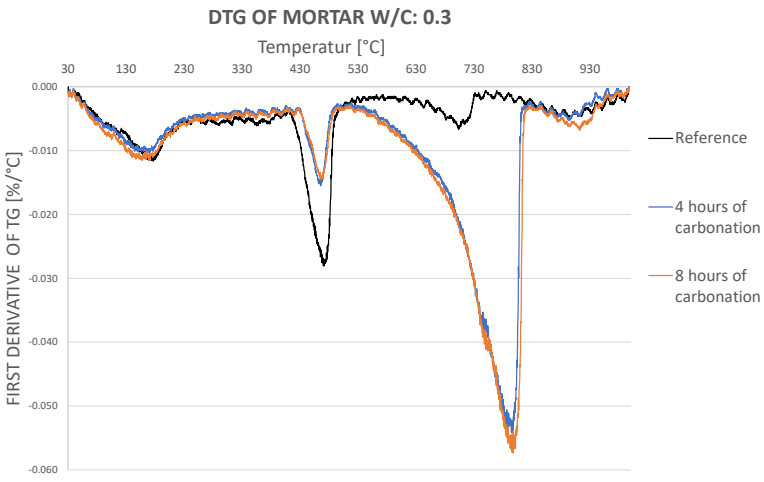

Figure 4.21: DTG for mortar with w/c ratio of 0.3

The mass losses% of mortar with w/c ratio of 0.6 in different temperature ranges are presented in figure 4.22 and table 4.9. The similar discussion, as for mortar with w/c ratio of 0.3, can be applied to the mortar with w/c ratio of 0.6. However, the main difference is the amount of mass loss% in the decarbonation of calcite. Like cement paste, the higher amount of w/c ratio would result in a lower amount of calcite formation.

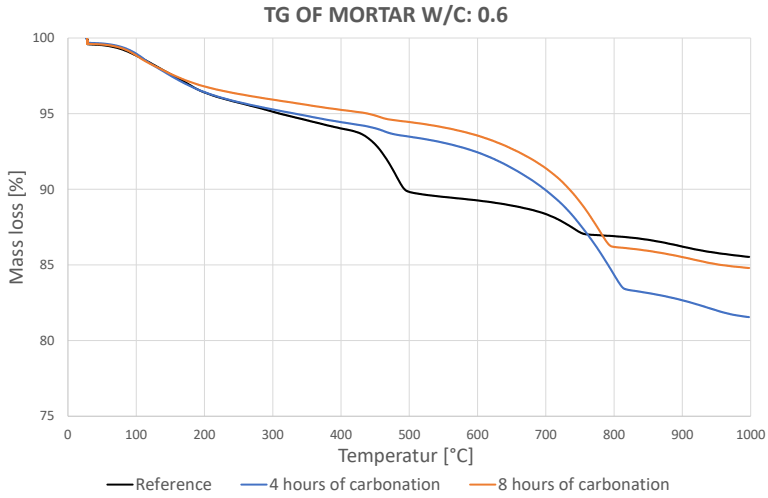

Figure 4.22: Thermal mass loss% for mortar with w/c ratio of 0.6

Table 4.9: Mass loss% of mortar with w/c ratio of 0.6 in different temperature range

	Mass loss% 105-420°C	Mass loss% 420-500°C	Mass loss% 500-1000°C
Reference	4.9 %	4.0 %	4.28 %
4 hours of carbonation	4.53 %	0.82 %	11.93 %
8 hours of carbonation	3.56 %	0.69 %	9.66 %

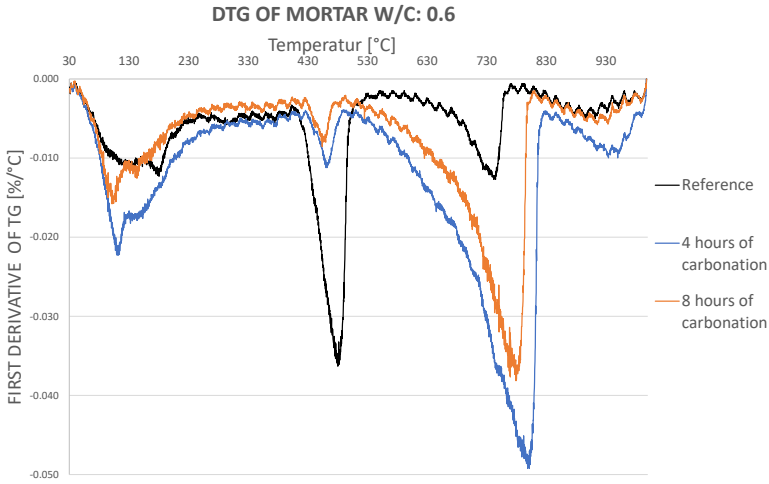

Figure 4.23: DTG for mortar with w/c ratio of 0.6

4.6.1 CO_2 Uptake Measurement by TGA

According to equation 3.4, the CO_2 loss can be determined as the result of the decomposition of calcium carbonate [45, 46]. Table 4.10 shows the CO_2 uptake in terms of cement wt% by using TGA.

Table 4.10: CO_2 uptake % by cement weight using TGA

		CO_2 uptake %	
		w/c: 0.3	w/c: 0.6
Cement Paste	4 H carbonation	6.79 %	4.39 %
	8 H carbonation	8 %	4.09 %
Cement Mortar	4 H carbonation	11.92 %	7.65 %
	8 H carbonation	11.31 %	5.38 %

To have a better understanding of CO_2 uptake in industrial products, table 4.11 is presented to show the CO_2 uptake (kg) per 1 m^2 of the cement-based wall with a thickness of 20 cm of products in different batches, although, cement paste (without sand) does not use commonly for wall production.

Table 4.11: CO_2 uptake (kg) per 1 m^2 of the cement-based wall with a thickness of 20 cm using TGA

		CO_2 uptake (kg)	
		w/c: 0.3	w/c: 0.6
Cement Paste	4 H carbonation	20.4	8.7
	8 H carbonation	24	8.1
Cement Mortar	4 H carbonation	10.5	7.2
	8 H carbonation	10	5

It seems that both, cement paste and mortar, with lower water-cement ratio, gained more carbonated products as a result of carbonation curing.
The small differences between CO_2 uptake %, presented in table 4.3 measured by mass curve method and the TGA method, can be due to the two facts; lower distribution of calcium carbonate crystals in powder samples in TGA and natural atmospheric carbonation of reference's powder sample while exposing to air during preparation, which can influence the accuracy of the result.

4.6.2 Determination of Hydration Degree

The determination of hydration degree was calculated for cement paste and mortar at the age of 6 days. Based on the mass loss% of different temperature ranges in accordance with Bhatty's methodology, that presented in table 3.14, the values of Ldh, Ldx, Ldc are found and by using equations 3.5 and 3.6 the hydration degree is then calculated. The values are shown in table 4.12.

Table 4.12: Values of Ldh, Ldx, Ldc and hydration degree

			Ldh%	Ldx%	Ldc%	Hydration degree %
Cement paste	w/c: 0.3	Reference	10.081	4.321	2.601	64
		4 H carbonation	7.609	3.285	10.484	63
		8 H carbonation	7.929	3.587	9.284	64
	w/c: 0.6	Reference	8.880	3.117	2.129	54
		4 H carbonation	7.536	2.978	6.341	55
		8 H carbonation	7.367	2.937	6.041	53
Mortar	w/c: 0.3	Reference	5.60	3.143	3.04	42
		4 H carbonation	4.545	1.993	14.636	52
		8 H carbonation	4.382	1.816	14.037	50
	w/c: 0.6	Reference	5.353	4.008	3.832	46
		4 H carbonation	4.677	1.407	11.181	44
		8 H carbonation	3.703	1.197	8.997	36

According to table 4.12, the cement paste showed a higher value of hydration degree compared to mortar. This might be due to the higher amount of cement phases, in cement paste samples, to hydrate. Moreover, almost all the samples with w/c ratio of 0.3 showed

a higher value of hydration degree in comparison with ratio of 0.6 which might be again due to the higher amount of cement used in the lower w/c ratio.
In cement paste, carbonation cured samples showed almost the same value of hydration degree as for their references, on the contrary, the carbonation cured mortar samples showed fluctuating values of hydration degree which make it hard to find a logical reason behind it. Since calcium carbonate would be formed as a result of the reaction between C_2S, C_3S, hydration products and CO_2, the value of hydration degree, for carbonation cured samples, was expected to be lower than their references due to the less amount of formed CH.
It is suggested that, although the hydration degree of reference samples can be determined decently by using Bhatty's methodology, however, it is not a proper methodology to use in the case of carbonation curing. More investigation is needed to propose a decent method for the determination of hydration degree in carbonation cured specimens.

4.6.3 Sulfate Resistivity

Although sulfate resistivity is not part of the experimental program, it can be a proof for a lower amount of $Ca(OH)_2$ presence in carbonation cured samples. Figure 4.24 shows the difference of sulfate resistivity in reference (in the right) and carbonation cured (in the left). As an example, the picture just selected from mortar with w/c ratio of 0.6. According to Rostami et al.,2011, sulfate resistance is due to the removal of CH in specimens [6]. It also corresponds to the lower amount of CH in carbonated cured specimens compare to their references, discussed in section 4.6.

Carbonated cured in the left side Reference in the right side

Figure 4.24: Sulfate resistivity

4.7 pH Level Results

The pH value of cement paste and mortar, at the age of 14 days, is presented in figure 4.25. Despite in calcium hydroxide reduction in carbonation cured samples (see section 4.6), due to the conversion of $Ca(OH)_2$ to $CaCO_3$, all the carbonation cured specimens, showed pH value of ≥ 12, suggesting that, although pH level would decrease at a very early age due to the dissolution of CO_2 to carbonate ions, carbonation curing is not detrimental in the long terms (at least after 14 days) with respect to carbonation induced corrosion due to the proper subsequent hydration that accompanied the early carbonation. The pH value in mortar carbonation cured samples is lower than the cement paste due to the lower amount of CH in their compounds. Taking into consideration that, other alkali ions (NaOH and KOH) contribute to the pH of pore solution and most likely are not carbonated yet, however, more investigation is needed to evaluate the effect of early carbonation curing on the reaction of other alkali ions that mentioned above.

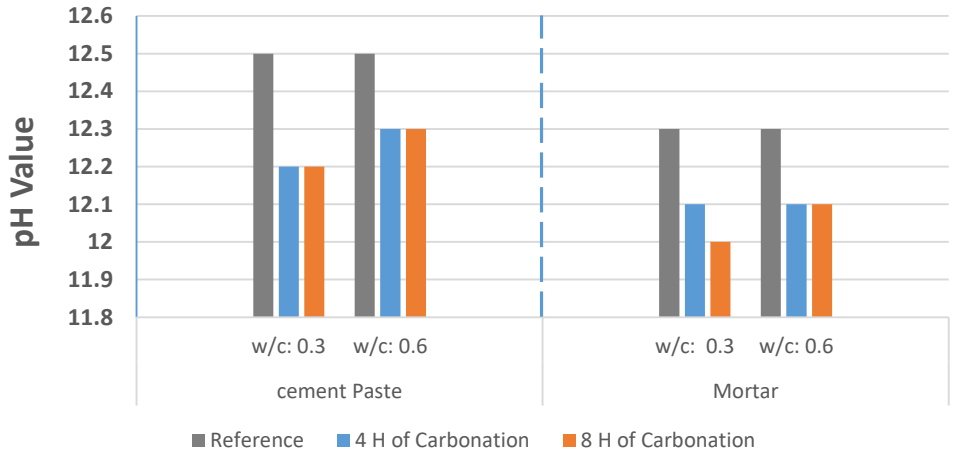

Figure 4.25: pH values of cement paste and mortar

4.8 Porosity and Hardened Density Results

4.8.1 Porosity

The porosity test was started at the age of 7 days from casting. Macro-porosity, suction porosity and total porosity have been measured for cement paste and mortar, which presented in figure 4.26 and figure 4.27, respectively. All the carbonation cured samples were compared with their references in terms of increase/decrease percentage.

In figure 4.26, all the samples with w/c ratio of 0.3 showed a lower volume of pores in comparison with the other batch with w/c ratio of 0.6. This is due to the lower water-cement ratio (the lower the w/c ratio, the less the capillary pores) and more amount of hydration products that occupied the space between solid parts of C-S-H gel (related to

gel pores). However, this reason is not in agreement with mortar batches shown in figure 4.27; it seems that the very low quantity of water for a large amount of solid phases (cement and sand), caused very low workability which resulted in more pore system, this also corresponds to the air content of mortar samples discussed in section 4.1.2.

According to figure 4.26, both the macro-porosity and suction-porosity decreased as a consequence of early carbonation curing. It is conclusive that, in carbonation cured specimens, the reaction of CO_2 with cement phases inside the pore system, formed $CaCO_3$; hence, the products occupied the free space between solid phases as well as a part of the volume originally filled with water that emptied as a result of the reaction. The high pressure of CO_2 gas during carbonation curing might result in diffusion of CO_2 in air/macro pores system, which resulted in a lower volume of macro-porosity in carbonation cured samples. These reasons are in agreement with the mortar carbonation cured samples, shown in figure 4.27, however, it seems that the reaction of CO_2 with cement phases, during carbonation curing, was more intense in decreasing the macro-pores in mortar specimens.
Moreover, the second four hours of carbonation curing did not have a significant effect on decreasing the volume of pores compared to the first four hours of carbonation.

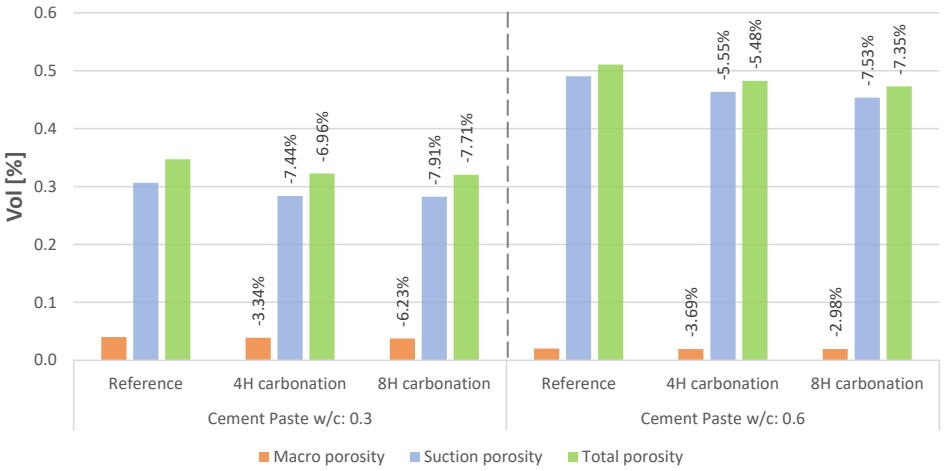

Figure 4.26: Porosity of cement paste samples

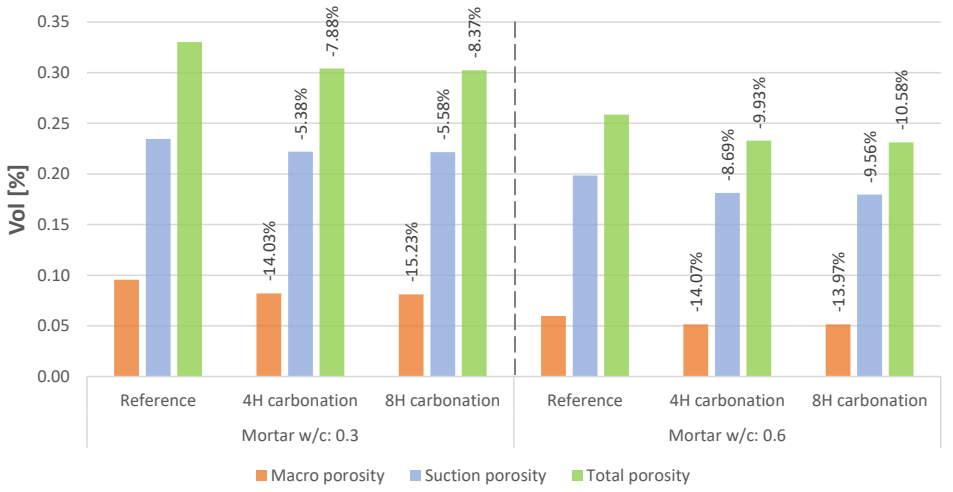

Figure 4.27: Porosity of mortar samples

4.8.2 Hardened Density

Figure 4.28 and figure 4.29 illustrate the hardened density of cement paste and mortar in three terms; normal density, dry density and solid density that explained in section 3.5.4. All the carbonation cured samples were compared with their references in terms of increase/decrease percentage.
Generally, density is correlated with porosity, but they have an inverse relationship; with the same used materials, the higher the pore volume, the lower the density. The volume of pore system is considered in the normal and dry density, hence, the lower value of density (normal and dry density) of cement paste with w/c ratio of 0.6, compare to 0.3, can be explained by having higher pore volume discussed in section 4.8.1. This also is in agreement with the lower amount of density (normal and dry density) of mortar with w/c ratio of 0.3, compare to 0.6. On the contrary, as for the solid density, since the pore volume does not consider in the calculation, no significant changes have been observed within all the samples. Besides, the very low value of dry density in cement paste with w/c ratio of 0.6 is most likely due to the high amount of free water left inside the samples.

All the carbonation cured specimens showed higher density (normal and dry density) compared to their references. Besides, the eight hours of carbonation curing showed a slight increase in dry density compare to 4 hours. This is due to the reaction of CO_2 with cement phases to form calcium carbonate rather than calcium hydroxide, since $CaCO_3$ has a higher density compare to $Ca(OH)_2$. The effect of carbonation reaction on pores system was discussed in section 4.8.1.

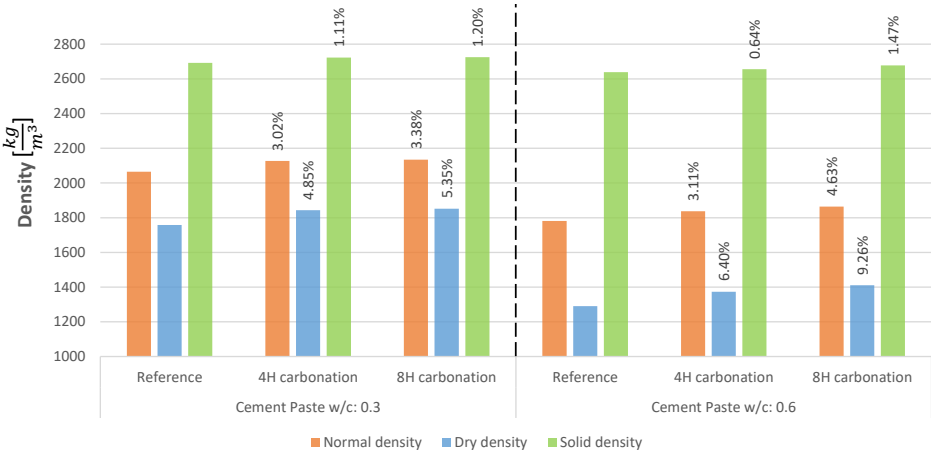

Figure 4.28: Density of cement paste samples

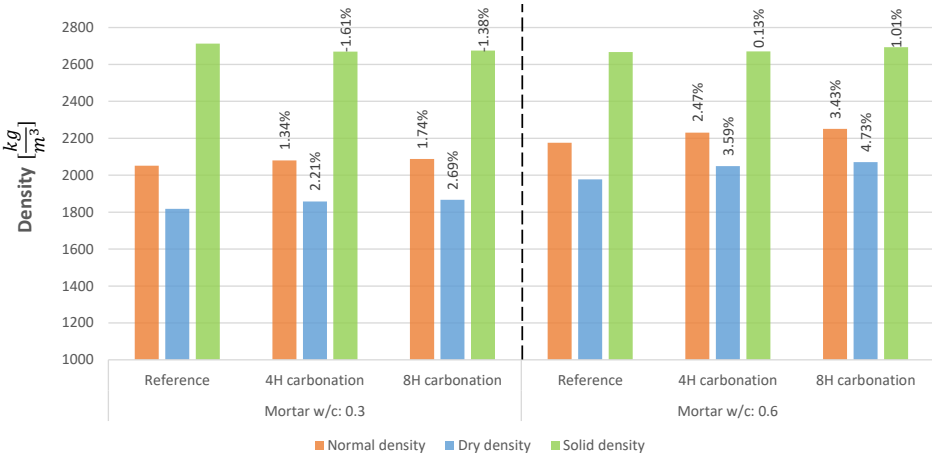

Figure 4.29: Density of mortar samples

4.9 SEM Results

The results in this section are based on the photomicrographs of samples taken by SEM. Figures [4.30-4.42] represent the micro-structure of all cement paste and mortar samples. In their caption, C_p and C_M are considered as cement paste and mortar, respectively.

The first four figures [4.30-4.33] are representative of reference samples in cement paste and mortar. The random-distributed blade-like crystals with the size of around 2 μm can be observed in all the reference samples, which are representative of calcium hydroxide formed as a result of hydration products. The granular shape crystals represent the C-S-H particles that have formed alongside $Ca(OH)_2$; previous research showed similar observations [53]. The EDS analysis test was done randomly for some photos to detect each element of crystals' composition. The elements were mainly Ca, Si, O and Al and there was no trace of carbon. All the EDS results are attached in Appendix C. XRD results have also provided supplementary evidence for these findings.

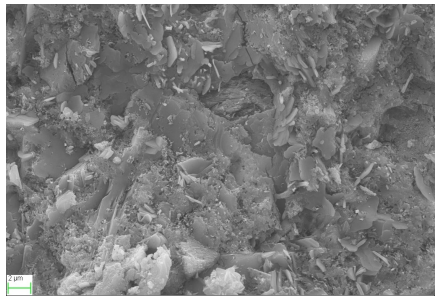

Figure 4.30: C_p, w/c:0.3, Reference

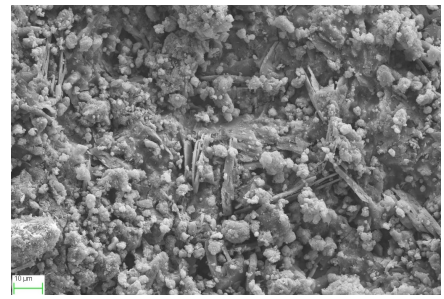

Figure 4.31: C_p, w/c:0.6, Reference

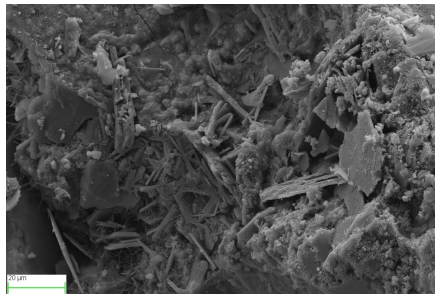

Figure 4.32: C_M, w/c:0.3, Reference

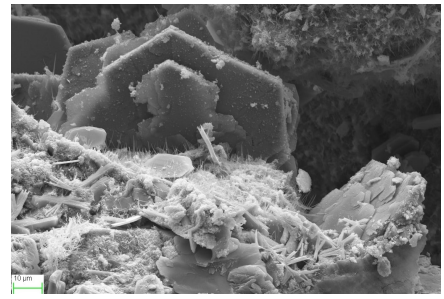

Figure 4.33: C_M, w/c:0.6, Reference

The findings are different in carbonation cured samples. The next four figures [4.34-4.37] are representative of four hours of carbonation curing for cement paste and mortar. The densely packed irregular and multiangular crystals, like a bloom of flowers, are covered and spread all over the place. They are considered as calcite (which is one of the calcium carbonate's polymorphs) with the size of around 1-2 μm; previous studies resulted in similar findings [53, 54]. The EDS results (see Appendix C) also showed the high presence of carbon in their composition. Moreover, the blade-like crystals (represent as $Ca(OH)_2$) were rarely observed in the samples which means that calcium carbonate, in-

stead of calcium hydroxide, were mainly formed during carbonation curing. The XRD and TGA results can serve as supporting evidence for the findings. It is also conclusive that the calcite crystals clustered have filled the space, which was originally filled with water and as a consequence, they made the carbonation cured specimens less porous (denser), in comparison with their reference, this corresponds to porosity results discussed in section 4.8.1. Besides, in some other photos, which provided in Appendix C, the pure calcite crystals could not be detected, instead, they were mixed with silica to form a hybrid of hydrates and carbonates.

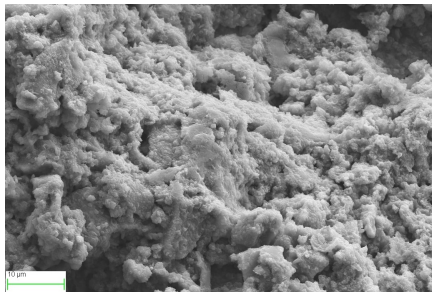

Figure 4.34: C_p, w/c:0.3, 4 H carbonation

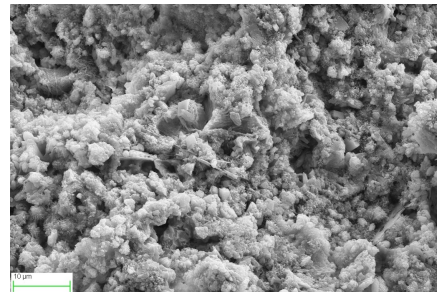

Figure 4.35: C_p, w/c:0.6, 4 H carbonation

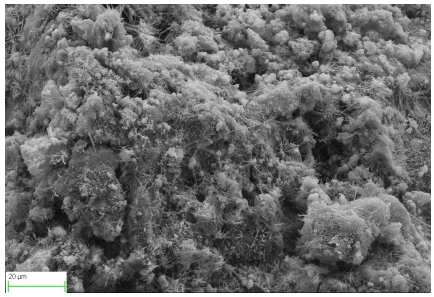

Figure 4.36: C_M, w/c:0.3, 4 H carbonation

Figure 4.37: C_M, w/c:0.6, 4 H carbonation

Figures [4.38-4.42] represents the micro-structure of cement paste and mortar samples with eight hours of carbonation curing. The findings were more or less different with four hours of carbonation curing. For instance, as for figure 4.38, the calcium carbonate seems to intermingled with C-S-H gel forming honeycomb-like crystals with a finer texture, similar to the results of the previous study [54]. In figure 4.39 the multiangular crystals, like 4 hours of carbonation cured samples, which considered as calcite, are incorporated alongside C-S-H. In figure 4.40, the densely packed needle-shaped crystals, like a bloom of flower, were formed above the honeycomb shape of crystals (mix of calcite and C-S-H), EDS results (see Appendix C) showed the presence of elements such as Si, Ca, O, C and Al in those needle-shaped crystals, suggesting that the mix of calcite and ettringite can be the reason of these types of crystals' formation, a previous study showed similar observations [53], another figure belongs to the same sample, but in a different spot is shown in figure 4.41 that shows the densely packed calcite crystals. In figure 4.42, the needle-shaped crystals could rarely be observed, instead, the pure densely packed calcite crystals

could be easily found in almost every spot. XRD and TGA results supported the evidence.

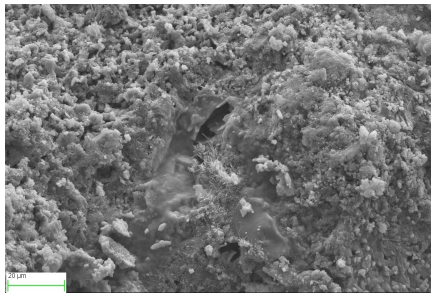

Figure 4.38: C_p, w/c:0.3, 8 H carbonation

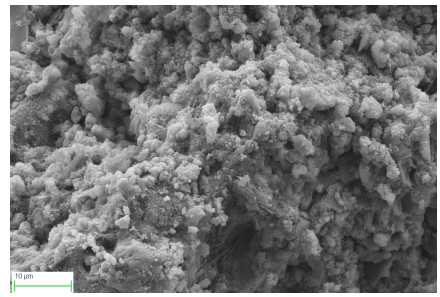

Figure 4.39: C_p, w/c:0.6, 8 H carbonation

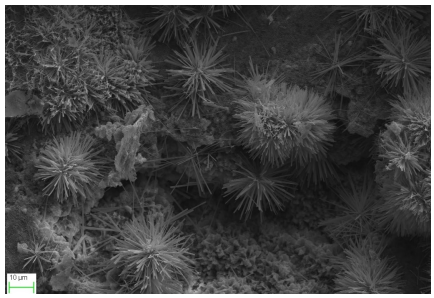

Figure 4.40: C_M, w/c:0.3, 8 H carbonation

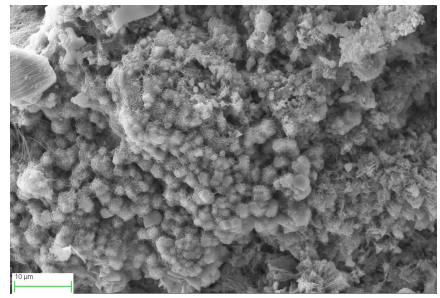

Figure 4.41: C_M, w/c:0.3, 8 H carbonation

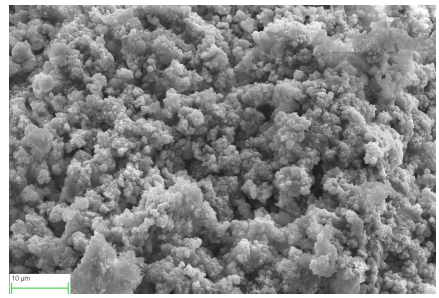

Figure 4.42: C_M, w/c:0.6, 8 H carbonation

4.10 Sources of Errors in the Experimental Program

In the following section, the sources of error, that could influence the results, are summarized below;

1. In the process of making powder sample, the whole specimen was crushed and milled and then kept in an airtight plastic bag. The composition of minerals, in different layers, is not exactly similar. Although the way of making powder was in such that the whole part of the cubic sample, layer by layer, was distributed roughly in the powder, there was a little chance of having more minerals belonged to outer/inner layers when it came to taking the sample for the TGA, XRD and pH level test that could influence the results.

2. The weathering carbonation of powder samples, while carrying on the tests (TGA, XRD, pH level), could affect the accuracy of the results.

3. In the porosity test, the pressure tank is a cylinder with a height of 44 cm and diameter of 12 cm that specimens were located from the bottom of the cylinder to the top. After depressurizing the tank, from 50 bars to atmosphere pressure, the interval between weighing the specimens on the top and bottom, could affect the amount of water in the macro-pore system for the specimens located in the lower part of the cylinder since a part of the water could be removed as a consequence of depressurizing.

Chapter 5

Conclusions

Numerous effects of early age carbonation curing on cement paste and mortar, in terms of chemical, mechanical and micro-structural changes have been observed and quantified in accordance with the experimental program. The following conclusions are summarized, based on both the literature and the results;

1. **Effect of fresh properties on carbonation curing**

    - Since it would not be possible to reduce the internal relative humidity to an ideal level of 50-60% within the first five hours after casting, water content has a vital role in obtaining a decent CO_2 uptake through carbonation curing process. The presence of high water quantity inside the pore system would inhibit the CO_2 gas ingress through the deep layers of specimens. This is in agreement of cement paste with w/c ratio of 0.6.
    - The presence of air content inside the specimens would be beneficial for CO_2 gas ingress, which would result in a higher carbon dioxide uptake.
    - Previously, it was believed that the high w/c ratio would result in a very low carbonation [37], however, as for cement paste with w/c ratio of 0.6, in spite of low increase rate in the early strength, it showed a decent CO_2 uptake. The high increase in both, early strength and CO_2 uptake, in the mortar with the same w/c ratio 0.6, is noticeable.

2. **Effect of pre-carbonation curing on carbonation curing**

    - The control of proper moisture loss in the specimens through the pre-carbonation curing is critical. In spite of not having enough data to find an optimum moister loss before carbonation curing, 5 hours of pre-carbonation curing, inside the climate chamber with RH of 60% and temperature of 25°C, resulted in CO_2 uptake of 15.5% and 9.4%, by cement weight after 8 hours of carbonation curing, for mortar and cement paste, respectively.

- Demolding after five hours of initial curing in a climate chamber is an ideal time to start carbonation curing since specimens are hardened enough to be transported without physical damages.

3. **CO_2 uptake**

   - Since the temperature, inside the airtight chamber, elevated very quickly within the first two hours of carbonation curing, which was followed by a reduction in temperature, it is conclusive that carbonation curing would be mainly efficient in the first two hours of carbonation.
   - On average, after 8 hours of carbonation curing, cement paste and mortar have the capacity of the CO_2 uptake around 23 kg and 15 kg, respectively, per square meter of cement-based wall products with a thickness of 20 cm.
   - By assuming the same carbonation methodology, Norway has the capacity to utilize 165000 tones of CO_2 into all concrete products annually, which can help to the reduction of global warming. Hence, early carbonation curing has shown to be a very promising sustainable technology.
   - Mortar samples showed higher potential for CO_2 uptake (around 15% of cement weight after 8 hours of carbonation curing) due to their porous nature, compared to cement paste, which is around 9% of cement weight.
   - TGA showed acceptable results regarding the estimation of CO_2 uptake.

4. **Effect of carbonation curing on mechanical and physical properties**

   - Generally, with proper pre-conditioning and mix design, carbonation curing would result in a significant rapid compressive strength due to the formation of calcium carbonate crystals at early age. This high-increase can be achieved in five hours of initial curing in climate chamber with RH of 60% and temperature of 25°C prior to a couple of hours of carbonation curing.
   - Although carbonation cured mortar with w/c ratio of 0.6 showed a decent rate of increase in compressive strength (41.9% after 8 hours of carbonation curing compare to its reference), in both, mortar and cement paste specimens with w/c ratio of 0.3, carbonation cured samples showed a higher rate of increase in strength compared to carbonation cured samples with w/c ratio of 0.6. Hence, water-cement ratio is an important parameter for carbonation curing.
   - Carbonation cured samples showed a reduction in the rate of increase in compressive strength, after 14-days; however, they still showed higher strength compared to their references. This reduction is likely due to the lower amount of Belite left in carbonation cured samples (according to XRD results), since Belite contributes significantly in the long term of strength.
   - Eight hours of carbonation curing did not show a significant increase in compressive strength in comparison with 4 hours of carbonation. This is due to the efficiency of carbonation curing, which is mainly within the first two hours of carbonation curing.

- Porosity is an important parameter for early carbonation curing. Since mortar is more porous than cement paste, due to the presence of sand, it showed a higher rate of increase in strength as well as a higher amount of CO_2 uptake. It demonstrated that mortar-like elements such as masonry concrete blocks can be ideal for carbonation curing because of their porous nature.

5. **Effect of carbonation curing on chemical and micro-structural properties**

   - TGA, XRD and SEM results were serving each other as supporting evidence in terms of chemical changes.
   - Carbonation curing resulted in the formation of calcium carbonate crystals due to the reaction of CO_2 with cement phases and hydration products itself. These reactions are exothermic, which resulted in vaporizing a part of the water, inside the pore system of specimens, during carbonation curing. Hence, as a solution to this, additional water can be sprayed, right after carbonation curing, to compensate a part of the water loss.
   - In the carbonation cured samples, less CH compounds were observed. This is due to the reaction of CO_2 with a part of cement phases to form calcium carbonate rather than CH, also, the carbonation of CH itself should be considered. In spite of less CH in carbonation cured samples, the pH value maintained above 12, which is not detrimental and not likely to start carbonation-induced corrosion. Moreover, due to this CH reduction, carbonation cured samples showed sulfate resistivity.
   - Both the macro-porosity and suction-porosity decreased as a consequence of early carbonation curing that calcium carbonate products occupied the free space between solid phases. The calcite crystals filled irregularly the originally water-filled space that would have been filled with hydration products.
   - Normal and dry density showed a slight increase in carbonation cured samples due to the rapid formation of calcium carbonate that has a higher density compare to CH.

Chapter 6

Future Work

The following items are my suggestions that can be proposed for future work within the field of early age carbonation curing;

- Investigation of CO_2 uptake by using flue gas CO_2 during carbonation curing, rather than high purity of carbon dioxide.
- Effect of early carbonation curing on the reaction of alkali ions such as NaOH and KOH that contribute to the pH of pore solution.
- Effect of early carbonation curing on the resistivity of chloride-induced corrosion in accordance with NORDTEST method NT build 443.
- Effect of early carbonation curing on purposely added calcium hydroxide powder into fresh concrete.
- A mathematical model to predict the strength and CO_2 uptake based on some important variable parameters.
- Effect of early carbonation curing on ultra-high performance concrete.
- Hydration degree of carbonation cured concrete.

Bibliography

[1] Fibertex, "Carbonation of concrete." https://www.fibertex.com/sites/fibertex.com/files/2020-05/Carbonation_0420.pdf, 2020.

[2] M. F. Bertos, S. Simons, C. Hills, and P. Carey, "A review of accelerated carbonation technology in the treatment of cement-based materials and sequestration of co2," *Journal of hazardous materials*, vol. 112, no. 3, pp. 193–205, 2004.

[3] S. Tech, "Solidia solutions [picture]." https://www.solidiatech.com/solutions.html.

[4] D. Zhang and Y. Shao, "Early age carbonation curing for precast reinforced concretes," *Construction and Building Materials*, vol. 113, pp. 134–143, 2016.

[5] Z. He, Z. Li, and Y. Shao, "Effect of carbonation mixing on co2 uptake and strength gain in concrete," *Journal of Materials in Civil Engineering*, vol. 29, no. 10, p. 04017176, 2017.

[6] V. Rostami, Y. Shao, and A. J. Boyd, "Durability of concrete pipes subjected to combined steam and carbonation curing," *Construction and Building Materials*, vol. 25, no. 8, pp. 3345–3355, 2011.

[7] C. Shi, M. Liu, P. He, and Z. Ou, "Factors affecting kinetics of co2 curing of concrete," *Journal of Sustainable Cement-Based Materials*, vol. 1, no. 1-2, pp. 24–33, 2012.

[8] C. Shi, M. Liu, Q. Zou, and F. He, "A study on factors influencing compressive strength of co2-cured concrete," in *International RILEM conference on advances in construction materials through science and engineering*, pp. 703–711, RILEM Publications SARL, 2011.

[9] A. Nanakoudis, "What is sem? scanning electron microscopy explained [picture]." https://www.thermofisher.com/blog/microscopy/what-is-sem-scanning-electron-microscopy-explained/1.

[10] P. K. Mehta and P. J. Monteiro, *Concrete microstructure, properties and materials*. 2017.

[11] J. Shieber, "Co2 in the atmosphere just exceeded 415 parts per million for the first time in human history," 2019.

[12] J. Young, R. Berger, and J. Breese, "Accelerated curing of compacted calcium silicate mortars on exposure to co2," *Journal of the american ceramic society*, vol. 57, no. 9, pp. 394–397, 1974.

[13] W. Klemm and R. Berger, "Accelerated curing of cementitious systems by carbon dioxide: Part i. portland cement," *Cement and Concrete Research*, vol. 2, no. 5, pp. 567–576, 1972.

[14] R. L. Berger and W. Klemm, "Accelerated curing of cementitious systems by carbon dioxide: Part ii. hydraulic calcium silicates and aluminates," *Cement and concrete Research*, vol. 2, no. 6, pp. 647–652, 1972.

[15] C. Shi and Y. Wu, "Studies on some factors affecting co2 curing of lightweight concrete products," *Resources, Conservation and Recycling*, vol. 52, no. 8-9, pp. 1087–1092, 2008.

[16] J. Zhang, C. Shi, Y. Li, X. Pan, C.-S. Poon, and Z. Xie, "Performance enhancement of recycled concrete aggregates through carbonation," *Journal of Materials in Civil Engineering*, vol. 27, no. 11, p. 04015029, 2015.

[17] R. Berger, J. Young, and K. Leung, "Acceleration of hydration of calcium silicates by carbon dioxide treatment," *Nature Physical Science*, vol. 240, no. 97, pp. 16–18, 1972.

[18] M. A. Venhuis and E. J. Reardon, "Vacuum method for carbonation of cementitious wasteforms," *Environmental science & technology*, vol. 35, no. 20, pp. 4120–4125, 2001.

[19] S. Kashef-Haghighi and S. Ghoshal, "Co2 sequestration in concrete through accelerated carbonation curing in a flow-through reactor," *Industrial & engineering chemistry research*, vol. 49, no. 3, pp. 1143–1149, 2010.

[20] Y. Shao, S. Monkman, and A. Boyd, "Recycling carbon dioxide into concrete: a feasibility study," in *ProceedingS of the 2010 Concrete Sustainability Conference*, 2010.

[21] G. Jónsson and O. Wallevik, "Information on the use of concrete in denmark, sweden, norway and iceland," *Icelandic Build. Res. Inst*, 2005.

[22] S. Jacobsen *et al.*, "Tkt 4215 concrete technology 1," *Trondheim: Norwegian University of Science and Technology-Department of Structural Engineering*, 2009.

[23] D. W. Pfeifer, "High performance concrete and reinforcing steel with a 100-year service life," *PCI journal*, vol. 45, no. 3, 2000.

[24] C. Cheng-Feng and C. Jing-Wen, "Strength and elastic modulus of carbonated concrete," *ACI materials journal*, vol. 102, no. 5, p. 315, 2005.

[25] J. J. Chang, W. Yeih, R. Huang, and J. M. Chi, "Mechanical properties of carbonated concrete," *Journal of the Chinese Institute of Engineers*, vol. 26, no. 4, pp. 513–522, 2003.

[26] W. Dias, "Reduction of concrete sorptivity with age through carbonation," *Cement and Concrete Research*, vol. 30, no. 8, pp. 1255–1261, 2000.

[27] H.-W. Song and S.-J. Kwon, "Permeability characteristics of carbonated concrete considering capillary pore structure," *Cement and Concrete Research*, vol. 37, no. 6, pp. 909–915, 2007.

[28] M. Collepardi, S. Collepardi, J. O. Olagot, and F. Simonelli, "The influence of slag and fly ash on the carbonation of concrete," in *Proc. of 8th CANMET/ACI Int. Conf. on Fly Ash, Silica Fume, Slag, and Natural Pozzolans in Concrete, held May*, pp. 23–29, 2004.

[29] H. T. Toennies, "Artificial carbonation of concrete masonry units," in *Journal Proceedings*, vol. 56, pp. 737–756, 1960.

[30] J. Young, R. Berger, and J. Breese, "Accelerated curing of compacted calcium silicate mortars on exposure to co2," *Journal of the american ceramic society*, vol. 57, no. 9, pp. 394–397, 1974.

[31] C. J. Goodbrake, J. F. Young, and R. L. Berger, "Reaction of beta-dicalcium silicate and tricalcium silicate with carbon dioxide and water vapor," *Journal of the American Ceramic Society*, vol. 62, no. 3-4, pp. 168–171, 1979.

[32] S. Kashef-Haghighi, Y. Shao, and S. Ghoshal, "Mathematical modeling of co2 uptake by concrete during accelerated carbonation curing," *Cement and concrete research*, vol. 67, pp. 1–10, 2015.

[33] S. Monkman and Y. Shao, "Assessing the carbonation behavior of cementitious materials," *Journal of Materials in Civil Engineering*, vol. 18, no. 6, pp. 768–776, 2006.

[34] N. DeCristofaro, V. Meyer, S. Sahu, J. Bryant, and F. Moro, "Environmental impact of carbonated calcium silicate cement-based concrete," in *Proceedings of 1st International Conference on Construction Materials for Sustainable Future, CoMS, Zadar, Croatia*, 2017.

[35] C. Shi, F. He, and Y. Wu, "Effect of pre-conditioning on co2 curing of lightweight concrete blocks mixtures," *Construction and Building materials*, vol. 26, no. 1, pp. 257–267, 2012.

[36] T. Zhang and O. E. Gjørv, "An electrochemical method for accelerated testing of chloride diffusivity in concrete," *Cement and Concrete Research*, vol. 24, no. 8, pp. 1534–1548, 1994.

[37] R. L. Berger and W. Klemm, "Accelerated curing of cementitious systems by carbon dioxide: Part ii. hydraulic calcium silicates and aluminates," *Cement and concrete Research*, vol. 2, no. 6, pp. 647–652, 1972.

[38] Q.-y. ZOU, C.-j. SHI, K.-r. ZHENG, and F.-q. HE, "Effect of pre-conditioning on co2 curing of block concretes," *Journal of Building Materials*, vol. 1, p. 024, 2008.

[39] C. Shi, Q. Zou, and F. He, "Study on co2 curing kinetics of concrete," *Journal of the Chinese Ceramic Society*, vol. 7, pp. 1179–84, 2010.

[40] Y. Leng, *Materials characterization : introduction to microscopic and spectroscopic methods*. Weinheim, Germany : Wiley-VCH, 2013.

[41] Bruker, "Handheld xrf: How it works." `https://www.bruker.com/products/x-ray-diffraction-and-elemental-analysis/handheld-xrf/how-xrf-works.html`, 2017.

[42] Bedwani, "X=ray fluorescence spectroscopy." `http://www.bedwani.ch/xrf/xrf_1/xrf.htm`, 2017.

[43] UCL, "University college london ucl-spectra emission line overlap checker." `https://www.ucl.ac.uk/archmat/tools/emission.php`, 2007.

[44] C. Yi, J. Shi, X. L. Zhao, W. H. Zhao, Q. Liu, and H. X. Liu, "Comprehensive assessment of green degree of building material using fuzzy ahp," in *Applied mechanics and materials*, vol. 71, pp. 769–777, Trans Tech Publ, 2011.

[45] M. Mahoutian, Z. Ghouleh, and Y. Shao, "Carbon dioxide activated ladle slag binder," *Construction and Building Materials*, vol. 66, pp. 214–221, 2014.

[46] V. S. Ramachandran and J. J. Beaudoin, *Handbook of analytical techniques in concrete science and technology: principles, techniques and applications*. Elsevier, 2000.

[47] C. J. Goodbrake, J. F. Young, and R. L. Berger, "Reaction of beta-dicalcium silicate and tricalcium silicate with carbon dioxide and water vapor," *Journal of the American Ceramic Society*, vol. 62, no. 3-4, pp. 168–171, 1979.

[48] P. Mounanga, A. Khelidj, A. Loukili, and V. Baroghel-Bouny, "Predicting ca (oh) 2 content and chemical shrinkage of hydrating cement pastes using analytical approach," *Cement and Concrete Research*, vol. 34, no. 2, pp. 255–265, 2004.

[49] J. I. Bhatty, "Hydration versus strength in a portland cement developed from domestic mineral wastes—a comparative study," *Thermochimica acta*, vol. 106, pp. 93–103, 1986.

[50] J. Rivera Lozano, "La hidratación de la pasta de cemento con adiciones activas," *PhD, Universidad Autónoma de Madrid*, 2004.

[51] A. S. for Testing and A. C. Material, "Standard test methods for chemical analysis of limestone, quicklime and hydrated lime," *Annual book of ASTM standards 4.01*, p. 36, 2006.

[52] W. Sha, E. O'Neill, and Z. Guo, "Differential scanning calorimetry study of ordinary portland cement," *Cement and Concrete Research*, vol. 29, no. 9, pp. 1487–1489, 1999.

[53] P. He, C. Shi, Z. Tu, C. S. Poon, and J. Zhang, "Effect of further water curing on compressive strength and microstructure of co2-cured concrete," *Cement and Concrete Composites*, vol. 72, pp. 80–88, 2016.

[54] Z. He, S. Wang, M. Mahoutian, and Y. Shao, "Flue gas carbonation of cement-based building products," *Journal of CO2 Utilization*, vol. 37, pp. 309–319, 2020.

Appendix

Appendix A - p.100

- Speedy Moisture Test Procedure
- pH Test Procedure

Appendix B - p.109

- Heat and Relative Humidity Development
- CO_2 Uptake % by Mass Curve Method
- 1-day Compressive Strength
- 14-days Compressive Strength
- TGA (Just one page as an example due to the large data)
- Porosity and Hardened Density

Appendix C - p.119

- SEM Images
- EDS Results

Appendix D - p.157

- Norcem Industrisement CEM I 52,5 R, Product Data
- Superplasticizer Porduct Data

Appendix A

- Speedy Moisture Test Procedure

1. SCOPE

1.1. Description of Test

This method describes the procedure for determining the moisture content of soils and other materials. The reaction of water with calcium carbide produces acetylene gas which activates a pressure gauge that is calibrated to read as percent moisture.

2. APPARATUS AND MATERIALS

2.1. Equipment Required

Speedy moisture test kit which includes, scoop, balance, speedy moisture meter, measuring spoon, steel balls, speedy absorbent, weights, small brush.

3. PROCEDURE

3.1. Test Procedure

Set up apparatus as shown on diagram in kit.

Clean the cap and body of moisture meter with brush.

Place three measures of speedy absorbent into body of moisture meter and also the two steel balls.

Weigh 26 grams of soil for testing - (the scale is calibrated to balance at exactly 26 g) and place sample to be tested in cap of meter.

With meter in horizontal position put cap on and tighten clamp.

Tip speedy meter to vertical position so absorbent contacts the soil, then return it to the horizontal position. Holding it with both hands, begin a circular motion so that balls are put into orbit inside the meter. Rotate for 10 seconds - rest for 20 seconds.

Repeat rotate - rest cycle until dial remains constant (usually about 3 minutes).

Hold meter in horizontal position and read dial when it comes to rest.

With speedy meter in vertical position carefully release pressure away from you, then empty contents and clean apparatus.

If moisture is in excess of 20%, then use half sample weight (13 grams). Use weight provided for this purpose, then follow same procedure except that the reading is multiplied by two.

4. RESULTS AND CALCULATIONS

4.1. Calculations

The reading on the dial is the moisture content based on the wet-weight of soil. Convert it to the dry-weight basis with the following formula.

$$\%\ Moist_{(DryWt.)} = \frac{\%Moist_{(WetWt.)}\ x100}{100 - \%Moist_{(Wet.Wt.)}}$$

4.2. R
Reporting Results

Report results on Form MR-20.

5. ADDED INFORMATION

Since the sample for moisture content is very small, great care must be taken to make sure the sample is representative.

This test is usually accurate to within about 1 or 2% of the true moisture content. If greater accuracy is required, use the oven dry method (STP 205-3).

Two problems often occur with the apparatus so be aware of them: one is the pressure gauge which may lose its calibration and the second is the tiny passage between the main chamber and the pressure gauge, which may become plugged. To avoid erroneous results, compare several speedy meter tests to duplicate oven-dry tests. If the difference is substantial, return the speedy meter to the central laboratory for repairs.

The steel balls in the main chamber are used to pulverize and mix the soil and absorbent. They should be put in orbit around the circumference of the chamber. Never use an end to end motion because the balls will seal off the opening to the pressure gauge by riveting it closed.

Because the dial readings give moisture content based on wet weight of soil, the results are lower than our normal dry-weight based tests. Below 10% the results are "close enough", but at 20%, the tests are 5% low, so corrections are needed. Use the formula given under "CALCULATIONS" to prepare a chart showing corrected moisture content for each dial reading.

- pH Test Procedure

Testing pH of Concrete

Need for a standard procedure

BY JENNIFER A. GRUBB, HEMANT S. LIMAYE, AND ASHOK M. KAKADE

Although concrete typically begins its life at a highly basic pH of about 13, the pH values at exposed surfaces soon fall as reactions occur between carbon dioxide from the atmosphere and alkalis in the concrete—a process known as carbonation. Over time, fronts of carbonated concrete, with pH values of about 8.5, advance below exposed surfaces.

It may be necessary to determine the depth of this front, as carbonated concrete can allow corrosion of reinforcing steel. This can be done by spraying a phenolphthalein indicator solution onto a fractured or cut surface of the concrete and noting the location of a color change. In this case, the color change occurs when the solution contacts a material with a pH of 9 to 9.5. The depth of the carbonation front can also be evaluated by using a drill to collect samples at selected depths. In this case, the pH of the powdered samples can be evaluated using the standard test methods described in the following sections.

It may also be necessary to evaluate the pH of a concrete floor surface, as the adhesives used to install vinyl flooring or carpet tiles can be damaged when applied to substrates with pH values exceeding 9 (many flooring manufacturers won't issue a warranty on their installed products unless the pH has been verified to be within acceptable ranges). Although paragraph 5.3 in ASTM F 710-05, "Standard Practice for Preparing Concrete Floors to Receive Resilient Flooring,"[1] indicates a procedure to be used to test concrete floors for alkalinity, we believe the procedure isn't adequate. We therefore propose an alternate standard procedure for testing the pH of concrete.

The information in this article was originally presented at the ACI Fall 2004 Convention, San Francisco, CA.

FUNDAMENTALS OF pH

pH is an approximate measure of acidity or alkalinity of a solution and is defined as the negative logarithm of the hydrogen ion (H^+) concentration. As the pH of a solution increases, the number of free hydrogen ions decreases, and a change in pH of one reflects a tenfold change in the H^+ concentration. For example, there are 10 times as many hydrogen ions available at a pH of 7 than at a pH of 8. The pH scale ranges from 0 to 14, and a pH of 7 is considered to be neutral. Substances with a pH less than 7 are acidic and substances with a pH greater than 7 are basic.

The following are examples showing the relationship between H^+ concentration and pH for various solutions:

- In a hydrogen chloride solution, or hydrochloric acid, the H^+ concentration is 1×10^{-2}, and the pH is 2;
- In water, the H^+ concentration is 1×10^{-7}, and the pH is 7;
- In saturated calcium hydroxide, the H^+ concentration is about $1 \times 10^{-12.4}$, and the pH is about 12.4; and
- In sodium hydroxide solution, the H^+ concentration is 1×10^{-14}, and the pH is 14.

Because pH is a measure of a solution, accurately measuring the pH of a solid substance such as concrete is a challenging task.

TABLE 1:
Reported pH values for concrete-related materials

Category	pH
Fresh cement	>12.5
Low alkali cement	12.7 to 13.1
High alkali cement	13.5 to 13.9
High alumina cement	11.4 to 12.5
Mixing water for concrete	6 to 9
Sea water	7.5 to 8.4
Hardened cement paste with ingress of sea water	12.0
Range of phenolphthalein solution (colorless to red)	8 to 10
Class F fly ash	>13.2
Silica fume slurry (equal mass of water & silica fume)	5.5
Reduction in pH due to 10% silica fume	0.5
Reduction in pH due to 20% silica fume	1.0
pH of silica fume concrete	>12.5

EVALUATION

Our evaluation included a literature survey, an informal survey of professionals and associations, and assessment of test standards and methods, including pH strips, pH pencils, and digital meters. In addition, we also quantified the influence of procedural variables on the measured test results.

Literature survey

Our literature survey revealed that there is plenty of literature available concerning the pH of concrete as it relates to carbonation, embedded steel corrosion, alkali-silica reaction, and the effects of mineral admixtures. There are, however, few published papers related to the measurement of concrete pH, especially with regard to a standard procedure. In addition, most of the literature doesn't indicate the procedures followed to measure the pH. Some of the reported pH values are summarized in Table 1.

Informal survey

We used telephone and e-mail surveys of leading petrographers, various trade associations, and test laboratory personnel to determine the procedures now commonly used to measure concrete pH. Although pH-indicating strips reportedly are the most widely used method, most respondents didn't indicate the use of a specific dilution ratio. Some petrographers did indicate they use the procedure provided in ASTM C 25[2] with a pH probe and digital meter, and personnel at a few testing laboratories reported that they measure concrete pH using a pH pencil.

Standards review

As stated previously, to measure the pH of solid materials such as lime, soil, or concrete, an aqueous solution of the powdered material must be created—this dilutes the concentration of the solid material. A review of various standards and commentaries indicates that dilution ratios vary between 1:9 and 1:20. The following are summaries of the methods used in the publications we reviewed:

- ASTM C 25, "Standard Test Methods for Chemical Analysis of Limestone, Quicklime, and Hydrated Lime"[2]: Mix 10 g (0.35 oz) of sample with 200 mL (6.8 fl oz) of deionized water. Stir for 30 minutes, and let the solution stand for 30 minutes. Measure pH with a pH probe and meter. Report pH value to four significant figures;
- ASTM F 710, "Standard Practice for Preparing Floors to Receive Resilient Flooring"[1]: Place several drops of distilled or deionized water on a clean concrete surface to form an approximately 25 mm (1 in.) diameter circle. After 60 ± 5 seconds, measure pH using a pH strip; and
- ICRI Guideline No. 03740, "Guideline for Inorganic Repair Material Data Sheet Protocol"[3]: Mix 10 g (0.35 oz) of sample passed through the 90 µm (No. 170) sieve with 90 g (3.2 oz) of distilled or deionized water for 1 minute. After settling, measure pH using pH paper or a pH probe and meter.

Influence of variables

We designed our experimental program to observe the effects of major variables such as the type of concrete, sample size, and dilution ratio. We also conducted a limited number of tests for other variables such as soaking or waiting time, sample gradation, and temperature. Our samples were prepared using cement paste; mortar; concrete with 0, 15, and 50% cement replacement by weight with fly ash; or concrete from an old sidewalk. The samples were pulverized using a vibratory micro-mill. Sample sizes of 5, 10, and 20 g (0.18, 0.35, and 0.71 oz) were diluted with distilled water, using dilution ratios of 1:1, 1:2, 1:4, 1:9, 1:20, and 1:50 before testing for pH. The pH readings were obtained using either a pH probe with a digital meter or pH strips. The prepared solution was not stirred during the measurement process.

TEST RESULTS AND DISCUSSION

Type of sample

The measured pH values for various mixtures of cement paste, mortar, and concrete are listed in Table 2. All of the prepared samples were less than 2 months old at the time of testing except for the sample from a 20-year-old exposed concrete sidewalk. The tests were conducted using 5 g (0.18 oz) samples with a dilution ratio of 1:2. The highest pH of 12.71 was obtained for cement paste with a water-cementitious material ratio (*w/cm*) of 0.40. The lowest pH of 10.45 was obtained for the 20-year-old sidewalk sample.

Amount of sample

For each type of mixture, pH was measured using 5, 10, and 20 g (0.18, 0.35, and 0.71 oz) of material with various dilution ratios. Sample graphs are shown in Fig. 1 to 4. The difference in pH was less than 0.30.

TABLE 2:
MEASURED pH VALUES FOR VARIOUS CONCRETE MATERIALS

Material	Measured pH*
0.4 *w/cm* cement paste	12.71
0.4 *w/cm* mortar	12.69
0.4 *w/cm* concrete	12.62
0.55 *w/cm* concrete	12.49
Concrete with 15% fly ash (0.45 *w/cm*)	12.58
Concrete with 50% fly ash (0.45 *w/cm*)	12.37
Concrete from 20-year-old sidewalk	10.45

*All values are for sample size of 5 g (0.18 oz) and dilution ratio of 1:2.

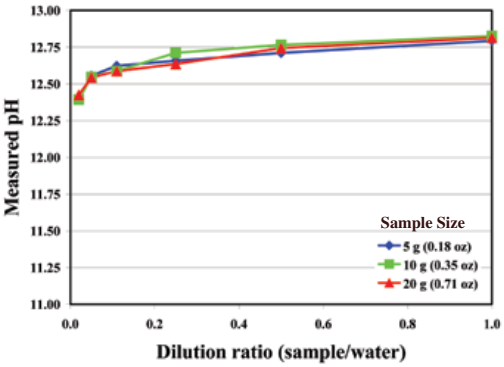

Fig. 1: Measured pH versus dilution ratio for cement paste with a 0.4 *w/cm*

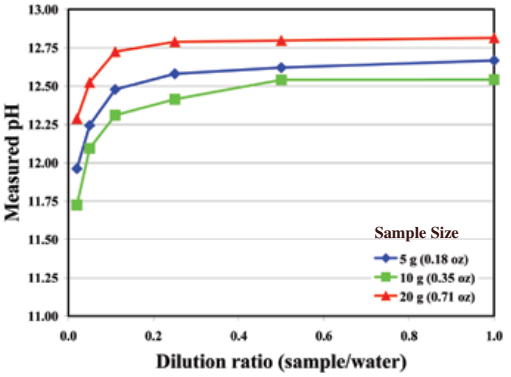

Fig. 2: Measured pH versus dilution ratio for concrete with a 0.4 *w/cm*

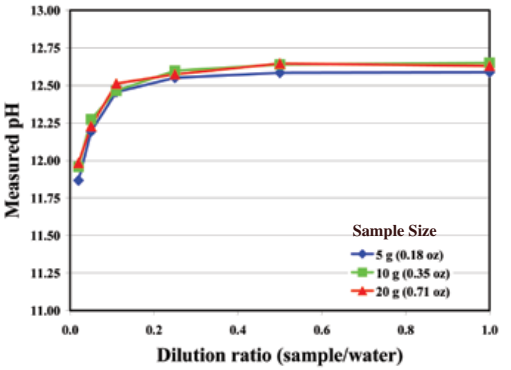

Fig. 3: Measured pH versus dilution ratio for concrete with 15% cement replacement by weight with fly ash

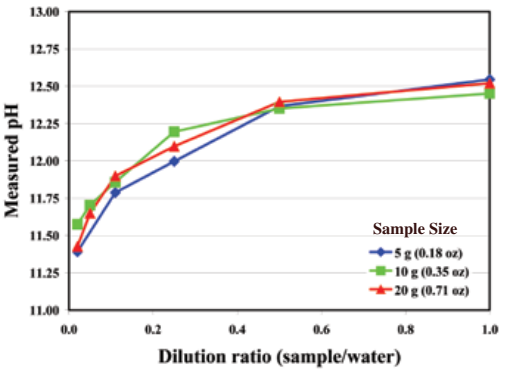

Fig. 4: Measured pH versus dilution ratio for concrete with 50% cement replacement by weight with fly ash

Dilution ratio

Figures 1 to 5 also show the effects of dilution ratio on pH values for various materials. The trend of increasing pH as the dilution ratio decreases from 1:50 to 1:1 is similar for all mixtures.

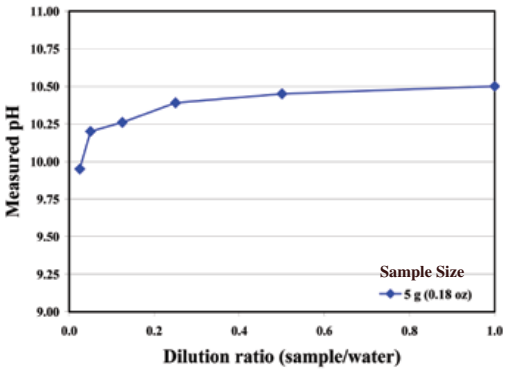

Fig. 5: Measured pH versus dilution ratio for carbonated concrete sample from a 20-year-old sidewalk

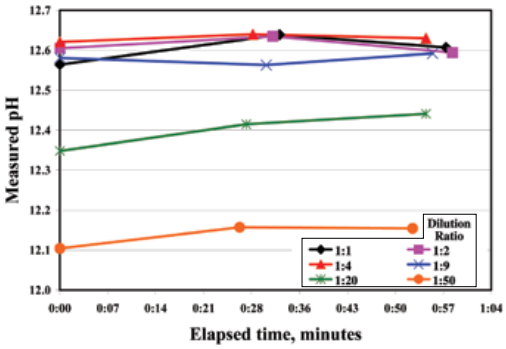

Fig. 6: Measured pH versus elapsed time for concrete with 0.4 *w/cm*

Soaking period

The graph in Fig. 6 illustrates the short time (1 hour) effect of soaking time on pH as a function of dilution ratio for a concrete sample. The change in pH was insignificant (less than 0.15) for all dilution ratios.

Sample gradation

Tests were conducted using powdered samples obtained from concrete with a *w/cm* of 0.40 and no fly ash. The pH measurements were conducted on the portion of the sample that was retained on the 2.00 mm (No. 10) sieve (large particles), the portion passing the 2.00 mm (No. 10) sieve and retained on the 850 µm (No. 20) sieve (intermediate particles), and the portion passing the 850 µm (No. 20) sieve (small particles) using a dilution ratio of 1:2. The pH values for the large particle size portion and the small particle size portion were found to be 11.55 and 12.48, respectively. Although the difference in pH was nearly 0.93, the pH of the combined sample was 12.37, indicating that it's not necessary to obtain a sample passing through the 850 µm (No. 20) sieve. The particle size distribution of the sample and measured pH values are shown in Table 3.

Temperature

Raising the temperature of a saturated solution of calcium hydroxide from 0 to 60 °C (32 to 140 °F) has been reported to decrease measured pH from 13.423 to 11.449.[4] The graph in Fig. 7 shows the effect of temperature found in the test program over a narrow temperature range.

COMPARISON OF TEST METHODS

The pH of a concrete slab was measured using a pH pencil, a pH probe with digital meter, and pH strips using the procedure indicated in ASTM F 710. As shown in Table 4, the measured values varied between 10 and 12. Color change obtained using a pH pencil (Fig. 8) was difficult to judge, as it was confusing to distinguish between the color match for pH values of 10 and 13.

To measure the pH of the slab with a pH probe and meter, a 0.3 g (0.011 oz) sample of concrete powder was obtained by sanding the surface, and the sample was mixed with 6 mL (0.2 fl oz) of distilled water. The mixture was contained in a sealed ring on the concrete slab (Fig. 9). With this method, a pH of 11.5 was obtained for a dilution ratio of 1:20.

When the procedure described in ASTM F 710 was used on a clean concrete surface, a pH of 10 was measured (Fig. 10). To improve the accuracy of the ASTM F 710 procedure,

TABLE 3:
EFFECT OF PARTICLE SIZE ON pH FOR A 5 g (0.18 oz) SAMPLE OF CONCRETE WITH A 0.4 *w/cm* USING A 1:2 DILUTION RATIO

Particle size	Distribution, %	Measured pH
Small, passing 850 µm (No. 20) sieve	59.6	12.48
Intermediate, passing 2.00 mm (No. 10) sieve and retained on 850 µm (No. 20) sieve	19.2	11.87
Large, retained on 2.00 mm (No. 10) sieve	21.2	11.55
Combined	100	12.37

a powdered sample of the concrete was collected by sanding the surface of the slab. The measurement was then taken using a pH strip dipped into the mixture. This procedure resulted in a measured pH of 12 for the same concrete. Even though pH values of 10 and 12 appear to be close, it should be noted that a pH value of 10 could be considered carbonated concrete, while a pH of 12 could be considered non-carbonated concrete.

TABLE 4:
COMPARISON OF TEST METHODS TO MEASURE SURFACE pH OF A CONCRETE SLAB

Method	Measured pH
ASTM F 710	10
Proposed method	12
pH pencil	?*
pH probe and meter	11.5

*Color change obtained using a pH pencil was difficult to judge, as it was confusing to distinguish between the color match for pH values of 10 and 13.

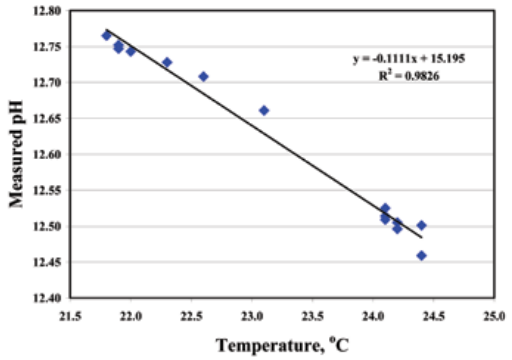

Fig. 7: Measured pH versus temperature

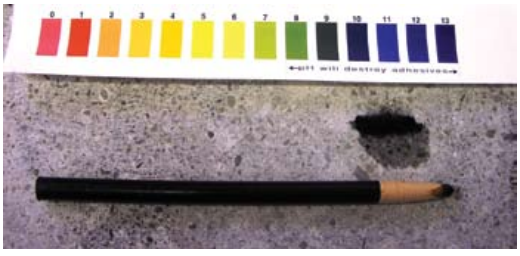

Fig. 8: Measuring pH using a pH pencil. It's difficult to distinguish color differences for pH values from 10 to 13

In another field test, the pH of a slab that had been previously tested by others using the ASTM F 710 procedure was found to have a pH of 7. The same slab was found to have a pH of 9 when the slab was sanded to obtain a powdered sample before conducting the ASTM F 710 procedure.

DISCUSSION AND CONCLUSIONS

Based on the test results from this study, dilution ratio and temperature have the greatest effect on measured pH values. All other factors such as particle size, amount of sample, and soaking time have less influence on the measured pH value. The use of a dilution ratio of 1:2 seems practical to make the pH measurement.

The pH measured on a powdered concrete sample of a slab was significantly different than the pH measured using the ASTM F 710 procedure. This shows that placing a few drops of deionized water on an undisturbed concrete surface is not enough to form a solution containing concrete particles. It's therefore our opinion that the procedure

Fig. 9: Measuring pH using a pH probe with a digital meter. Here, the pH is shown to be 11.53

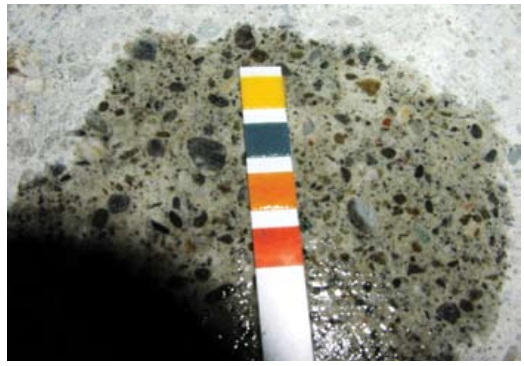

Fig. 10: The pH of clean concrete surface is measured using a pH strip and the procedure provided in ASTM F 710. Here, the pH is shown to be 10

provided in ASTM F 710 doesn't provide a true indication of concrete pH, and the procedure should be modified.

The experience gained during our testing program also showed that it's not convenient to measure the pH of the concrete slab with a pH probe with a meter. The probe that we used needs at least 6 mL (0.2 fl oz) of solution to measure pH. At a dilution ratio of 1:2, this requires 3 g (0.11 oz) of powdered sample. Sanding a concrete surface to obtain this much powder is time-consuming and laborious. Therefore, we recommend that the probe and meter be used only in a laboratory with a larger concrete sample.

Because floor adhesive is only in contact with the surface of the concrete slab, flooring industry personnel are only interested in measuring the pH of the concrete surface. To achieve proper adhesion of resilient flooring, most manufacturers recommend abrasive cleaning or bead blasting of the slab to remove surface residue. Therefore, it makes sense to measure pH by sanding the surface of the slab. For carbonation and embedded steel corrosion-related issues, it's necessary to measure the pH of the concrete at various depths with more precision. Therefore, it's our opinion that two different procedures are needed: one for using pH strips to measure the pH of the concrete surface in the field, and one for using a pH probe to measure the pH at various depths within the concrete in the laboratory.

RECOMMENDED TEST PROCEDURES

Field test for pH measurement of a concrete surface

- Clean the surface using a wire brush. Be sure to remove dirt, concrete sealer, and old adhesive residue;
- Gather 0.5 g (0.018 oz) of concrete powder by hand sanding an approximately 50 x 50 mm (2 x 2 in.) area with 50-grit general-purpose sandpaper;
- Thoroughly mix the concrete powder with 10 to 12 drops of fresh distilled water with a small, flat plastic stirrer. Let stand for 60 seconds;
- Insert a pH strip into the mixture. Compare the strip to the color chart to determine the pH; and
- Note the temperature of the concrete surface.

Laboratory test for pH measurement of concrete

- Calibrate the pH probe and meter using the manufacturer's directions and appropriate buffer solutions;
- Collect 5 g (0.18 oz) of concrete powder at the required depth using a drill;
- Use a plastic stirrer to mix the concrete powder with 10 mL (0.34 fl oz) of fresh distilled water at a temperature of 22 ± 1 °C (72 ± 2 °F);
- Filter the mixture using No. 40 filter paper;
- Insert the pH probe into the mixture. Read the pH to one decimal place; and
- Note the temperature of the mixture.

Acknowledgments

The authors are grateful for the comments and opinions provided by persons who responded to the e-mails and telephone calls of our informal survey.

References

1. ASTM F 710-05, "Standard Practice for Preparing Concrete Floors to Receive Resilient Flooring," ASTM International, West Conshohocken, PA, 2005, 6 pp.

2. ASTM C 25-06, "Standard Test Methods for Chemical Analysis of Limestone, Quicklime, and Hydrated Lime," ASTM International, West Conshohocken, PA, 2006, 36 pp.

3. Guideline No. 03740, "Guideline for Inorganic Repair Material Data Sheet Protocol," International Concrete Repair Institute, Des Plaines, IL, 2003, 10 pp. (Available at http://www.icri.org/committees/03740DataSheetProtocol_11082004_linenumberedDraft.pdf)

4. Bates, R.G., *Determination of pH—Theory and Practice*, 2nd Edition, John Wiley & Sons, New York, NY, 1973, 479 pp.

Selected for reader interest by the editors after independent expert evaluation and recommendation.

Jennifer A. Grubb performed the testing for this research in 2004 while an intern at Concrete Science, Inc., Hayward, CA, and is now an Engineer at Simpson Gumpertz & Heger, Inc., Boston, MA. She received her BS in civil engineering from Cornell University in 2003 and her ME in structural materials from the University of California at Berkeley in 2005.

ACI member **Hemant S. Limaye** is a Principal Engineer with Concrete Science, Inc. He is also a member of the American Society of Mechanical Engineers. His interests include nondestructive methods, sensors, instrumentation, and testing methodologies.

ACI member **Ashok M. Kakade** is a Principal Engineer with Concrete Science, Inc., where he is a professional engineer involved in the evaluation of and repair recommendations for concrete structures. He is also a member of ASTM International, the American Society of Civil Engineers, and the International Concrete Repair Institute.

Appendix B

- Cement Paste data logger

>>Logging Name:RH cement paste
>>Sample Points:98
>>Sample Rate:300 sec.
>>Temperature Unit:Celsius

NO.	Time(minute)	TEMPERATURE	RELATIVE-HUMIDITY
1	0	34.8	60.1
2	5	36.7	60.8
3	10	38.4	61.5
4	15	40	61.8
5	20	41.4	62.5
6	25	42.6	63.2
7	30	43.8	63.7
8	35	44.9	64.2
9	40	46	64.5
10	45	47	64.7
11	50	47.9	64.3
12	55	48.8	64.5
13	60	49.5	64.6
14	65	50.1	64.6
15	70	50.6	64.5
16	75	51.1	64.4
17	80	51.4	64
18	85	51.8	63.6
19	90	52	63.2
20	95	52.2	62.5
21	100	52.3	61.9
22	105	52.4	61.2
23	110	52.4	60.5
24	115	52.4	60
25	120	52.3	59.6
26	125	52.1	59.2
27	130	52	58.9
28	135	51.8	58.5
29	140	51.6	58.3
30	145	51.4	58.2
31	150	51.2	58
32	155	50.9	57.9
33	160	50.6	57.8
34	165	50.4	57.7
35	170	50.1	57.6
36	175	49.8	57.6
37	180	49.6	57.5
38	185	49.3	57.4
39	190	49.1	57.3
40	195	48.7	57.1
41	200	48.4	57

42	205	48.2	56.8
43	210	47.9	56.7
44	215	47.2	55.9
45	220	45.2	88.4
46	225	43.6	79.9
47	230	33.5	79.9
48	235	38.4	74.8
49	240	39.7	62.7
50	245	39.6	62.2
51	250	39.5	61.9
52	255	39.3	61.7
53	260	39.1	61.5
54	265	38.8	61.4
55	270	38.5	61.2
56	275	38.2	61
57	280	37.9	60.8
58	285	37.6	60.6
59	290	37.4	60.4
60	295	37.1	60.2
61	300	36.8	60
62	305	36.5	59.8
63	310	36.3	59.6
64	315	36	59.4
65	320	35.8	59.2
66	325	35.6	58.9
67	330	35.4	58.7
68	335	35.1	58.5
69	340	34.9	58.4
70	345	35.1	56.3
71	350	34.7	56
72	355	34.4	55.8
73	360	34.2	55.7
74	365	34	55.6
75	370	33.8	55.4
76	375	33.6	55.3
77	380	33.4	55.2
78	385	33.2	55.1
79	390	33	55
80	395	32.9	54.9
81	400	32.7	54.9
82	405	32.5	54.8
83	410	32.4	54.7
84	415	32.2	54.6
85	420	32.1	54.5
86	425	31.9	54.4
87	430	31.7	54.3
88	435	31.6	54.2

89	440	31.4	54.2
90	445	31.3	54.1
91	450	31.2	54
92	455	31	53.9
93	460	30.9	53.9
94	465	30.7	53.8
95	470	30.6	53.8
96	475	30.5	53.7
97	480	30.4	53.6
98	485	28.6	68.2

- Cement Mortar data logger

>>Logging Name:RH cement mortar
>>Sample Points:99
>>Sample Rate:300 sec.
>>Temperature Unit:Celsius

NO.	Time(minutes)	TEMPERATURE	RELATIVE-HUMIDITY
1	0	27.5	59.3
2	5	39.7	61.8
3	10	42.9	63.8
4	15	43.6	64.3
5	20	43.5	64.3
6	25	43.1	64.1
7	30	42.5	63.6
8	35	42	62.2
9	40	41.5	62
10	45	41.1	61.8
11	50	40.7	61.7
12	55	40.3	61.5
13	60	40	61.3
14	65	39.7	61.1
15	70	39.4	60.9
16	75	39.1	60.7
17	80	38.8	60.5
18	85	38.5	60.3
19	90	38.3	60.1
20	95	38	60
21	100	37.8	59.8
22	105	37.5	59.6
23	110	37.4	59.4
24	115	37.1	59.2
25	120	36.9	59
26	125	36.7	58.8
27	130	36.5	58.6
28	135	36.3	58.5
29	140	36.1	58.3
30	145	36	58.2
31	150	35.8	58
32	155	35.6	58
33	160	35.4	57.8
34	165	35.2	57.7
35	170	35.1	57.6
36	175	34.9	57.5
37	180	34.7	57.4
38	185	34.6	57.3
39	190	34.4	57.2
40	195	34.2	57.1
41	200	34.1	57.1
42	205	33.9	57

43	210	33.8	56.9
44	215	33.7	56.8
45	220	33.5	56.7
46	225	33.4	56.6
47	230	33.2	56.6
48	235	33.1	56.5
49	240	28	89.1
50	245	26.6	86.3
51	250	32.9	56.4
52	255	32.8	56.3
53	260	32.7	56.3
54	265	32.5	56.2
55	270	32.4	56.2
56	275	32.3	56.1
57	280	32.2	56
58	285	32	56
59	290	31.9	55.9
60	295	31.8	55.9
61	300	31.7	55.8
62	305	31.6	55.8
63	310	31.4	55.7
64	315	31.3	55.6
65	320	31.2	55.6
66	325	31.1	55.6
67	330	31	55.5
68	335	30.9	55.5
69	340	30.7	56.1
70	345	30.2	54.4
71	350	29.7	54.1
72	355	29.5	54.1
73	360	29.4	53.9
74	365	29.3	53.5
75	370	29.2	53.1
76	375	29	52.9
77	380	28.9	52.8
78	385	28.8	52.6
79	390	28.7	52.6
80	395	28.6	52.5
81	400	28.4	52.5
82	405	28.4	52.4
83	410	28.3	52.4
84	415	28.2	52.3
85	420	28.1	52.3
86	425	28.1	52.3
87	430	27.9	52.2
88	435	27.9	52.2
89	440	27.8	52.2

90	445	27.7	52.1
91	450	27.6	52.1
92	455	27.5	52
93	460	27.5	52
94	465	27.4	51.9
95	470	27.3	51.9
96	475	27.3	51.8
97	480	27.2	51.8
98	485	27.1	51.7
99	490	27.1	51.7

- CO_2 uptake % (mass curve method)

	scale value (g)
First 4 H of curing (cement paste)	
after vacuum in the beginning	0
injecting CO2 after 4 hours	360
vacuum in the end	260
Second 4 H of curing (cement paste)	
after vacuum in the beginning	0
injecting CO2 after 4 hours	120
vacuum in the end	20
First 4 H of curing (mortar)	
after vacuum in the beginning	0
injecting CO2 after 4 hours	300
vacuum in the end	160
Second 4 H of curing (mortar)	
after vacuum in the beginning	0
injecting CO2 after 4 hours	100
vacuum in the end	10

Cement paste	total cement amount in chamber (kg) in first 4 H	3.177
	CO2 uptake by cement weight after first 4 H	8.18%
	total cement amount in chamber (kg) in second 4 H	1.588
	CO2 uptake by cement weight after second 4 H	1.26%
	Total CO2 uptake by cement weight	9.44%
Mortar	total cement amount in chamber (kg) in first 4 H	1.16
	CO2 uptake by cement weight after first 4 H	13.79%
	total cement amount in chamber (kg) in second 4 H	0.58
	CO2 uptake by cement weight after second 4 H	1.72%
	Total CO2 uptake by cement weight	15.51%

- 1-day compressive strength test

Cement Paste w/c=0.3	Sample 1	Sample 2	Sample 3	Mean
Reference	40.62	43.71	42.14	42.15666667
4 Hours of CO2 Curing	53.95	62.15	59.12	58.40666667
8 Hours of CO2 Curing	59.35	63.5	Error	61.425
Cement Paste w/c=0.6				
Reference	20.7	19.2	18.89	19.59666667
4 hours of carbonation curing	20.22	21.03	20.34	20.53
8 hours of carbonation curing	19.49	23.23	18.64	20.45333333
Cement Mortar w/c=0.3				
Reference	15.43	12.98	14.3	14.23666667
4 hours of carbonation curing	27.43	26.52	Error	26.975
8 hours of carbonation curing	32.07	33.62	30.55	32.08
Cement Mortar w/c=0.6				
Reference	15.14	14.48	14.45	14.69
4 hours of carbonation curing	19.99	18.61	18.04	18.88
8 hours of carbonation curing	20.17	21.51	Error	20.84

- 14-day compressive strength test

Cement Paste w/c=0.3	Sample 1	Sample 2	Sample 3	Mean
Reference	59.7	65.99	62.82	62.83666667
4 Hours of CO2 Curing	55.25	71.15	77.1	67.83333333
8 Hours of CO2 Curing	74.95	64.84	72.13	70.64
Cement Paste w/c=0.6				
Reference	27.85	27.17	26.51	27.17666667
4 hours of carbonation curing	28.06	28.45	29.15	28.55333333
8 hours of carbonation curing	30.33	30.43	30.87	30.54333333
Cement Mortar w/c=0.3				
Reference	20.32	23.5	17.18	20.33333333
4 hours of carbonation curing	33.57	27.12	30.69	30.46
8 hours of carbonation curing	Error	38.35	33.53	35.94
Cement Mortar w/c=0.6				
Reference	33.5	33.54	31.49	32.84333333
4 hours of carbonation curing	33.17	30.65	29.96	31.26
8 hours of carbonation curing	32.09	33.68	33.7	33.15666667

- An example of TGA data

Huge amount of data cannot be fitted in the appendix

CM,0.6,R					CM,0.6,4C					CM,0.6,8C				
Temperatur [°C]	HF [mW]	Masse [mg]	DTG [%/°C]	Masse [%]	Temperatur [°C]	HF [mW]	Masse [mg]	DTG [%/°C]	Masse [%]	Temperatur [°C]	HF [mW]	Masse [mg]	DTG [%/°C]	Masse [%]
27.7254	-7.4096	42.5116	-0.009132	100	26.6971	-7.7202	64.3311	-0.016575	100	27.8654	-7.8895	50.2945	-0.033613	100
27.7473	-7.4166	42.5114	0.025641	99.9995295	26.7152	-7.7221	64.3308	-0.045977	99.9995337	27.8773	-7.8926	50.2941	-0.666667	99.9992047
27.7395	-7.4227	42.5112	-0.016760	99.9990591	26.7239	-7.7234	64.3304	-0.012739	99.9989119	27.8779	-7.8927	50.2937	-0.043103	99.9984094
27.7574	-7.4295	42.5109	-0.041667	99.9983534	26.7553	-7.7244	64.3300	-0.222222	99.9982901	27.8895	-7.8912	50.2932	-0.041667	99.9974152
27.7646	-7.4382	42.5106	-0.018750	99.9976477	26.7580	-7.7280	64.3294	-0.029412	99.9973574	27.9039	-7.8928	50.2926	-0.045455	99.9962223
27.7806	-7.4430	42.5103	-0.024845	99.996942	26.7750	-7.7293	64.3289	-0.200000	99.9965802	27.9171	-7.8922	50.2920	-0.187500	99.9950293
27.7967	-7.4447	42.5099	-0.078947	99.9960011	26.7775	-7.7329	64.3284	-0.059524	99.995803	27.9203	-7.8906	50.2914	-1.000000	99.9938363
27.8005	-7.4460	42.5096	-0.026490	99.9952954	26.7859	-7.7378	64.3279	-0.022388	99.9950257	27.9209	-7.8883	50.2908	-2.000000	99.9926433
27.8156	-7.4490	42.5092	0.041096	99.9943545	26.8127	-7.7432	64.3273	-0.030303	99.9940931	27.9212	-7.8804	50.2902	-0.026316	99.9914504
27.8083	-7.4531	42.5089	-0.024691	99.9936488	26.8292	-7.7452	64.3268	-0.038961	99.9933158	27.9440	-7.8779	50.2896	-0.066667	99.9902574
27.8245	-7.4574	42.5085	-0.045977	99.9927079	26.8446	-7.7463	64.3262	-0.052632	99.9923832	27.9515	-7.8768	50.2891	#DIV/0!	99.9892632
27.8332	-7.4606	42.5081	-0.119048	99.991767	26.8560	-7.7468	64.3256	-0.018868	99.9914505	27.9515	-7.8749	50.2885	-0.043478	99.9880703
27.8374	-7.4632	42.5076	-0.020513	99.9905908	26.8825	-7.7465	64.3251	-0.750000	99.9906733	27.9653	-7.8713	50.2879	0.250000	99.9868773
27.8569	-7.4650	42.5072	-0.714286	99.9896499	26.8833	-7.7468	64.3245	-0.049587	99.9897406	27.9629	-7.8659	50.2873	-0.035928	99.9856843
27.8576	-7.4655	42.5067	-0.056818	99.9884737	26.8954	-7.7481	64.3239	-0.022321	99.9888079	27.9796	-7.8608	50.2867	-0.545455	99.9844913
27.8664	-7.4658	42.5062	-0.071429	99.9872976	26.9178	-7.7511	64.3234	-0.042017	99.9880307	27.9807	-7.8566	50.2861	-0.037975	99.9832984
27.8720	-7.4613	42.5058	-0.046296	99.9863567	26.9297	-7.7520	64.3229	-0.044776	99.9872534	27.9965	-7.8515	50.2855	-0.833333	99.9821054
27.8828	-7.4593	42.5053	-0.200000	99.9851805	26.9431	-7.7510	64.3223	-0.038168	99.9863208	27.9971	-7.8463	50.2850	-0.086957	99.9811113
27.8853	-7.4601	42.5048	-0.025974	99.9840044	26.9562	-7.7493	64.3218	-0.029762	99.9855435	28.0040	-7.8426	50.2844	-0.049180	99.9799183
27.9007	-7.4606	42.5044	-0.052632	99.9830634	26.9730	-7.7460	64.3213	-0.048077	99.9847663	28.0162	-7.8383	50.2838	1.500000	99.9787253
27.9083	-7.4568	42.5040	0.097561	99.9821225	26.9834	-7.7409	64.3208	-0.020921	99.9839891	28.0158	-7.8321	50.2832	0.200000	99.9775323

- Porosity and density of cement paste

	Cement Paste w/c: 0.3			Cement Paste w/c: 0.6		
	Reference	4H carbonation	8H carbonation	Reference	4H carbonation	8H carbonation
g1 [kg]	0.22327	0.23225	0.2278	0.14974	0.16756	0.16501
g2 [kg]	0.26222	0.26802	0.26254	0.20666	0.2241	0.2181
g3 [kg]	0.127	0.126	0.123	0.116	0.122	0.117
g4 [kg]	0.26734	0.27293	0.26719	0.20899	0.22646	0.22038
Normal density	2064.72441	2127.142857	2134.471545	1781.55172	1836.885246	1864.102564
Difference %		3.02%	3.38%		3.11%	4.63%
Volume [m^3]	0.000127	0.000126	0.000123	0.000116	0.000122	0.000117
Dry density	1758.03	1843.25	1852.03	1290.86	1373.44	1410.34
Difference %		4.85%	5.35%		6.40%	9.26%
Solid density	2692.271	2722.105	2724.554	2638.590	2655.468	2677.430
Difference %		1.11%	1.20%		0.64%	1.47%
Suction porosity	0.307	0.284	0.282	0.491	0.463	0.454
Difference %		-7.44%	-7.91%		-5.55%	-7.53%
Macro porosity	0.040	0.039	0.038	0.020	0.019	0.019
Difference %		-3.34%	-6.23%		-3.69%	-2.98%
Total porosity	0.347	0.323	0.320	0.511	0.483	0.473
Difference %		-6.96%	-7.71%		-5.48%	-7.35%

- Porosity and density of mortar

	Mortar w/c: 0.3			Mortar w/c: 0.6		
	Reference	4H carbonation	8H carbonation	Reference	4H carbonation	8H carbonation
g1 [kg]	0.2272	0.2285	0.22958	0.23734	0.24587	0.25272
g2 [kg]	0.25652	0.2558	0.25682	0.26117	0.26763	0.27463
g3 [kg]	0.125	0.123	0.123	0.12	0.12	0.122
g4 [kg]	0.26846	0.2659	0.26678	0.26835	0.2738	0.28091
Normal density	2052.16	2079.674797	2087.96748	2176.41667	2230.25	2251.065574
Difference %		1.34%	1.74%		2.47%	3.43%
Volume [m³]	0.000125	0.000123	0.000123	0.00012	0.00012	0.000122
Dry density	1817.60	1857.72	1866.50	1977.83	2048.92	2071.48
Difference %		2.21%	2.69%		3.59%	4.73%
Solid density	2713.160	2669.393	2675.758	2667.041	2670.468	2693.956
Difference %		-1.61%	-1.38%		0.13%	1.01%
Suction porosity	0.235	0.222	0.221	0.199	0.181	0.180
Difference %		-5.38%	-5.58%		-8.69%	-9.56%
Macro porosity	0.096	0.082	0.081	0.060	0.051	0.051
Difference %		-14.03%	-15.23%		-14.07%	-13.97%
Total porosity	0.330	0.304	0.302	0.258	0.233	0.231
Difference %		-7.88%	-8.37%		-9.93%	-10.58%

Appendix C

- SEM Images

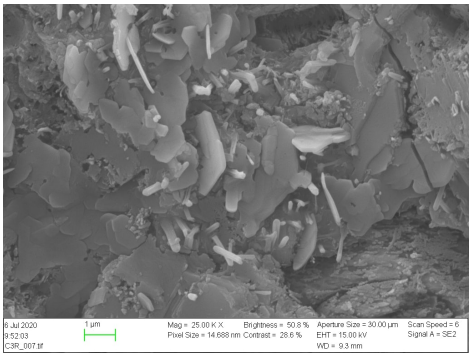

C_p w/c: 0.3, Reference

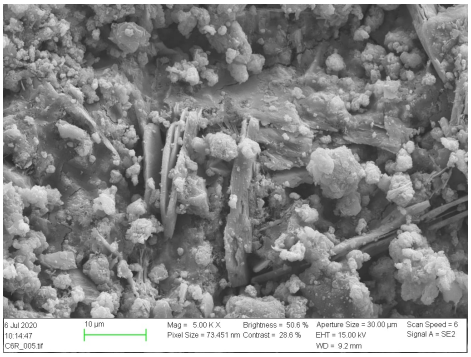

C_p w/c: 0.6, Reference

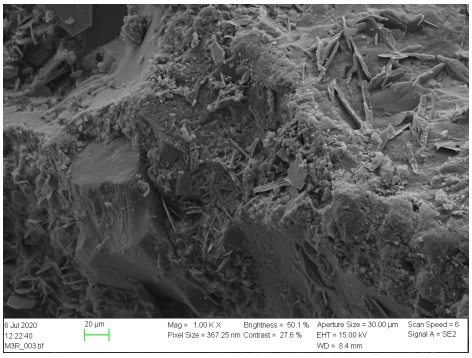

C_M w/c: 0.3, Reference

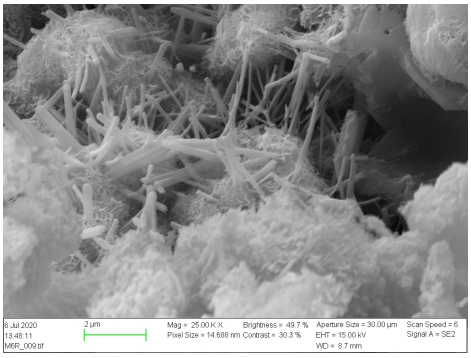

C_M w/c: 0.6, Reference

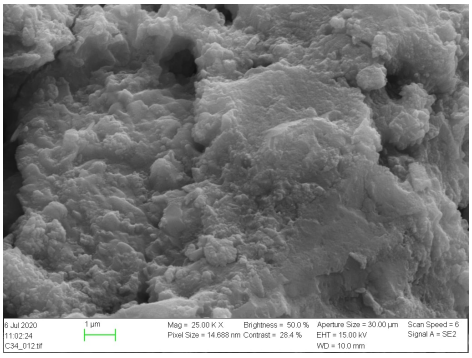

C_p w/c: 0.3, 4H carbonation

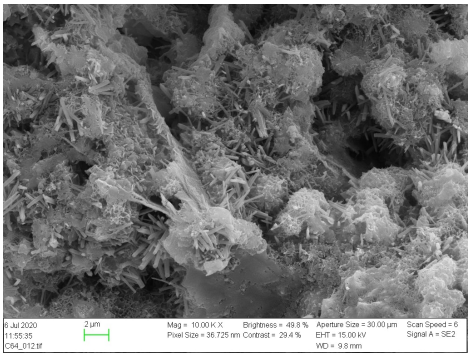

C_p w/c: 0.6, 4H carbonation

C_M w/c: 0.3, 4H carbonation

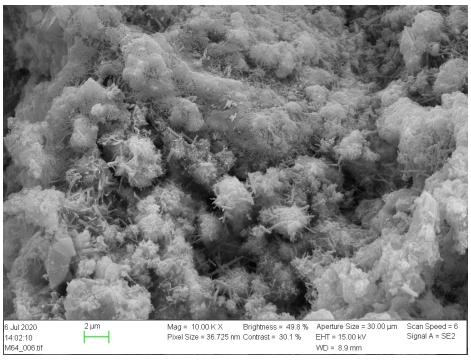

C_M w/c: 0.6, 4H carbonation

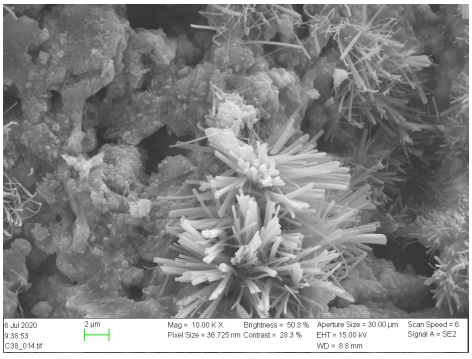

C_p w/c: 0.3, 8H carbonation

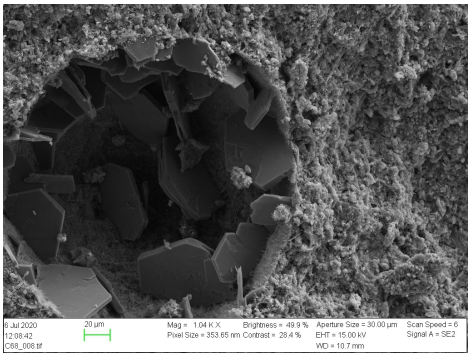

C_p w/c: 0.6, 8H carbonation

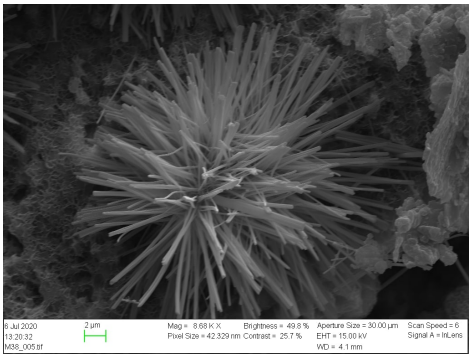

C_M w/c: 0.3, 8H carbonation

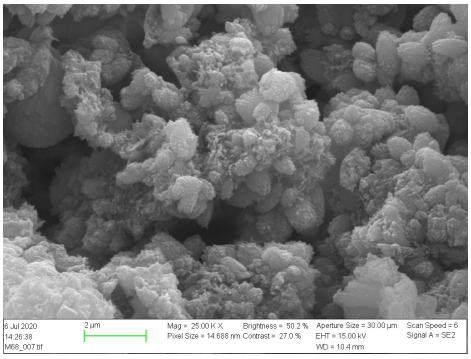

C_M w/c: 0.6, 8H carbonation

- EDS results
Cement paste, w/c:0.3, Reference

EDAX TEAM

Mohammad Cement 2020

Author: student
Creation: 07/06/2020 9:53:43 AM

Sample Name: C3R

Area 1

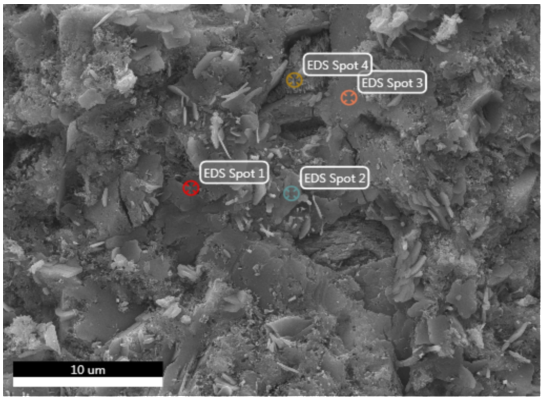

Notes:

EDS Spot 1

kV:	Mag:	Takeoff:	Live Time(s):	Amp Time(µs):	Resolution:(eV)
15	10000	36	30	7.68	125.8

EDS Spot 1 - Det 1

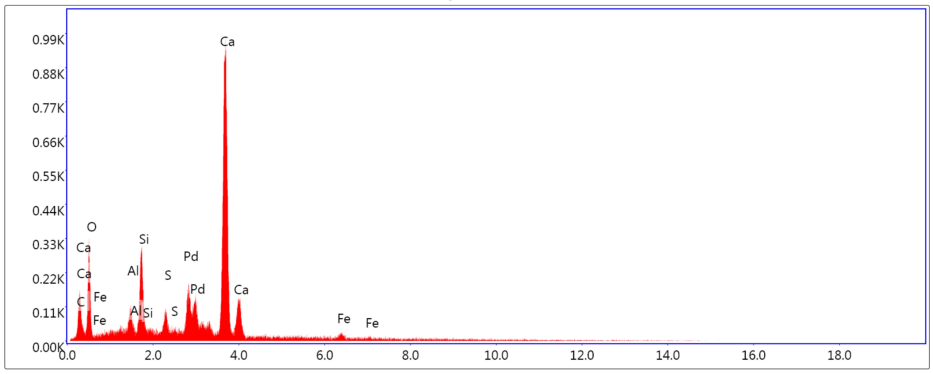

Lsec: 30.0 25 Cnts 2.025 keV Det: Octane Elite 25

eZAF Smart Quant Results with SEC (BCNOF_2017-09-14)

Element	Weight %	Atomic %	Net Int.	Error %	Kratio	Z	A	F
C K	0.86	1.93	2.92	80.91	0.0030	1.1640	0.3437	1.0000
O K	28.78	48.69	129.01	11.97	0.0397	1.1117	0.1402	1.0000
AlK	1.44	1.44	35.01	13.32	0.0089	0.9849	0.7096	1.0045
SiK	5.52	5.32	149.02	6.89	0.0397	1.0058	0.8031	1.0063
S K	1.89	1.59	41.33	12.96	0.0150	0.9837	0.9008	1.0160
CaK	58.73	39.67	757.53	2.66	0.4877	0.9456	0.9907	1.0027
FeK	2.79	1.35	14.38	33.48	0.0205	0.8368	0.9717	1.0222

EDS Spot 2

kV:	15	Mag: 10000	Takeoff: 36	Live Time(s): 30	Amp Time(µs): 7.68	Resolution:(eV) 125.8

EDS Spot 2 - Det 1

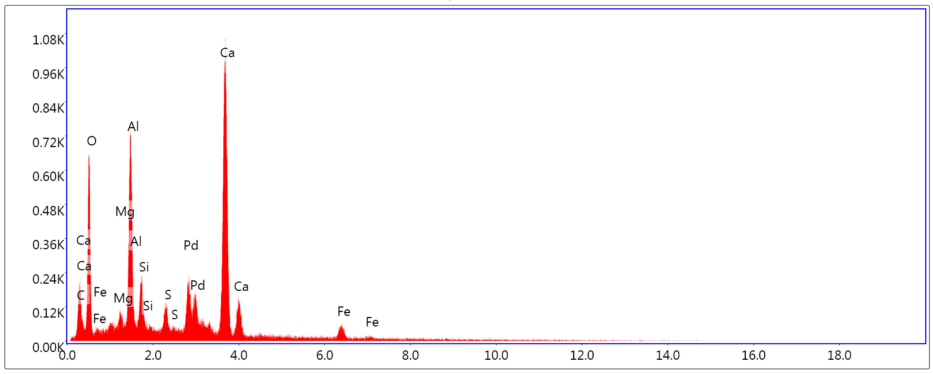

Lsec: 30.0 50 Cnts 2.025 keV Det: Octane Elite 25

eZAF Smart Quant Results with SEC (BCNOF_2017-09-14)

Element	Weight %	Atomic %	Net Int.	Error %	Kratio	Z	A	F
C K	1.91	3.93	8.16	38.21	0.0055	1.1511	0.2811	1.0000
O K	34.36	52.95	303.91	10.77	0.0607	1.0987	0.1809	1.0000
MgK	1.03	1.05	34.02	15.17	0.0055	1.0108	0.5902	1.0027
AlK	11.25	10.28	422.94	5.56	0.0700	0.9725	0.7164	1.0033
SiK	2.64	2.32	101.25	10.06	0.0175	0.9930	0.7484	1.0052
S K	2.03	1.56	66.12	11.15	0.0156	0.9710	0.8811	1.0132
CaK	41.84	25.74	820.82	2.83	0.3436	0.9329	0.9846	1.0052
FeK	4.94	2.18	39.27	17.31	0.0365	0.8247	0.9813	1.0254

EDS Spot 3

kV: 15 Mag: 10000 Takeoff: 36 Live Time(s): 30 Amp Time(µs): 7.68 Resolution:(eV) 125.8

EDS Spot 3 - Det 1

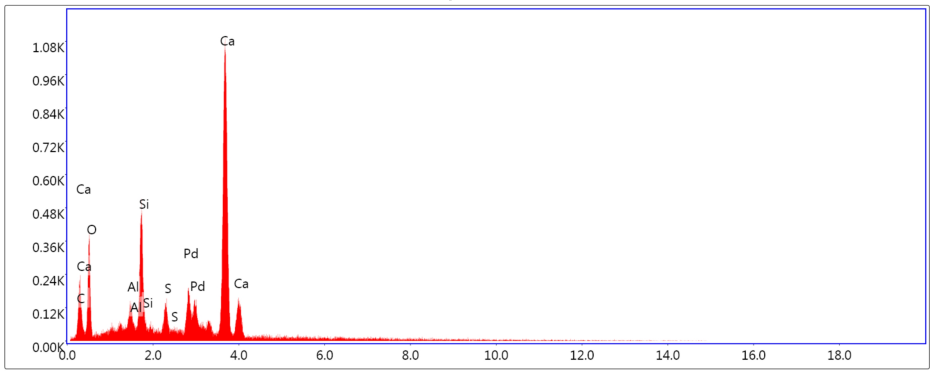

Lsec: 30.0 49 Cnts 2.025 keV Det: Octane Elite 25

eZAF Smart Quant Results with SEC (BCNOF_2017-09-14)

Element	Weight %	Atomic %	Net Int.	Error %	Kratio	Z	A	F
C K	1.96	4.24	6.99	39.53	0.0061	1.1550	0.3005	1.0000
O K	29.46	47.86	161.62	11.77	0.0416	1.1027	0.1434	1.0000
AlK	2.24	2.16	67.41	9.68	0.0144	0.9765	0.7302	1.0049
SiK	8.07	7.47	264.23	4.92	0.0590	0.9972	0.8143	1.0063
S K	2.98	2.42	77.51	10.91	0.0236	0.9751	0.8948	1.0153
CaK	55.29	35.86	848.80	2.60	0.4581	0.9371	0.9870	1.0018

EDS Spot 4

kV:	Mag:	Takeoff:	Live Time(s):	Amp Time(µs):	Resolution:(eV)
15	10000	36	30	7.68	125.8

EDS Spot 4 - Det 1

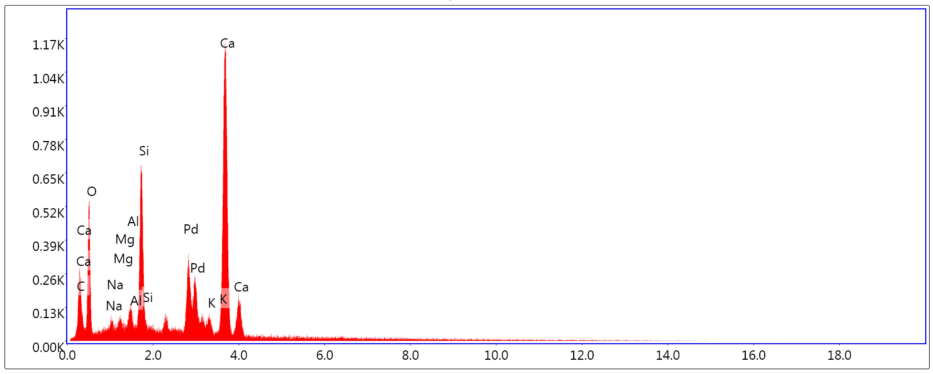

Lsec: 30.0 47 Cnts 2.025 keV Det: Octane Elite 25

eZAF Smart Quant Results with SEC (BCNOF_2017-09-14)

Element	Weight %	Atomic %	Net Int.	Error %	Kratio	Z	A	F
C K	0.01	0.02	0.03	99.99	0.0000	1.1517	0.3176	1.0000
O K	33.58	53.53	231.41	11.32	0.0483	1.0994	0.1553	1.0000
NaK	1.12	1.25	20.72	22.54	0.0041	0.9954	0.4382	1.0015
MgK	0.88	0.93	26.48	18.53	0.0045	1.0116	0.5914	1.0028
AlK	1.66	1.57	56.88	11.19	0.0098	0.9733	0.7186	1.0048
SiK	10.11	9.18	380.84	4.70	0.0688	0.9938	0.8089	1.0057
K K	2.14	1.40	47.98	13.07	0.0170	0.9178	0.9766	1.0545
CaK	50.50	32.14	895.71	2.65	0.3914	0.9337	0.9835	1.0021

Cement paste, w/c:0.6, Reference

EDAX TEAM

Mohammad Cement 2020

Author: student
Creation: 07/06/2020 10:13:22 AM

Sample Name: C6R

Area 1

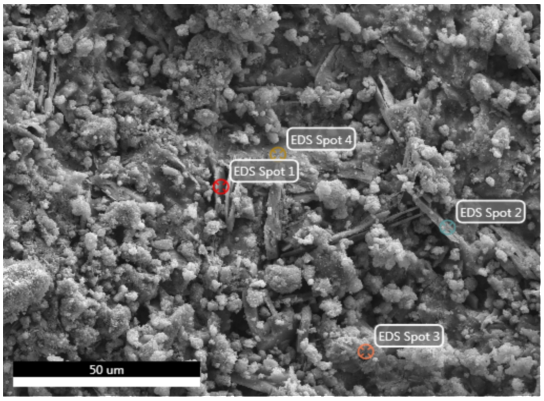

Notes:

EDS Spot 1

kV:	Mag:	Takeoff:	Live Time(s):	Amp Time(µs):	Resolution:(eV)
15	2500	35.8	30	7.68	125.8

EDS Spot 1 - Det 1

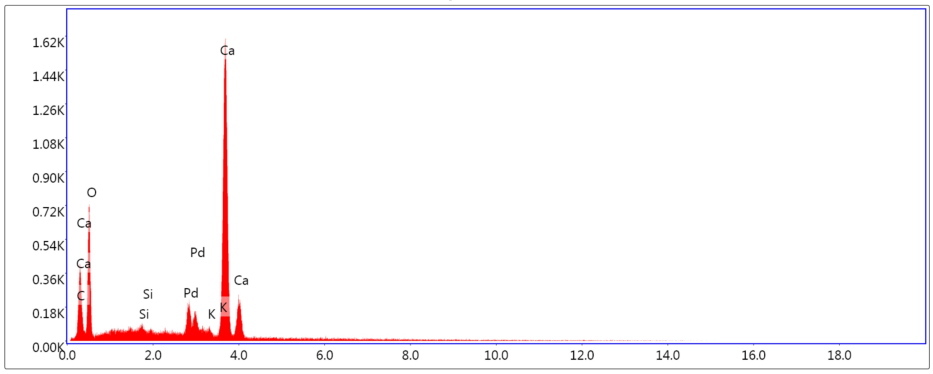

Lsec: 30.0 35 Cnts 2.025 keV Det: Octane Elite 25

eZAF Smart Quant Results with SEC (BCNOF_2017-09-14)

Element	Weight %	Atomic %	Net Int.	Error %	Kratio	Z	A	F
C K	0.00	0.01	0.03	99.99	0.0000	1.1457	0.4881	1.0000
O K	40.94	63.34	324.91	10.99	0.0608	1.0937	0.1486	1.0000
SiK	0.63	0.55	28.42	21.27	0.0046	0.9887	0.8067	1.0073
K K	1.10	0.69	30.53	16.37	0.0097	0.9131	0.9947	1.0673
CaK	57.33	35.41	1244.95	2.30	0.4872	0.9290	0.9999	1.0017

EDS Spot 2

kV:	Mag:	Takeoff:	Live Time(s):	Amp Time(µs):	Resolution:(eV)
15	2500	35.8	30	7.68	125.8

EDS Spot 2 - Det 1

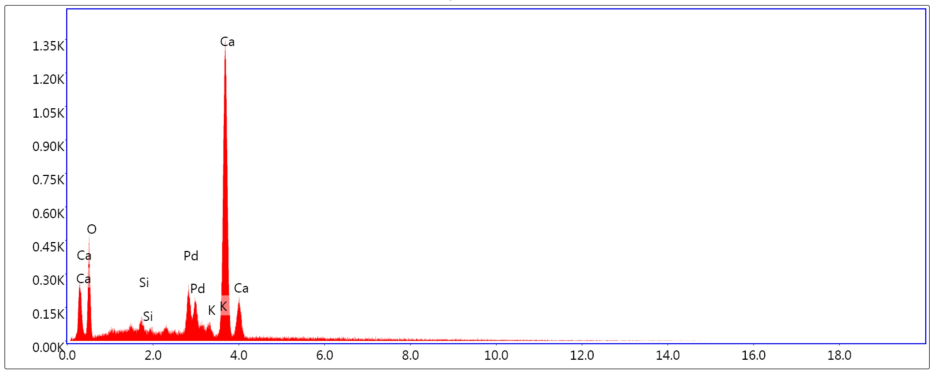

Lsec: 30.0 47 Cnts 2.025 keV Det: Octane Elite 25

eZAF Smart Quant Results with SEC (BCNOF_2017-09-14)

Element	Weight %	Atomic %	Net Int.	Error %	Kratio	Z	A	F
O K	34.36	56.56	186.27	11.71	0.0448	1.1051	0.1347	1.0000
SiK	1.02	0.95	34.77	17.01	0.0072	0.9997	0.8068	1.0073
K K	1.82	1.23	38.12	13.12	0.0156	0.9235	0.9935	1.0658
CaK	62.80	41.26	1025.75	2.40	0.5157	0.9397	0.9969	1.0014

EDS Spot 3

kV:	Mag:	Takeoff:	Live Time(s):	Amp Time(µs):	Resolution:(eV)
15	2500	35.8	30	7.68	125.8

EDS Spot 3 - Det 1

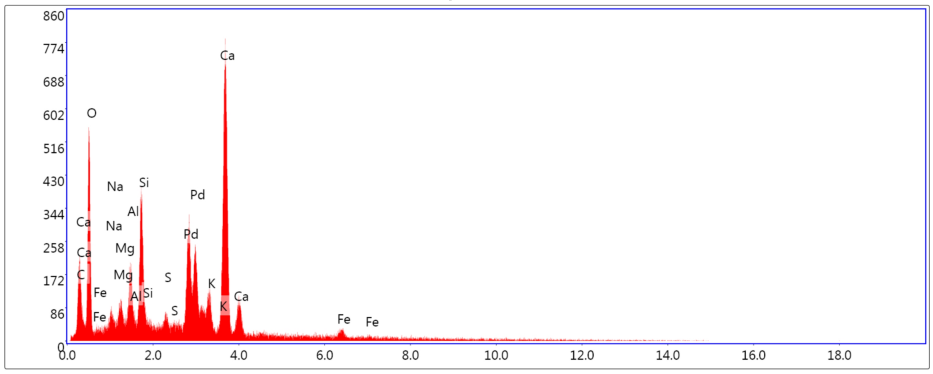

eZAF Smart Quant Results with SEC (BCNOF_2017-09-14)

Element	Weight %	Atomic %	Net Int.	Error %	Kratio	Z	A	F
C K	0.01	0.02	0.03	99.99	0.0000	1.1480	0.3105	1.0000
O K	38.15	58.63	246.64	11.09	0.0605	1.0957	0.1801	1.0000
NaK	1.07	1.15	15.49	28.91	0.0036	0.9920	0.4246	1.0014
MgK	1.35	1.36	31.94	15.62	0.0063	1.0080	0.5780	1.0025
AlK	3.36	3.06	91.20	9.11	0.0185	0.9699	0.7037	1.0042
SiK	6.89	6.03	204.46	5.88	0.0434	0.9903	0.7865	1.0055
S K	0.94	0.72	22.79	21.31	0.0066	0.9683	0.8853	1.0145
K K	4.07	2.56	73.06	10.39	0.0305	0.9144	0.9752	1.0456
CaK	40.56	24.88	580.11	3.16	0.2975	0.9302	0.9773	1.0045
FeK	3.60	1.58	21.04	27.57	0.0239	0.8223	0.9806	1.0264

EDS Spot 4

kV:	15	Mag: 2500	Takeoff: 35.8	Live Time(s): 30	Amp Time(µs): 7.68	Resolution:(eV) 125.8

EDS Spot 4 - Det 1

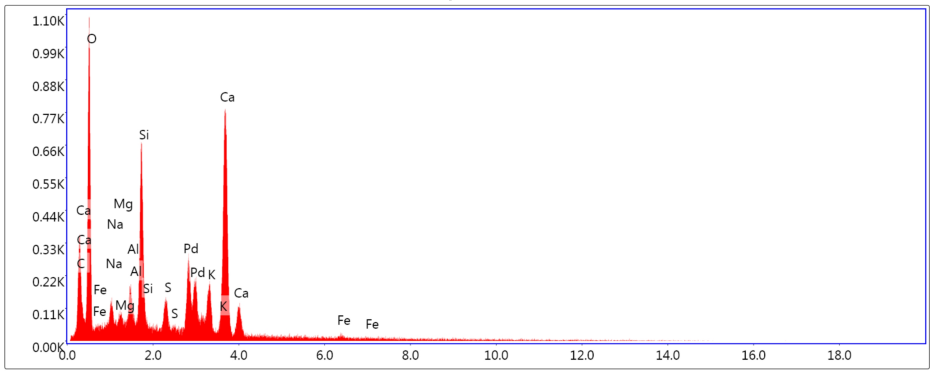

Lsec: 30.0 44 Cnts 2.025 keV Det: Octane Elite 25

eZAF Smart Quant Results with SEC (BCNOF_2017-09-14)

Element	Weight %	Atomic %	Net Int.	Error %	Kratio	Z	A	F
C K	0.01	0.01	0.03	99.99	0.0000	1.1303	0.2805	1.0000
O K	45.86	64.89	505.37	10.20	0.0902	1.0781	0.2126	1.0000
NaK	2.57	2.53	55.91	13.80	0.0095	0.9755	0.4422	1.0015
MgK	1.17	1.09	40.60	13.26	0.0058	0.9910	0.5871	1.0027
AlK	2.35	1.97	93.36	9.14	0.0138	0.9534	0.7134	1.0046
SiK	8.84	7.13	385.24	4.89	0.0595	0.9733	0.8009	1.0054
S K	2.24	1.58	77.65	11.71	0.0164	0.9514	0.8848	1.0136
K K	4.72	2.73	121.28	9.08	0.0368	0.8981	0.9723	1.0417
CaK	31.26	17.66	641.82	3.15	0.2397	0.9136	0.9735	1.0044
FeK	1.00	0.40	8.50	60.89	0.0070	0.8067	0.9860	1.0346

Cement paste, w/c:0.3, 8 hours carbonation

EDAX TEAM

Mohammad Cement 2020

Author: student
Creation: 07/06/2020 9:06:17 AM

Sample Name: C38

Area 1

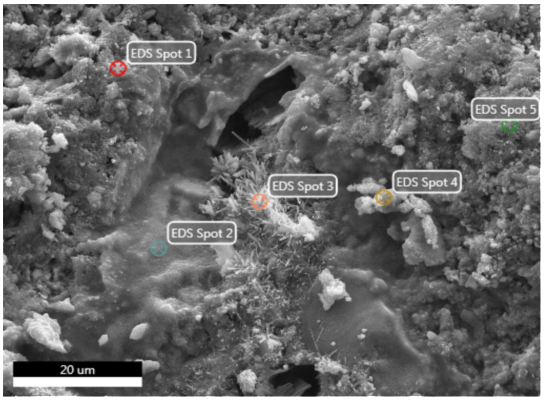

Notes:

EDS Spot 1

kV:	Mag:	Takeoff:	Live Time(s):	Amp Time(µs):	Resolution:(eV)
15	4305	35.6	30	7.68	125.8

EDS Spot 1 - Det 1

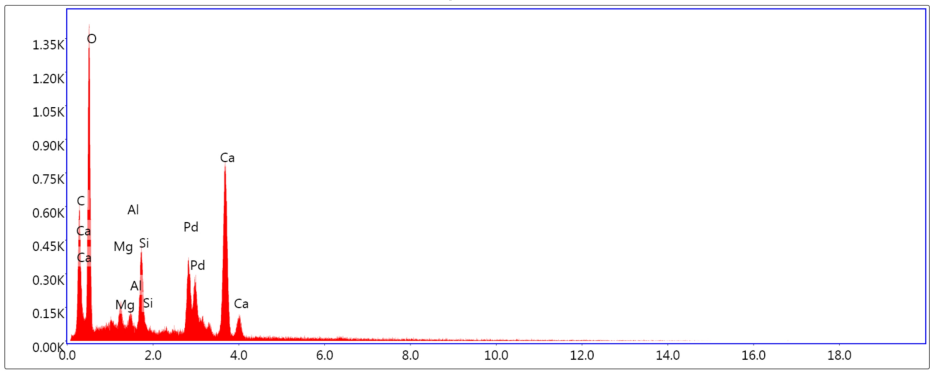

Lsec: 30.0 38 Cnts 2.025 keV Det: Octane Elite 25

eZAF Smart Quant Results with SEC (BCNOF_2017-09-14)

Element	Weight %	Atomic %	Net Int.	Error %	Kratio	Z	A	F
C K	10.24	16.51	68.43	11.69	0.0342	1.0978	0.3776	1.0000
O K	52.27	63.25	687.09	9.82	0.1014	1.0463	0.2303	1.0000
MgK	2.49	1.98	97.97	9.41	0.0116	0.9608	0.6024	1.0025
AlK	1.34	0.96	59.32	11.92	0.0072	0.9240	0.7193	1.0043
SiK	5.04	3.47	245.68	5.61	0.0313	0.9432	0.8132	1.0056
CaK	28.61	13.82	664.71	3.01	0.2047	0.8846	0.9993	1.0051

EDS Spot 2

kV:	15	Mag: 4305	Takeoff: 35.6	Live Time(s): 30	Amp Time(µs): 7.68	Resolution:(eV) 125.8

EDS Spot 2 - Det 1

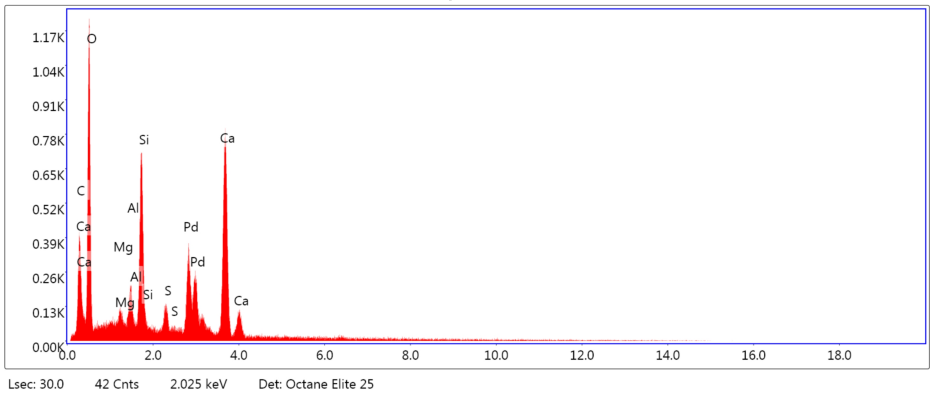

eZAF Smart Quant Results with SEC (BCNOF_2017-09-14)

Element	Weight %	Atomic %	Net Int.	Error %	Kratio	Z	A	F
C K	5.94	10.25	26.83	17.45	0.0152	1.1115	0.2800	1.0000
O K	47.98	62.21	555.97	10.02	0.0928	1.0597	0.2225	1.0000
MgK	1.80	1.54	65.86	10.66	0.0089	0.9735	0.6120	1.0029
AlK	2.73	2.10	112.07	8.02	0.0154	0.9364	0.7318	1.0048
SiK	9.63	7.11	428.35	4.70	0.0617	0.9559	0.8133	1.0052
S K	2.09	1.35	73.11	12.04	0.0144	0.9342	0.8878	1.0131
CaK	29.83	15.44	625.54	3.02	0.2179	0.8968	0.9880	1.0046

EDS Spot 3

kV:	15	Mag: 4305	Takeoff: 35.6	Live Time(s): 30	Amp Time(µs): 7.68	Resolution:(eV) 125.8

EDS Spot 3 - Det 1

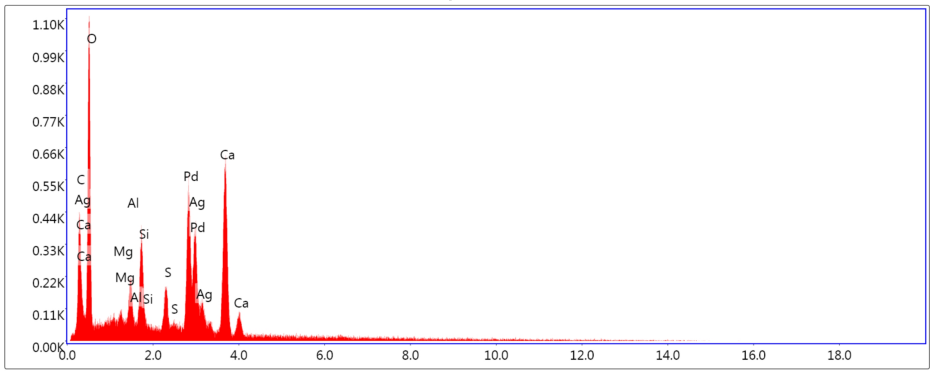

Lsec: 30.0 52 Cnts 2.025 keV Det: Octane Elite 25

eZAF Smart Quant Results with SEC (BCNOF_2017-09-14)

Element	Weight %	Atomic %	Net Int.	Error %	Kratio	Z	A	F
C K	6.40	11.31	31.48	14.98	0.0166	1.1263	0.3162	1.0000
O K	48.47	64.33	544.02	10.12	0.0849	1.0746	0.2234	1.0000
MgK	1.49	1.30	50.28	12.18	0.0063	0.9883	0.5872	1.0029
AlK	3.06	2.41	117.60	8.23	0.0151	0.9508	0.7109	1.0048
SiK	5.03	3.80	211.28	6.11	0.0285	0.9708	0.7938	1.0067
S K	3.23	2.14	110.98	9.69	0.0204	0.9492	0.8979	1.0161
AgL	7.27	1.43	100.79	11.93	0.0405	0.7082	1.0692	1.0098
CaK	25.06	13.28	496.87	3.65	0.1618	0.9118	0.9663	1.0041

EDS Spot 4

kV:	Mag:	Takeoff:	Live Time(s):	Amp Time(µs):	Resolution:(eV)
15	4305	35.6	30	7.68	125.8

EDS Spot 4 - Det 1

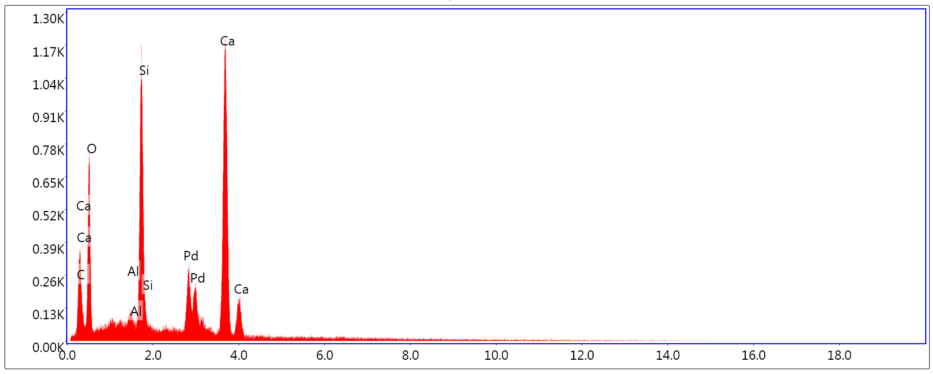

Lsec: 30.0 42 Cnts 2.025 keV Det: Octane Elite 25

eZAF Smart Quant Results with SEC (BCNOF_2017-09-14)

Element	Weight %	Atomic %	Net Int.	Error %	Kratio	Z	A	F
C K	4.66	9.00	22.41	17.95	0.0131	1.1337	0.2880	1.0000
O K	36.47	52.95	335.88	10.79	0.0581	1.0818	0.1706	1.0000
AlK	1.48	1.28	64.00	10.16	0.0091	0.9570	0.7409	1.0053
SiK	14.21	11.75	667.92	4.05	0.0998	0.9771	0.8282	1.0052
CaK	43.18	25.02	937.87	2.66	0.3386	0.9175	0.9872	1.0029

EDS Spot 5

kV:	Mag:	Takeoff:	Live Time(s):	Amp Time(µs):	Resolution:(eV)
15	4305	35.6	30	7.68	125.8

EDS Spot 5 - Det 1

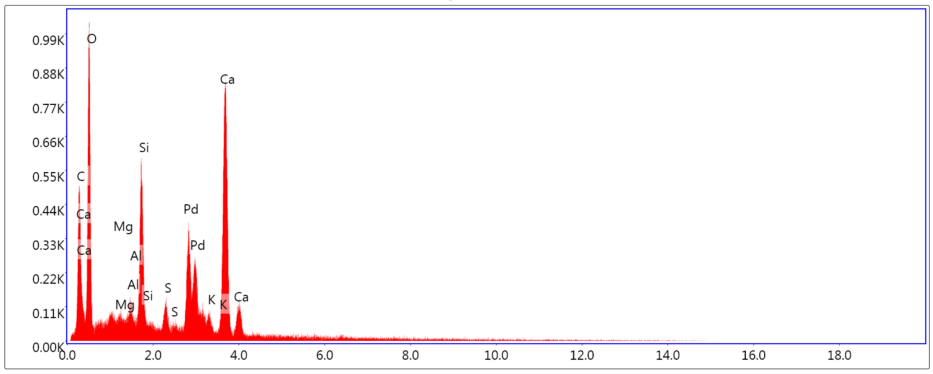

Lsec: 30.0 47 Cnts 2.025 keV Det: Octane Elite 25

eZAF Smart Quant Results with SEC (BCNOF_2017-09-14)

Element	Weight %	Atomic %	Net Int.	Error %	Kratio	Z	A	F
C K	2.06	3.74	9.36	99.99	0.0058	1.1210	0.3132	1.0000
O K	48.98	66.79	470.78	10.28	0.0862	1.0692	0.2050	1.0000
MgK	0.95	0.85	30.14	16.96	0.0044	0.9826	0.5934	1.0027
AlK	1.45	1.17	52.93	12.31	0.0080	0.9452	0.7221	1.0048
SiK	7.96	6.18	319.36	5.15	0.0505	0.9650	0.8143	1.0057
S K	1.71	1.16	54.44	12.04	0.0117	0.9432	0.8966	1.0146
K K	1.40	0.78	33.17	18.82	0.0103	0.8903	0.9787	1.0517
CaK	35.50	19.33	669.54	3.01	0.2559	0.9056	0.9873	1.0037

Cement paste, w/c:0.6, 4 hours carbonation

EDAX TEAM

Mohammad Cement 2020

Author: student
Creation: 07/06/2020 11:45:41 AM

Sample Name: C64

Area 1

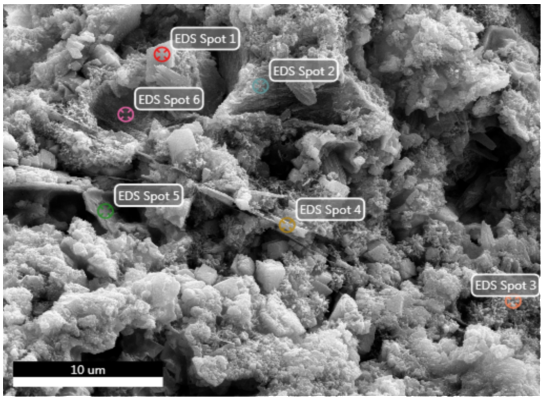

Notes:

EDS Spot 1

kV:	15	Mag: 10000	Takeoff: 37	Live Time(s): 30	Amp Time(µs): 7.68	Resolution:(eV) 125.8

EDS Spot 1 - Det 1

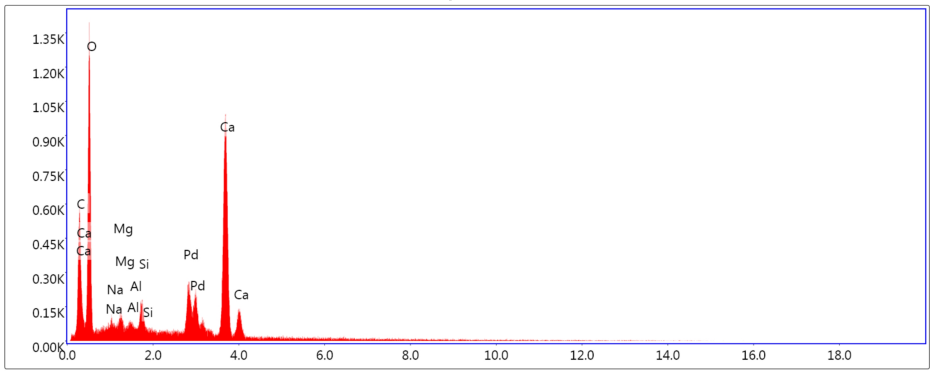

Lsec: 30.0 49 Cnts 2.025 keV Det: Octane Elite 25

eZAF Smart Quant Results with SEC (BCNOF_2017-09-14)

Element	Weight %	Atomic %	Net Int.	Error %	Kratio	Z	A	F
C K	6.62	11.21	49.70	12.31	0.0277	1.1081	0.4376	1.0000
O K	52.06	66.17	613.16	9.95	0.1020	1.0565	0.2150	1.0000
NaK	1.47	1.30	32.79	17.99	0.0052	0.9554	0.4329	1.0013
MgK	1.57	1.31	57.11	11.29	0.0077	0.9705	0.5863	1.0023
AlK	0.71	0.54	29.63	17.95	0.0041	0.9335	0.7113	1.0041
SiK	1.89	1.37	87.41	8.55	0.0127	0.9530	0.8103	1.0063
CaK	35.68	18.10	787.83	2.69	0.2768	0.8941	1.0022	1.0040

EDS Spot 2

kV:	Mag:	Takeoff:	Live Time(s):	Amp Time(µs):	Resolution:(eV)
15	10000	37	30	7.68	125.8

EDS Spot 2 - Det 1

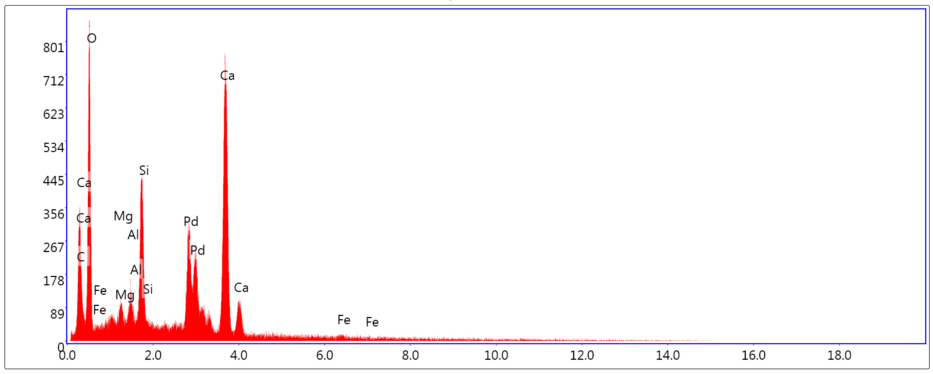

Lsec: 30.0 42 Cnts 2.025 keV Det: Octane Elite 25

eZAF Smart Quant Results with SEC (BCNOF_2017-09-14)

Element	Weight %	Atomic %	Net Int.	Error %	Kratio	Z	A	F
C K	5.29	9.48	24.50	16.97	0.0162	1.1197	0.3433	1.0000
O K	45.73	61.54	401.63	10.43	0.0795	1.0680	0.2037	1.0000
MgK	1.61	1.43	47.64	12.07	0.0077	0.9815	0.6033	1.0026
AlK	1.97	1.57	65.74	10.80	0.0108	0.9442	0.7251	1.0045
SiK	7.57	5.80	276.07	5.21	0.0477	0.9639	0.8127	1.0054
CaK	36.94	19.84	637.53	3.00	0.2666	0.9047	0.9941	1.0042
FeK	0.88	0.34	6.19	66.17	0.0057	0.7987	0.9869	1.0339

EDS Spot 3

kV: 15 Mag: 10000 Takeoff: 37 Live Time(s): 30 Amp Time(µs): 7.68 Resolution:(eV) 125.8

EDS Spot 3 - Det 1

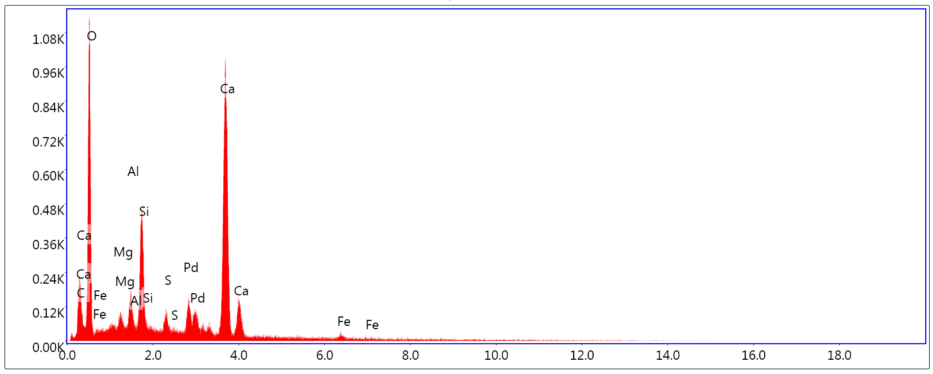

Lsec: 30.0 40 Cnts 2.025 keV Det: Octane Elite 25

eZAF Smart Quant Results with SEC (BCNOF_2017-09-14)

Element	Weight %	Atomic %	Net Int.	Error %	Kratio	Z	A	F
C K	1.36	2.63	8.30	34.24	0.0054	1.1409	0.3455	1.0000
O K	45.96	66.44	530.40	10.13	0.1027	1.0889	0.2051	1.0000
MgK	1.24	1.18	46.05	12.02	0.0072	1.0018	0.5824	1.0027
AlK	2.01	1.73	85.69	9.25	0.0138	0.9639	0.7082	1.0048
SiK	5.92	4.87	277.53	5.18	0.0468	0.9843	0.7982	1.0065
S K	1.26	0.91	48.07	15.56	0.0111	0.9625	0.8965	1.0170
PdL	5.27	1.14	85.01	8.75	0.0406	0.7153	1.0656	1.0119
CaK	35.56	20.52	786.64	2.93	0.3216	0.9248	0.9737	1.0040
FeK	1.42	0.59	12.98	34.78	0.0118	0.8176	0.9833	1.0314

EDS Spot 4

kV:	15	Mag: 10000	Takeoff: 37	Live Time(s): 30	Amp Time(µs): 7.68	Resolution:(eV) 125.8

EDS Spot 4 - Det 1

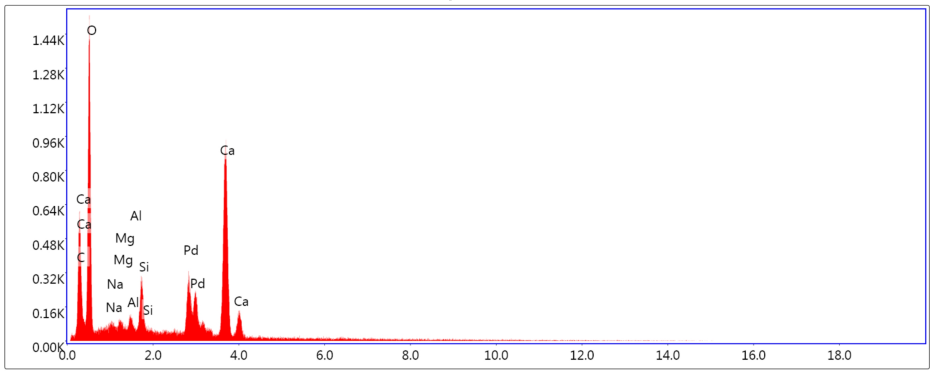

Lsec: 30.0 43 Cnts 2.025 keV Det: Octane Elite 25

eZAF Smart Quant Results with SEC (BCNOF_2017-09-14)

Element	Weight %	Atomic %	Net Int.	Error %	Kratio	Z	A	F
C K	6.07	10.19	42.86	13.08	0.0229	1.1062	0.4056	1.0000
O K	53.44	67.36	677.78	9.75	0.1084	1.0546	0.2282	1.0000
NaK	1.71	1.50	39.05	16.15	0.0060	0.9536	0.4367	1.0013
MgK	1.28	1.06	47.53	12.23	0.0062	0.9687	0.5886	1.0024
AlK	1.24	0.93	52.46	11.97	0.0070	0.9317	0.7153	1.0041
SiK	3.32	2.39	155.82	6.13	0.0217	0.9511	0.8103	1.0060
CaK	32.94	16.58	736.93	2.68	0.2489	0.8922	1.0003	1.0044

EDS Spot 5

kV:	15	Mag: 10000	Takeoff: 37	Live Time(s): 30	Amp Time(µs): 7.68	Resolution:(eV) 125.8

EDS Spot 5 - Det 1

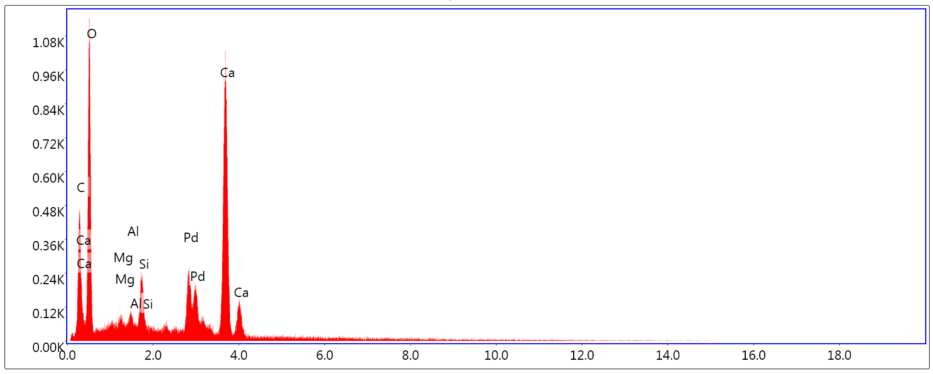

eZAF Smart Quant Results with SEC (BCNOF_2017-09-14)

Element	Weight %	Atomic %	Net Int.	Error %	Kratio	Z	A	F
C K	5.26	9.17	35.60	14.11	0.0213	1.1133	0.4244	1.0000
O K	50.93	66.62	529.51	10.22	0.0946	1.0617	0.2043	1.0000
MgK	1.17	1.01	39.91	13.24	0.0058	0.9756	0.5910	1.0024
AlK	1.10	0.85	42.73	13.31	0.0064	0.9384	0.7185	1.0043
SiK	2.95	2.20	127.05	6.96	0.0198	0.9580	0.8136	1.0063
CaK	38.60	20.16	791.12	2.68	0.2984	0.8990	1.0010	1.0036

EDS Spot 6

kV:	Mag:	Takeoff:	Live Time(s):	Amp Time(µs):	Resolution:(eV)
15	10000	37	30	7.68	125.8

EDS Spot 6 - Det 1

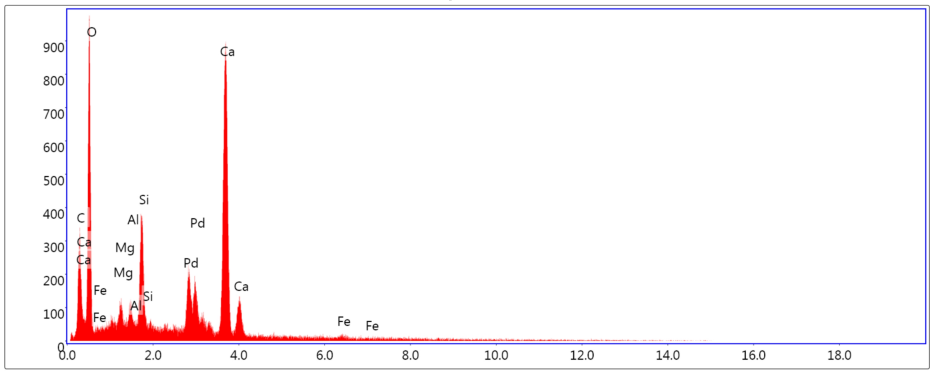

Lsec: 30.0 37 Cnts 2.025 keV Det: Octane Elite 25

eZAF Smart Quant Results with SEC (BCNOF_2017-09-14)

Element	Weight %	Atomic %	Net Int.	Error %	Kratio	Z	A	F
C K	3.63	6.61	20.10	18.97	0.0132	1.1224	0.3706	1.0000
O K	47.22	64.47	451.19	10.37	0.0886	1.0706	0.2004	1.0000
MgK	1.81	1.62	58.05	11.02	0.0093	0.9841	0.5934	1.0025
AlK	1.35	1.09	49.01	11.73	0.0080	0.9466	0.7153	1.0043
SiK	5.61	4.37	225.50	5.45	0.0386	0.9665	0.8090	1.0057
CaK	39.35	21.44	752.77	2.73	0.3124	0.9072	0.9962	1.0040
FeK	1.02	0.40	7.92	62.83	0.0073	0.8010	0.9858	1.0324

Cement paste, w/c:0.6, 8 hours carbonation

EDAX TEAM

Mohammad Cement 2020

Author: student
Creation: 07/06/2020 12:09:56 PM

Sample Name: C68

Area 1

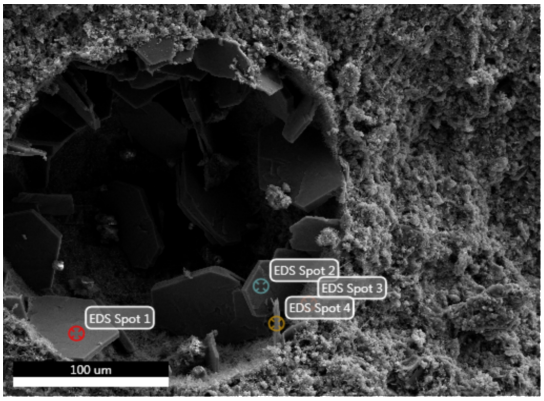

Notes:

EDS Spot 1

kV:	15	Mag: 1038	Takeoff: 37.8	Live Time(s): 30	Amp Time(µs): 7.68	Resolution:(eV) 125.8

EDS Spot 1 - Det 1

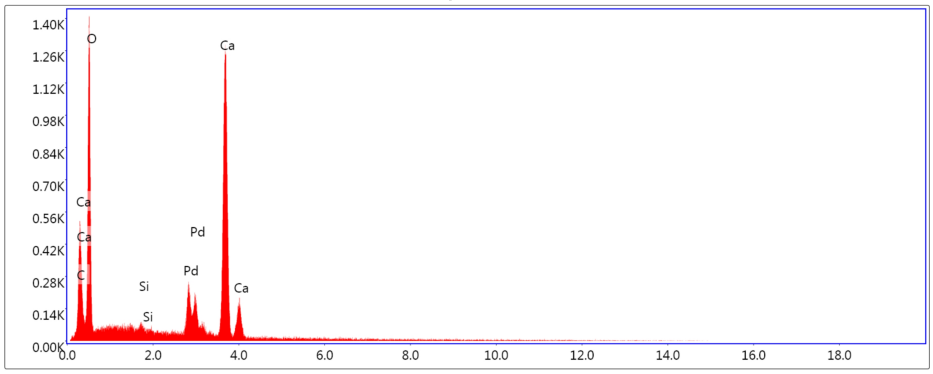

Lsec: 30.0 38 Cnts 2.025 keV Det: Octane Elite 25

eZAF Smart Quant Results with SEC (BCNOF_2017-09-14)

Element	Weight %	Atomic %	Net Int.	Error %	Kratio	Z	A	F
C K	1.68	3.00	15.34	23.41	0.0083	1.1175	0.5009	1.0000
O K	54.96	73.72	643.57	10.06	0.1049	1.0659	0.2021	1.0000
SiK	0.26	0.20	12.79	41.77	0.0018	0.9621	0.8169	1.0070
CaK	43.10	23.08	1003.02	2.54	0.3475	0.9030	1.0049	1.0031

EDS Spot 2

kV:	Mag:	Takeoff:	Live Time(s):	Amp Time(µs):	Resolution:(eV)
15	1038	37.8	30	7.68	125.8

EDS Spot 2 - Det 1

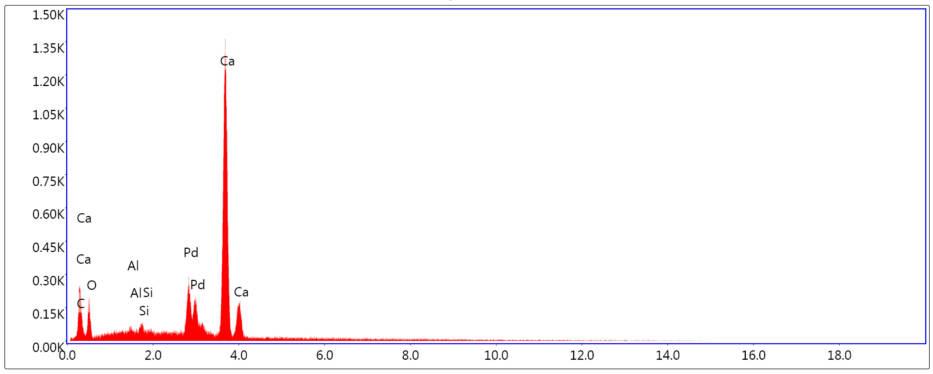

eZAF Smart Quant Results with SEC (BCNOF_2017-09-14)

Element	Weight %	Atomic %	Net Int.	Error %	Kratio	Z	A	F
C K	0.65	1.63	3.32	79.33	0.0033	1.1798	0.4961	1.0000
O K	21.16	39.62	80.20	13.11	0.0236	1.1272	0.1163	1.0000
AlK	0.24	0.27	6.01	64.84	0.0015	0.9994	0.7114	1.0046
SiK	0.76	0.81	20.91	24.58	0.0054	1.0208	0.8111	1.0075
CaK	77.18	57.67	1009.09	2.38	0.6314	0.9604	1.0009	1.0007

EDS Spot 3

kV:	15	Mag: 1038	Takeoff: 37.8	Live Time(s): 30	Amp Time(µs): 7.68	Resolution:(eV) 125.8

EDS Spot 3 - Det 1

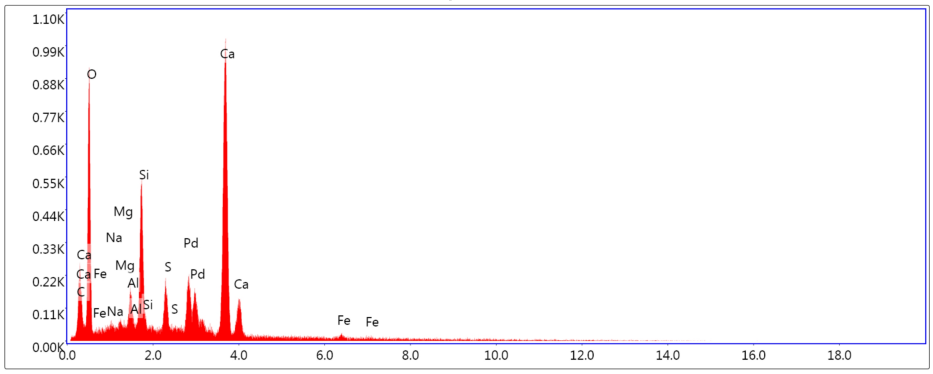

Lsec: 30.0 49 Cnts 2.025 keV Det: Octane Elite 25

eZAF Smart Quant Results with SEC (BCNOF_2017-09-14)

Element	Weight %	Atomic %	Net Int.	Error %	Kratio	Z	A	F
C K	1.60	3.08	7.53	39.03	0.0048	1.1337	0.2997	1.0000
O K	42.66	61.72	412.18	10.47	0.0792	1.0817	0.1938	1.0000
NaK	0.47	0.47	9.71	46.51	0.0018	0.9790	0.4423	1.0014
MgK	0.56	0.54	19.08	20.89	0.0030	0.9947	0.5999	1.0027
AlK	2.10	1.80	81.18	9.21	0.0131	0.9569	0.7287	1.0046
SiK	7.21	5.94	303.31	4.93	0.0511	0.9770	0.8143	1.0059
S K	3.20	2.31	107.36	9.31	0.0247	0.9552	0.9000	1.0140
CaK	40.77	23.55	804.31	2.75	0.3287	0.9174	0.9881	1.0038
FeK	1.42	0.59	11.37	41.26	0.0103	0.8104	0.9835	1.0303

EDS Spot 4

kV:	15	Mag: 1038	Takeoff: 37.8	Live Time(s): 26	Amp Time(µs): 7.68	Resolution:(eV) 125.8

EDS Spot 4 - Det 1

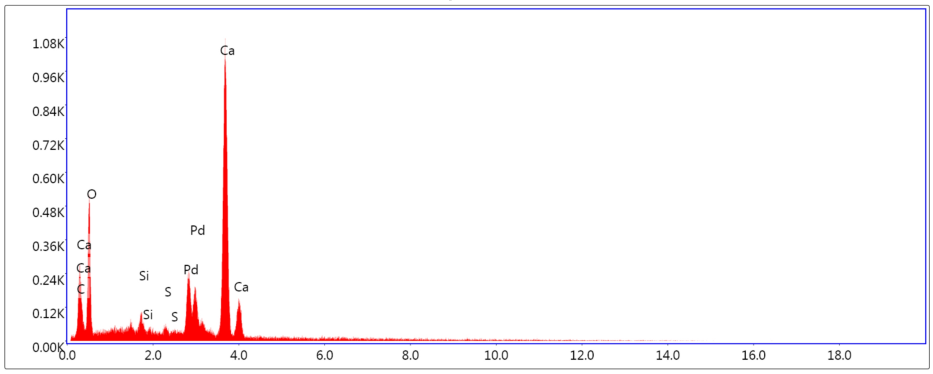

Lsec: 26.0 47 Cnts 2.025 keV Det: Octane Elite 25

eZAF Smart Quant Results with SEC (BCNOF_2017-09-14)

Element	Weight %	Atomic %	Net Int.	Error %	Kratio	Z	A	F
C K	1.33	2.69	7.99	38.39	0.0059	1.1415	0.4631	1.0000
O K	40.97	62.02	265.44	11.11	0.0590	1.0896	0.1575	1.0000
SiK	1.30	1.12	45.31	14.78	0.0088	0.9848	0.8172	1.0072
S K	0.70	0.53	20.02	22.87	0.0053	0.9630	0.9296	1.0187
CaK	55.70	33.65	917.53	2.50	0.4334	0.9252	1.0012	1.0019

Cement paste, w/c:0.3, 8 hours carbonation

EDAX TEAM

Mohammad Cement 2020

Author: student
Creation: 07/06/2020 9:27:34 AM

Sample Name: C38

Area 2

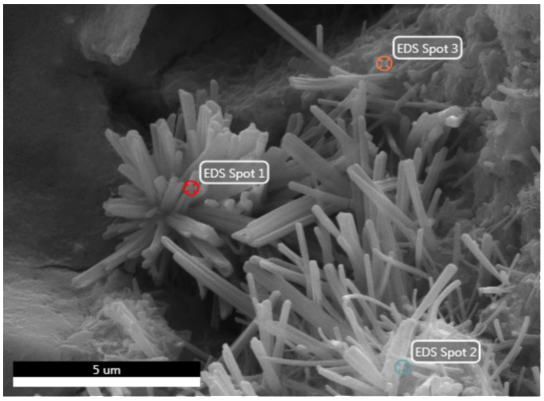

Notes:

EDS Spot 1

kV: 15 Mag: 25000 Takeoff: 35.5 Live Time(s): 30 Amp Time(µs): 7.68 Resolution:(eV) 125.8

EDS Spot 1 - Det 1

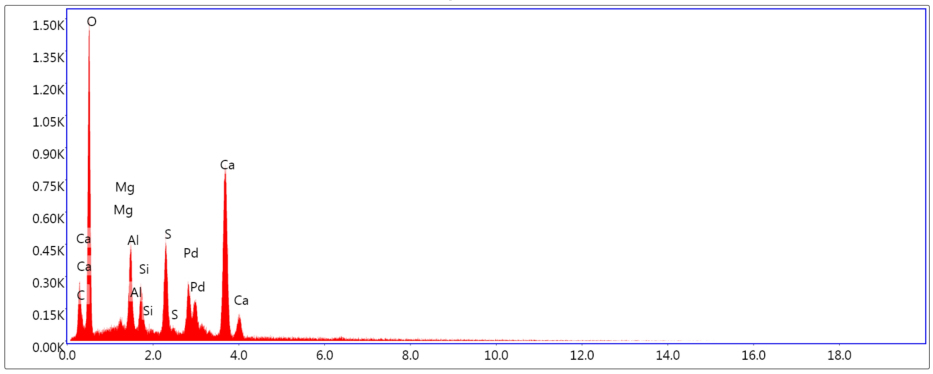

Lsec: 30.0 47 Cnts 2.025 keV Det: Octane Elite 25

eZAF Smart Quant Results with SEC (BCNOF_2017-09-14)

Element	Weight %	Atomic %	Net Int.	Error %	Kratio	Z	A	F
C K	1.79	3.17	7.81	39.67	0.0044	1.1162	0.2507	1.0000
O K	51.66	68.63	672.86	9.74	0.1111	1.0643	0.2320	1.0000
MgK	1.25	1.09	48.24	12.58	0.0064	0.9778	0.6025	1.0029
AlK	5.64	4.45	248.02	6.19	0.0338	0.9406	0.7280	1.0042
SiK	2.71	2.05	126.77	8.55	0.0181	0.9602	0.7916	1.0065
S K	7.64	5.06	295.14	4.49	0.0574	0.9384	0.9086	1.0121
CaK	29.31	15.54	659.26	2.99	0.2271	0.9008	0.9832	1.0046

EDS Spot 2

kV:	Mag:	Takeoff:	Live Time(s):	Amp Time(µs):	Resolution:(eV)
15	25000	35.5	30	7.68	125.8

EDS Spot 2 - Det 1

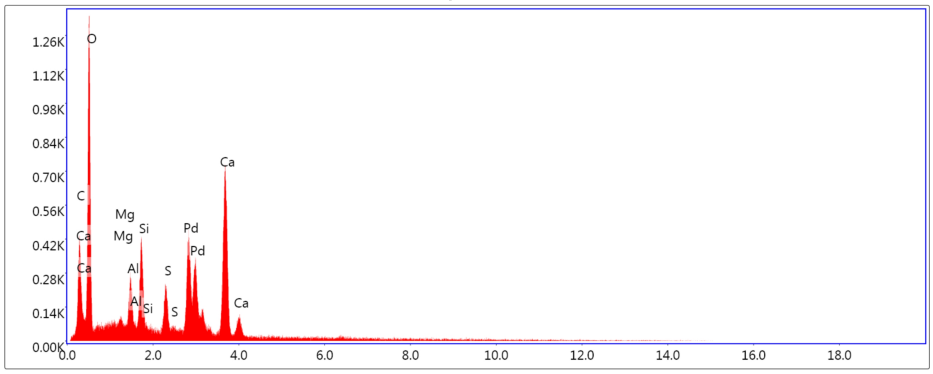

Lsec: 30.0 41 Cnts 2.025 keV Det: Octane Elite 25

eZAF Smart Quant Results with SEC (BCNOF_2017-09-14)

Element	Weight %	Atomic %	Net Int.	Error %	Kratio	Z	A	F
C K	6.25	10.51	28.58	17.17	0.0154	1.1062	0.2896	1.0000
O K	51.80	65.39	619.67	9.76	0.0985	1.0545	0.2347	1.0000
MgK	1.43	1.19	50.50	11.93	0.0065	0.9685	0.6056	1.0028
AlK	3.47	2.59	138.65	7.50	0.0182	0.9315	0.7296	1.0045
SiK	5.33	3.84	230.62	5.71	0.0316	0.9509	0.8071	1.0059
S K	3.94	2.48	137.65	8.21	0.0258	0.9292	0.9053	1.0131
CaK	27.79	14.01	571.33	3.11	0.1895	0.8919	0.9897	1.0050

EDS Spot 3

kV:	Mag:	Takeoff:	Live Time(s):	Amp Time(µs):	Resolution:(eV)
15	25000	35.5	30	7.68	125.8

EDS Spot 3 - Det 1

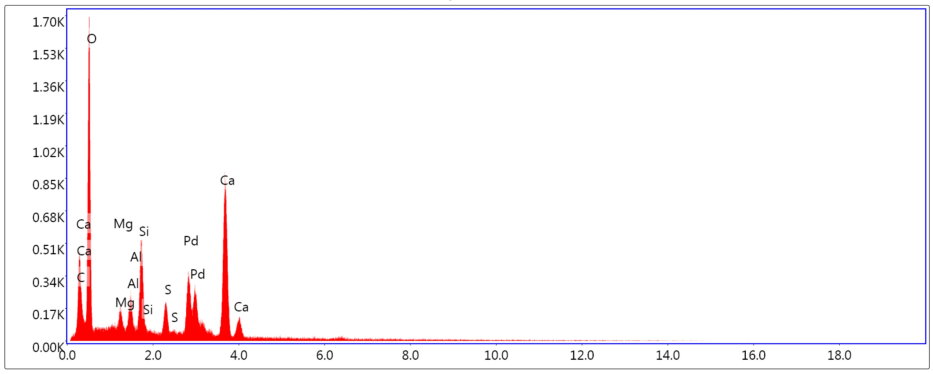

Lsec: 30.0 40 Cnts 2.025 keV Det: Octane Elite 25

eZAF Smart Quant Results with SEC (BCNOF_2017-09-14)

Element	Weight %	Atomic %	Net Int.	Error %	Kratio	Z	A	F
C K	4.91	8.27	27.11	17.35	0.0135	1.1060	0.3002	1.0000
O K	53.57	67.76	767.17	9.59	0.1128	1.0543	0.2414	1.0000
MgK	2.20	1.83	90.00	9.41	0.0106	0.9683	0.6023	1.0027
AlK	2.57	1.93	118.27	8.03	0.0143	0.9313	0.7211	1.0045
SiK	6.06	4.37	304.74	5.39	0.0387	0.9507	0.8064	1.0057
S K	2.76	1.74	111.92	9.32	0.0194	0.9291	0.9016	1.0134
CaK	27.92	14.09	668.65	2.93	0.2050	0.8917	0.9910	1.0051

Cement mortar, w/c:0.3, 8 hours carbonation

EDAX TEAM

Mohammad Cement 2020

Author: student
Creation: 07/10/2020 9:13:38 AM

Sample Name: M38

Area 3

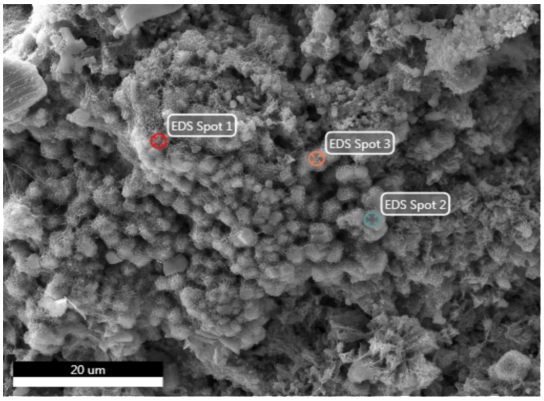

Notes:

EDS Spot 1

kV:	15	Mag: 5000	Takeoff: 38.9	Live Time(s): 50	Amp Time(µs): 7.68	Resolution:(eV) 125.8

EDS Spot 1 - Det 1

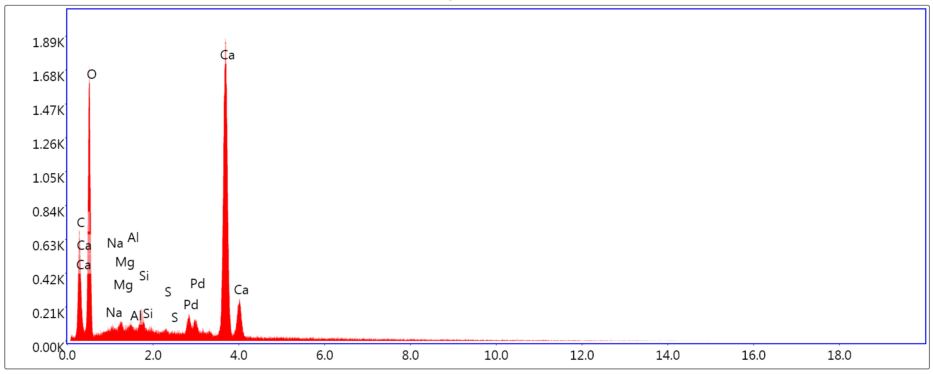

Lsec: 50.0 0 Cnts 0.000 keV Det: Octane Elite 25

eZAF Smart Quant Results

Element	Weight %	Atomic %	Net Int.	Error %	Kratio	Z	A	F
C K	1.87	3.62	25.01	13.64	0.0098	1.1392	0.4600	1.0000
O K	45.33	65.91	454.88	10.15	0.0907	1.0873	0.1839	1.0000
NaK	0.59	0.60	11.85	27.77	0.0025	0.9844	0.4270	1.0014
MgK	0.83	0.80	27.45	12.87	0.0049	1.0003	0.5829	1.0025
AlK	0.59	0.51	22.43	16.55	0.0041	0.9625	0.7114	1.0046
SiK	1.32	1.09	55.46	8.03	0.0106	0.9828	0.8094	1.0075
S K	0.45	0.32	15.50	22.01	0.0040	0.9610	0.9243	1.0198
PdL	3.60	0.79	52.44	10.48	0.0283	0.7143	1.0815	1.0154
CaK	45.41	26.35	896.82	2.41	0.4157	0.9234	0.9884	1.0025

EDS Spot 2

kV:	15	Mag: 5000	Takeoff: 38.9	Live Time(s): 50	Amp Time(µs): 7.68	Resolution:(eV) 125.8

EDS Spot 2 - Det 1

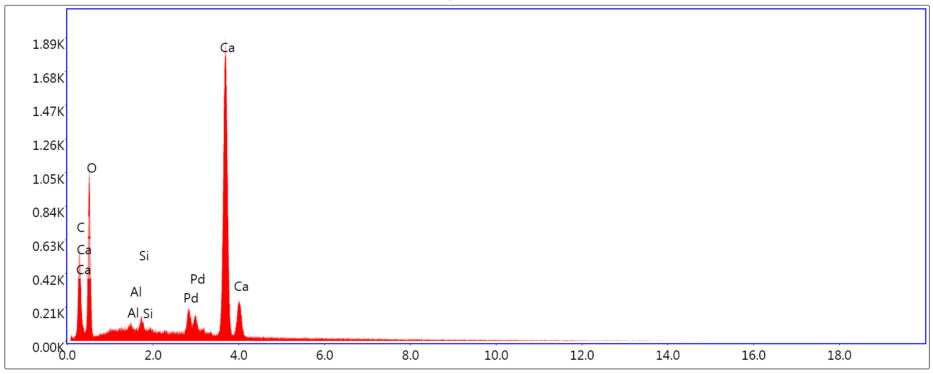

Lsec: 50.0 0 Cnts 0.000 keV Det: Octane Elite 25

eZAF Smart Quant Results

Element	Weight %	Atomic %	Net Int.	Error %	Kratio	Z	A	F
C K	1.96	3.91	21.57	14.73	0.0099	1.1404	0.4805	1.0000
O K	40.80	61.26	282.93	10.67	0.0662	1.0885	0.1609	1.0000
AlK	0.75	0.67	22.76	15.49	0.0049	0.9635	0.7216	1.0044
SiK	1.12	0.96	37.58	9.24	0.0084	0.9838	0.8171	1.0071
CaK	55.38	33.20	875.24	2.27	0.4759	0.9242	1.0021	1.0019

EDS Spot 3

kV:	15	Mag: 5000	Takeoff: 38.9	Live Time(s): 50	Amp Time(µs): 7.68	Resolution:(eV) 125.8

EDS Spot 3 - Det 1

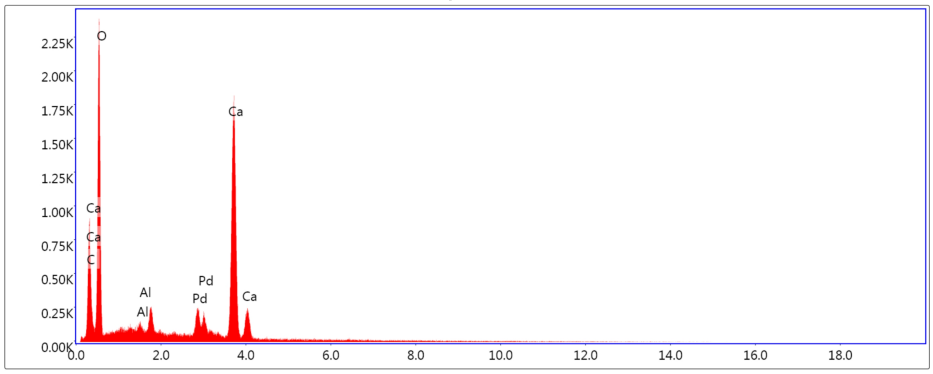

Lsec: 50.0 0 Cnts 0.000 keV Det: Octane Elite 25

eZAF Smart Quant Results

Element	Weight %	Atomic %	Net Int.	Error %	Kratio	Z	A	F
C K	2.76	4.85	41.24	11.22	0.0140	1.1144	0.4966	1.0000
O K	55.23	72.80	658.53	9.76	0.1137	1.0628	0.2114	1.0000
AlK	0.95	0.74	37.66	9.46	0.0059	0.9395	0.7221	1.0041
CaK	41.06	21.61	850.45	2.36	0.3413	0.9001	1.0046	1.0033

Appendix D

- Norcem Industrisement product data

PRODUKTDATABLAD

INDUSTRISEMENT

CEM I 52,5 R

SIST REVIDERT JULI 2016

Sementen tilfredsstiller kravene i NS-EN 197-1:2011 til Portlandsement CEM I 52,5 R.

Egenskap		Deklarerte data	Krav ifølge NS-EN 197-1:2011
Finhet (Blaine m^2/kg)		550	
Spesifikk vekt (kg/dm^3)		3,13	
Volumbestandighet (mm)		1	≤ 10
Begynnendestørkning (min)		110	≥ 45
Trykkfasthet (MPa)	1 døgn	33	
	2 døgn	41	≥ 30
	7 døgn	50	
	28 døgn	59	≥ 52,5
Sulfat (% SO_3)		≤ 4,0	≤ 4,0
Klorid (% Cl^-)		≤ 0,085	≤ 0,10
Vannløselig krom (ppm Cr^{6+})		≤ 2	≤ 2 [1]
Alkalier (% Na_2O_{ekv})		1,3	
Klinker (%)		96	95-100
Sekundærebestanddeler (%)		4	0-5

1. I henhold til EU forordning REACH Vedlegg XVII punkt 47 krom VI forbindelser.

NORCEM
HEIDELBERGCEMENT Group

Norcem AS, Postboks 142, Lilleaker, 0216 Oslo
Tlf. 22 87 84 00 firmapost@norcem.no www.norcem.no

- Superplasticizer product data

MAPEI

Dynamon SX-N

Superplasticising admixture

PRODUCT DESCRIPTION
Dynamon SX-N is a very efficient liquid superplasticising admixture, based on modified acrylic polymers.
The product belongs to the **Dynamon System** based on the DPP (Design Performance Polymers) technology, a new chemical process that can model the admixture's properties in relation to specific performances required for concrete. The process is developed by means of a complete design and production of monomers (an exclusive Mapei know-how).

AREAS OF APPLICATION
Dynamon SX-N is an all-round product to be used in nearly all types of concrete to improve the workability and/or reduce the amount of water needed.

Some specific applications are:

- Concrete with reduced permeability with specifications as to very high mechanical strength and to long durability in aggressive environments.
- Concrete with high levels of workability (consistency classes S4 or S5 - according to EN 206)
- Self-compacting concrete where high slump retention is required. If extra stabilisation is needed, a viscosity enhancing agent, **Viscofluid** or **Viscostar** can be used.
- Production of frost resistant concrete - in combination with air entraining agents (AEA), **Mapeair**. The correct type and amount of AEA is dependent on the properties of the other available ingredients.
- Concrete for flooring where a smooth concrete with high workability is aimed for. Larger dosages and lower tempe ratures may increase the retardation.

TECHNICAL PROPERTIES
Dynamon SX-N is an aqueous solution of active acrylic polymers that very efficiently disperses clusters of cement grains.

This effect can in principle be used in the following three ways:

1. To reduce the amount of added water, yet retain the same workability. Lower water to cement ratio means higher mechanical strength, reduced permeability and increased durability.
2. To increase workability compared to concrete with equal water to cement ratio. With the same mechanical strength the casting is facilitated.
3. To reduce both the amount of water and the amount of cement without changing the concrete's mechanical strength. In this way it is possible to

Dynamon SX-N

reduce the total cost of the concrete (less cement), reduce the concrete's shrinkage potential for (less water) and reduce the possibility of cracks due to temperature gradients (less hydration heat). Especially with concretes that normally have high amounts of cement, this effect is very important.

COMPATIBILITY WITH OTHER PRODUCTS

Dynamon SX-N can be combined with other admixtures from Mapei; such as a set-accelerating admixture, **Mapefast** or a set-retarding admixture, **Mapetard**. The product is also compatible with air entraining admixtures to produce frost resistant concrete, **Mapeair**.

The choice of admixture is done after an evaluation of the properties of the other ingredients in the mix.

DOSAGE

To obtain the prescribed properties (i.e. strength, durability, workability, cement reduction), **Dynamon SX-N** is added in dosages between 0.4 and 2.0% of the amount of cement + fly ash + microsilica. Increased dosages will also increase the slump retention, i.e. the time to be able to work with the concrete.

Higher dosages and lower temperatures will delay the setting of the concrete. To obtain correct knowledge, tests with actual parameters are advisable, especially before larger pours.

As opposed to traditional superplasticisers based on melamines or naphtalenes, the maximum effect of **Dynamon SX-N** is obtained regardless of when it isaddes during the mixing procedure it is added, but the time of addition can influence the mixing time. If at least 80 % of the mixing water is added before **Dynamon SX-N** the required mixing time will generally be shortest. It is nevertheless important to perform using the actual mixing equipment.

Dynamon SX-N can also be added directly into the truck on site. The concrete should then be mixed at full speed at least for one minute pr m^3 of concrete, and never shorter than 5 minutes.

PACKAGING

Dynamon SX-N is available in 25 liter cans, 200 liter drums, 1000 liter IBC tanks and in tank.

STORAGE

The product must be stored at temperatures between +8 and +35°C, and will retain its properties for at least one year if stored unopened in its original packaging. If the product is exposed to direct sunlight, colour variation may occur, but this will not affect the technical properties of the product.

SAFETY INSTRUCTIONS FOR PREPARATION AND INSTALLATION

Instructions for the safe use of our products can be found on the latest version of the SDS available from our website www.mapei.no

PRODUCT FOR PROFESSIONAL USE.

WARNING

Although the technical details and recommendations contained in this product data sheet correspond to the best of our knowledge and experience, all the above - information must, in every case, be taken as merely indicative and subject to confirmation after long-term practical application: for this reason, anyone who intends to use the product must ensure beforehand that it is suitable for the envisaged application: in every case, the user alone is fully responsible for any consequences deriving from the use of the product.

Please refer to the current version of the technical data sheet, available from our web site www.mapei.no

LEGAL NOTICE

The contents of this Technical Data Sheet ("TDS") may be copied into another project-related document, but the resulting document shall not supplement or replace requirements per the TDS in force at the time of the MAPEI product installation.
The most up-to-date TDS can be downloaded from our website www.mapei.no
ANY ALTERATION TO THE WORDING OR REQUIREMENTS CONTAINED OR DERIVED FROM THIS TDS EXCLUDES THE RESPONSIBILITY OF MAPEI.

All relevant references for the product are available upon request and from www.mapei.no

Dynamon SX-N

TECHNICAL DATA (typical values)	
PRODUCT IDENTITY	
Appearance:	liquid
Colour:	yellowish brown
Viscosity:	easy flowing; < 30 mPa·s
Solids content (%:)	18.5 ± 1.0
Density (g/cm³):	1.06 ± 0.02
pH:	6.5 ± 1
Chloride content (%):	< 0.05
Alkali content (Na_2O-equivalents) (%):	< 2.0

6392-07-2017(GB)

MAPEI®
BUILDING THE FUTURE